ISTANBUL TECHNICAL UNIVERSITY ★ GRADUATE SCHOOL OF SCIENCE ENGINEERING AND TECHNOLOGY

ROADHEADER PERFORMANCE PREDICTION USING PORTABLE LINEAR CUTTING MACHINE

M.Sc. THESIS

Can POLAT

Department of Mining Engineering

Mining Engineering Programme

APRIL 2015

ISTANBUL TECHNICAL UNIVERSITY ★ GRADUATE SCHOOL OF SCIENCE ENGINEERING AND TECHNOLOGY

ROADHEADER PERFORMANCE PREDICTION USING PORTABLE LINEAR CUTTING MACHINE

M.Sc. THESIS

Can POLAT
(505121014)

Department of Mining Engineering

Mining Engineering Programme

Thesis Advisor: Assoc. Prof. Dr. Cemal BALCI

APRIL 2015

İSTANBUL TEKNİK ÜNİVERSİTESİ ★ FEN BİLİMLERİ ENSTİTÜSÜ

TAŞINABİLİR DOĞRUSAL KAZI SETİ İLE KOLLU GALERİ AÇMA MAKİNALARININ PERFORMANS TAHMİNİNE YÖNELİK ÇALIŞMALAR

YÜKSEK LİSANS TEZİ

Can POLAT
(505121014)

Maden Mühendisliği Anabilim Dalı

Maden Mühendisliği Programı

Tez Danışmanı: Doç. Dr. Cemal BALCI

NİSAN 2015

Can Polat, a M.Sc. student of ITU Graduate School of Science Engineering and Technology student ID 505121014, successfully defended the thesis entitled "ROADHEADER PERFORMANCE PREDICTION USING PORTABLE LINEAR CUTTING MACHINE", which he prepared after fulfilling the requirements specified in the associated legislations, before the jury whose signatures are below.

Thesis Advisor :	**Assoc.Prof. Dr. Cemal BALCI** İstanbul Technical University	....
Jury Members :	**Prof. Dr. Nuh BİLGİN** İstanbul Technical University	....
	Assoc. Prof. Dr. İbrahim OCAK İstanbul University	....

Date of Submission : 23.03.2015
Date of Defense : 21.04.2015

FOREWORD

I would like to express my deep appreciation to my thesis advisor Assoc. Prof. Dr. Cemal Balcı for spending time on this research and his valuable guidance thruoght my study.

I am also grateful to Prof. Dr. Nuh Bilgin, Prof. Dr. Hanifi Copur and Assoc. Prof. Dr. Deniz Tumaç for their valuable comments and their help during this period.

I would like to say thank to Research Assist. Ramazan Comaklı, Research Assist. Emre Avunduk and Research Assist. Aydın Shaterpoor for their help and encouragement.

I am grateful to work with PLT Mining Manufacturing and Trading Inc. and Mustafa Tokat for their support in the field study.

I would like to say thanks to supporter of the project, named as "Investigation of some rock cuttability parameters to select mechanical excavators by a developed portable linear rock cutting machine" Scientific and Technological Research Council of Turkey (TUBITAK 112M859).

April 2015

Can POLAT
(Mining Engineer)

TABLE OF CONTENTS

Page

ABBREVIATIONS

SE_{opt}	**:**Specific Energy at Optimum Cutting Conditions
E_{dyn}	**:** Dynamic Elasticity Modulus
E_{sta}	**:** Static Elasticity Modulus
σ_C	: Compressive strength
σ_T	: Tensile Strength
d	: Depth of Cut
F’C	**:** Peak Cutting Force
F’N	**:** Peak Normal Force
F’S	**:** Peak Side Force
FC	**:** Cutting Force
FN	**:** Normal Force
FS	**:** Side force
ICR	**:** Instantaneous Cutting Rate
k	**:** Energy Transfer Ratio
P	**:** Power
Q	**:** Yield per Unit Length of Cut
RMCI	**:** Rock Mass Cuttability Index
RPI	**:** Roadheader Penetration Index
s	**:** Spacing
SE	**:** Specific Energy
SHRV	**:** N 24 Schmidt Hammer Rebound Value
w	**:** Tool Width
α	**:** Rake Angle
β	**:** Clearance Angle
θ	**:** Breakout Angle
ρ	**:** Density
Φ	: Tip Angle

LIST OF TABLES **Page**

LIST OF FIGURES

Page

ROADHEADER PERFORMANCE PREDICTION USING PORTABLE LINEAR CUTTING MACHINE

SUMMARY

This thesis is about the field of rock cutting. Mining and tunneling industries are using mechanized excavation machineries since 1950's. Design principles and performance prediction of these machineries are important due to economical reasons. Futhermore, these machineries have various advantages over the drilling and blasting method. Main purpose of the study is to introduce rock cutting experiments in Portable Linear Cutting Machine (PLCM) using conical picks. This study is a part of scientific research supported by Scientific and Technological Research Council of Turkey (TUBITAK 112M859).

In the first part of this study some rock samples subjected to physical and mechanical property tests, which are located in the Istanbul Technical University (ITU) Rock Mechanization Laboratory. All experiments carried out according to International Sociecty for Rock Mechanics (ISRM) and American Society for Testing and Materials (ASTM) methods (Natural Unit Weight, Uniaxial Compressive Strength, Brazilian Tensile Strength, Determination of P and S waves, Young Modulus, Schmidt Hammer, Shore Scleroscope). Then, two type of conical and a chisel cutter used in the rock cutting tests with PLCM. Cutters used in this study compared among each other on their forces and specific energy. Cutting force and specific energy prediction correlated with physical and mechanical properties and results checked with existing literature.

For the field study, coal mine owned by PLT Mining Manufacturing and Trading Inc, located in Amasya Suluova Basin is visited. Two axial having 75 kW cutting power roadheaders working on excavation of the main galleries are analyzed. Field performance of the roadheaders studied in the mine and rock samples representing the excavated formation taken from the face. After, for the field performance prediction, rock samples concreted and subjected to rock cutting experiments with two conical and one chisel pick. Specific energy results are used in existing models defined by

different researchers to find out this new testing machine can be used in performance prediction of roadheaders or not.

Finally, results obtained from rock cutting experiments with mini scale conical and chisel picks are compared with the theoretical models. Moreover, empirical equations related with physical and mechanical properties are correlated with unrelieved and relieved cutting force results. Some of the predictions are giving high correlation coefficents but it is always better to perform a cutting experiment to design or select a mechanical excavator instead of using empirical or theoretical models.

TAŞINABİLİR DOĞRUSAL KAZI SETİ İLE KOLLU GALERİ AÇMA MAKİNALARININ PERFORMANS TAHMİNİNE YÖNELİK ÇALIŞMALAR

ÖZET

Bu tez çalışması kazı mekaniği alanında yapılmış olup, kazı makinalarının tasarımı ve performans analizi üzerine yeni teknolojilerin kullanılmasını amaçlamıştır. Mekanize kazı makinaları madenlerde ve tünellerde 1950 li yıllardan itibaren kullanılmaktadır. Başlıca bu makinalar tünel açma makinaları, kollu galeri açma makinaları, tamburlu kesiciler, sürekli kazıcılar, hidrolik kazı makinaları ve kömür sabanları ve kuyu açma makinaları olarak sıralanabilir. Bu makinalar maden ve tünel kazısında kullanılmakta ve delme patlama yöntemine göre oldukça fazla avantaj sağlamaktadır. Bu makinaların tasarım prensipleri ve arazi performansları projelendirme aşamasından itibaren yapılacak işin ekonomik sınırlarını belirlemektedir.

TÜBİTAK 112M859 kodlu proje çevçevesinde geliştirilen yeni küçük boyutlu kazı seti (PLCM), kazı makinalarının projelendirme safhasında, şu an literatürde bulunan yöntemlere göre daha ucuz ve basit bir şekilde deney yürütülmesini amaçlamıştır. Bu proje çerçevesinde mini boyuttaki keskilerin tümünün (konik, kama, disk) kesme deneylerinde kullanılması amaçlanmaktadır. Bu sayede oldukça vakit alan tam boyutlu kesme seti ve yeterli sonuç veremeyen küçük boyutlu kazı seti geride bırakılıp, tasarım aşamasında hızlı bir şekilde deneylerin yürütülmesi planlanmaktadır. Bu tez çerçevesinde mini boyuttaki konik ve kama keskiler çalışılmış, bu keskileri kullanan kollu galeri açma makinalarının arazi performansı tahmin edilmeye çalışılmış ve keskiler literatürde önerilen modeller ile karşılaştırılmıştır.

Tezin ilk kısmında İTÜ Kazı ve Mekanizasyon Laboratuarında bilimsel araştırma için bulunan ve ayrıca arazi çalışmaları sırasında toplanan kaya numuneleri fiziksel ve mekanik deneylere tabii tutulmuştur. Bütün deneyler ISRM veya ASTM standartlarına uygun yapılmış ve sonuçlar irdelenmiştir (Birim Hacim Ağırlık, Tek eksenli basınç dayanımı, Dolaylı Çekme Dayanımı, Sonik Hız Deneyi, Elastisite Modulü, Schmidt Sertlik Çekici, Shore Scleroscope). Ardından geliştirilen yeni küçük boyutlu kesme cihazında deneyler iki adet konik ve bir adet kama keski ile yürütülmüştür.

Deneyler basınç dayanımı 9.1 ila 160.7 MPa arasında ve çekme dayanımı 1.14 ila 14.9 Mpa arasında değişen kayalar ile yapılmıştır. Deneyler yürütülürken kama keskiler ile yardımsız olarak farklı kesme derinlikleri seçilmiş ve kayaçlar ile tepkileri ölçülmüştür. Konik keskiler ile yapılan deneyler sadece 5 mm kesme derinliğinde yapılmıştır. Ayrıca konik keskilerde yardımlı olarak da yürütülmüştür.

İlk olarak yapılan deneyler, keskiler arasında karşılaştırılmış sonrasında fiziksel ve mekanik özelliklerin kesme kuvvetine ve spesifik enerjiye olan etkileri araştırılmıştır. Bu çalışmalar halihazırda varolan literatür ile karşılaştırılmış ve yeni geliştirilen deney aletinin kazı mekaniği alanında nasıl bir güvenirlik ile kullanılabileceği araştırılmıştır. Elde edilen sonuçlar arasında keskilerin arasında tasarım parametrelerine bağlı sonuçlar olduğunu ve bunların düzeltme faktörleri kullanarak gerçek boyuttaki keskiler ile arasındaki ilişki ileriki çalışmalar ile sonuçlandırılacaktır.

Arazi çalışmaları dahilinde PLT Madencilik Sanayi ve Ticaret Anonim Şirketine ait ait Suluova kömür işletmeleri ziyaret edilmiştir. Hazırlık galerisi kazısında çalışan eksenel tip 75 kW kesme gücüne sahip iki adet kollu galeri açma makinası incelenmiştir, arazi verileri yerinde kayıt edilmiş ve makinanın çalıştığı formasyonu temsil eden kaya örnekleri alınmıştır. Daha sonra laboratuarda arazi performans tahmini için mini boyuttaki konik keskiler ve kama indeks keski ile deneyler yapılmıştır. Yapılan deneyler kama keskilerde yardımsız ve farklı kesme derinliklerinde, konik keskilerde ise sadece 5 mm kesme derinliğinde optimum keskiler arası mesafe elde edilerek yapılmıştır. Elde edilen deney sonuçları varolan modeller ile birlikte incelenmiş ve hangi modelin en yakın sonucu verdiği irdelenmiştir.

Sonuç kısmında, bazı modellerin yeni deney yöntemi ile birlikte kullanılarak yakın sonuçlar verdiği gözlemlenmiştir. İstatistiksel modeller tek başına kullanıldığında yapılan tahmin değerleri genel olarak gerçeğe yakın sonuç vermediği sonucu elde edilmiştir. Bu modeller kullanılırken modelin sahip olduğu veri tabanı iyi anlaşılmalı ve sonuçlar çok düzgün bir şekilde yorumlanmalıdır. Aksi takdirde elde edilen sonuçlar gerçeği yansıtmayabilir ve tasarım aşamasında hata yapılmasına yol açabilir.

Daha sonra, pik kesme kuvveti tahmini için geliştirilen teorik ve yarı teorik modeller için yapılan deneyler doğrultusunda uygun değerler kullanılarak çözümlenmiştir. Elde edilen sonuçlar konik keski ve kama keski deneylerinin sonuçları ile karşılaştırılmıştır. Teorik ve yarı teorik modeller ile düşük, orta ve yüksek dereceli korelasyon değerleri elde edilmiştir. Bu bölümde teorik ve yarı teorik modellerin mekanize kazı makinaları tasarımı ve performans tahmini aşamasında kullanılması amaçlanmıştır. Fakat yüksek korelasyon değerleri elde edilse bile, bu modellerin tasarım aşamasında kullanılması oldukça kısıtlıdır. Bu yüzden her zaman kazı deneyleri yürütmek, diğer yöntemlere göre göreceli olarak daha uygun sonuçlar verecektir. Mühendislerin maden veya tünel tasarımı aşamasında bu yöntemlere başvurması önerilmektedir.

Son olarak, araştırmacılar tarafından önerilen ampirik modeller konik keskiler ile yürütülen yardımlı ve yardımsız deney sonuçları ile karşılaştırılmıştır. Ampirik modellerden tahmin edilen kesme kuvveti değeri deney sonuçları ile yüksek korelasyon katsayılı sonuçlar vermektedir. Fakat, proje aşamasında her zaman kesme deneyleri yapılması ampirik ve teorik yöntemlere göre daha sağlıklı sonuçlar vermektedir.

Bu tez çalışması "Mekanize Kazı Makinalarının Şeçiminde Kullanılmak Üzere Bazı Kayaçların Kesilebilirlik Özellikleri Araştırılarak Taşınabilir Doğrusal Kaya Kesme Cihazının Geliştirilmesi" (TÜBİTAK 112M859) isimli projenin bir çalışmasıdır. Yapılan tez çerçevesinde mini boyuttaki konik keskilerin bu deney aleti üzerinde hangi güvenle kullanılabileceği araştırılmış, var olan ampirik, teorik ve yarı teorik modeller ile ilişkileri araştırılmıştır. Ayrıca yapılan arazi çalışması ile kollu galeri açma makinaları seçimi ve tasarımında varolan modeller ile nasıl kullanılacağı araştırılmıştır.

İleriki çalışmalarda arazi verilerinin sayısı arttırılıp, bu konu üzerinde yeni bir abak geliştirilmesi planlanmaktadır. Ek olarak disk keskiler ile çalışmalar yürütülmeli ve tünel açma makinaları için benzer çalışmalar yapılmalıdır. Yeni geliştirilen bu deney aleti sayesinde doğrusal kesme deneyleri, diğer yöntemlere göre çok daha hızlı yürütülebilmekte ve sonuçlar daha hızlı irdelenebilmektedir. Yürütülecek bilimsel çalışmalar sonunda madencilik alanına yeni bir deney aleti kazandırılması amaçlanmaktadır.

1. INTRODUCTION AND PURPOSE OF THESIS

Mechanized excavation is developing day-by-day throught the world. Due to needs of the sociecty, extraction of mineral and excavation of tunnels must done in a safer, faster and economical way. Newly developed PLCM is much faster and easier than the preceding experiment methods. Completion of this thesis might help mechanized excavation laboratory studies for rock cutting testing.

Purpose of this thesis is to develop a PLCM within a project sponsored by Scientific and Technological Research Council of Turkey. Afterwards a series of experiments carried out in order to perform experiments with mini scaled conical picks and chisel picks used by McFeat and Smith.

Firstly, to understand the relationships between the chisel and conical cutters a group of experiments done with rock samples having uniaxial compressive strength ranges 9.1 to 160.7 MPa. After the rock cutting experiments, the relationship between chisel and mini scale conical cutters are investigated according to orthogonal forces and specific energy. Also, cutting force and specific energy prediction by using physical and mechanical properties done in this thesis and checked through the existing literature.

Secondly, in the field study part, Amasya-Suluova coal mine is visited. Roadheader performance measured during the excavation of main galleries and rock samples are taken from the face to perform rock mechanics and rock cutting experiments in the laboratory. After, results of actual field performance compared with laboratory studies and statistical models given in the literature.

Finally, in the last two parts, rock cutting experiment results for conical and chisel picks compared with theoretical and ampirical models in order to understand which models are giving the closest results with mini scaled cutters.

2. LITERATURE REVIEW

Conical cutting tools are mainly used in roadheaders, drum shearers and sometimes in tunnel boring machines to excavate rock and coal. They are generally used in the range of soft to hard rock. There are mainly three types of picks which are radial, forward attack and point attack these tools can be seen in Figure 2.1 simultaneously [1].

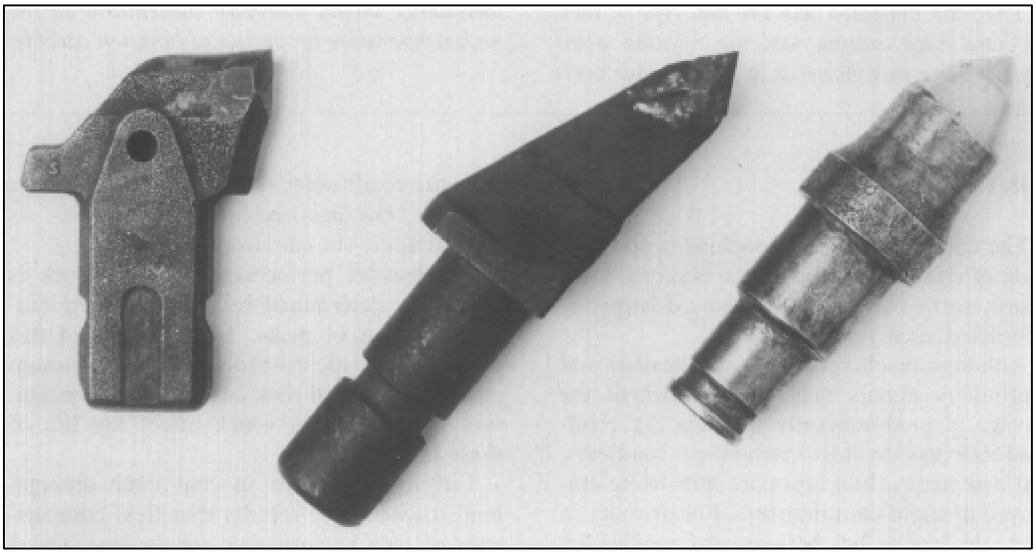

Figure 2.1 : Radial, forward attack and point attack picks [1].

2.1 Cutting Force of the Point Attack Tools

In point attack cutters design parameters are rake angle, tip angle, clearance angle and attack angle. Orthogonal forces acting on a cutting tool can be classified as normal, cutting and side forces. These angles and forces can be seen in Figure 2.2 and 2.3 simultaneously.

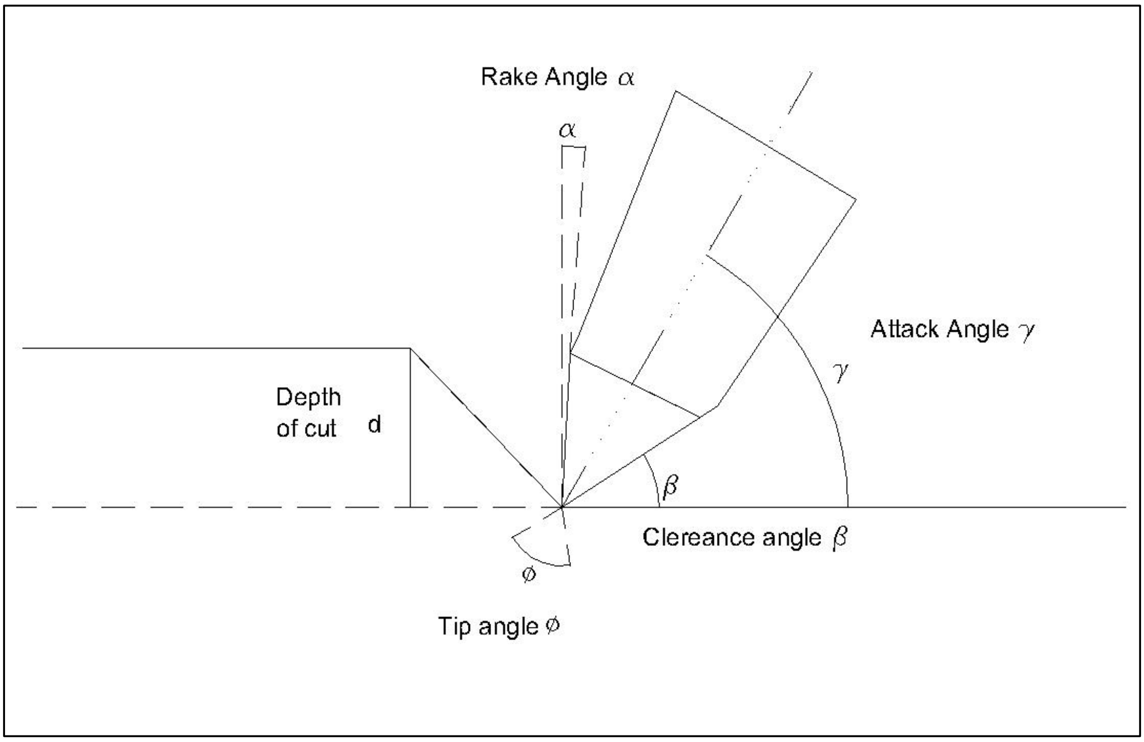

Figure 2.2 : Angles affecting point attack picks performance.

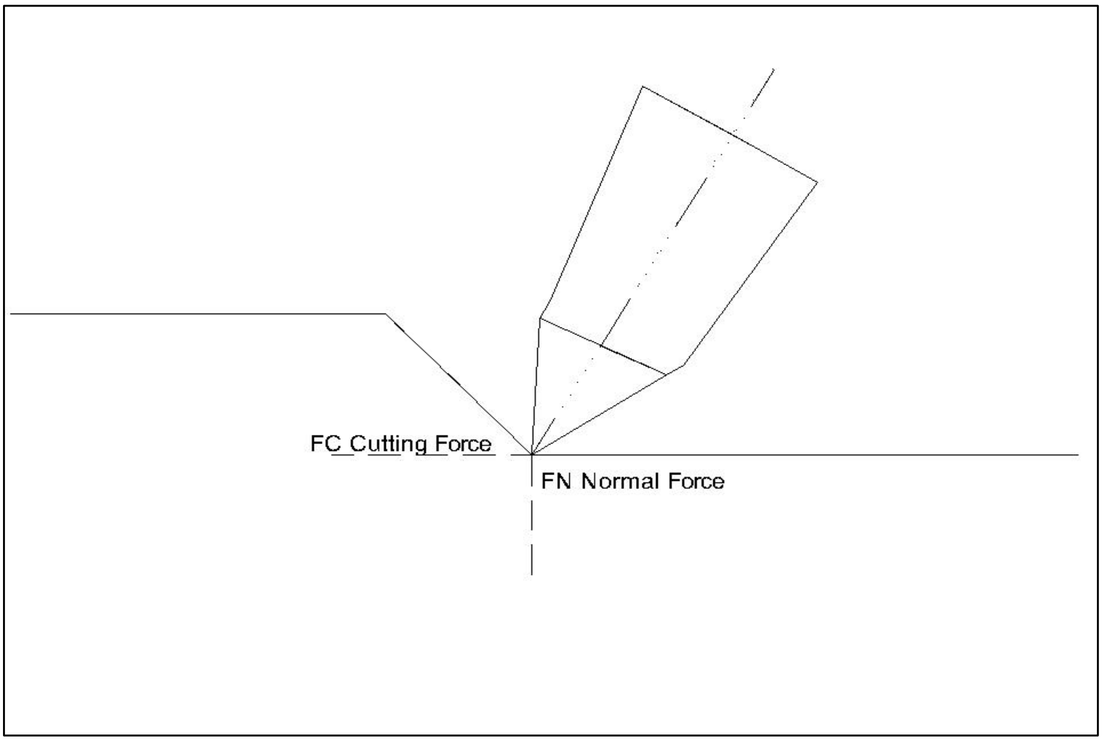

Figure 2.3 : Forces acting on a conical cutter.

It is very crucial to estimate cutting forces acting on a pick. There are three theoretical models and these models are briefly explained in the following paragraphs.

Evans (1984) state a model to predict cutting force acting on a point attack tool based on tensile and compressive strength. The formulation is given in Equation 2.1 [2].

$$F'C = \frac{16\,\Pi\, d^2\, \sigma_T^2}{\cos^2\left(\frac{\phi}{2}\right)\sigma_C} \qquad \textbf{(2.1)}$$

Where;

- F’C= peak cutting force
- d= depth of cut
- σ_T= tensile strength
- Φ= tip angle
- σ_C= compressive strength

Göktan (1997) modified the Evans’ theory and add friction angle between rock and cutter in the formulation. In this formulation compressive strength is taken out from the equation. The formulation given in Equation 2.2 [3].

$$F'C = \frac{4\,\Pi\;\sigma_T\, d^2 \sin^2(\phi/2+\psi)}{\cos(\phi/2+\psi)} \qquad \textbf{(2.2)}$$

Where;

- F’C= peak cutting force
- d= depth of cut
- σ_T= tensile strength
- Φ= tip angle
- ψ= friction angle between rock and cutter

Roxborough and Lıu (1995) modified the formula given by Evans for the point attack tools. The formulation is given in Equation 2.3 [4]

$$F'C = \frac{16\,\Pi\,\sigma_C\, d^2\, \sigma_T^2}{\left[2\sigma_T + \left(\sigma_C \cos\left(\frac{\phi}{2}\right)\left(\frac{1+\tan\psi}{\mathrm{Tan}\left(\frac{\psi}{2}\right)}\right)\right)\right]^2} \qquad \textbf{(2.3)}$$

Where;

- F'C= peak cutting force
- d= depth of cut
- σ_T= tensile strength
- Φ= tip angle
- σ_C= compressive strength

Bilgin et al. (2006) carried out a research on dominant rock properties affecting conical picks and found some formulations for predicting normal and cutting forces. These equations is given in Table 2.1.

Table 2.1 : Force estimation formulas [5].

Unrelieved Cutting	Relieved Cutting (at optimum s/d)
FC/d = 0.826 σ_C + 21.76	FC/d = 2.347 $\sigma_C^{0.785}$
FC/d = 12.625 σ_t + 8.78	FC/d = 16.794 $\sigma_t^{0.721}$
FC/d = 4.452 $e^{0.0058\,SH}$	FC/d = 3.292 $e^{0.0058\,SH}$
FC/d = 12.278 $E_{dyn}^{0.519}$	FC/d = 8.485 $E_{dyn}^{0.557}$
FC/d = 28.974 $E_{sta}^{0.413}$	FC/d = 21.051 $E_{sta}^{0.432}$
FN/d = 1.217 $\sigma_C^{1.104}$	FN/d = 0.752 $\sigma_C^{1.151}$
FN/d = 15.74 $\sigma_t^{0.915}$	FN/d = 10.687 $\sigma_t^{0.947}$
FN/d = 1.723 $e^{0.079\,SH}$	FN/d = 1.141 $e^{0.079\,SHRV}$
FN/d = 20.893$E_{sta}^{0.589}$	FN/d = 14.136 $E_{sta}^{0.596}$
FN/d = 8.236 $E_{dyn}^{0.633}$	FN/d = 5.266 $E_{dyn}^{0.668}$

Where;

- SE_{opt} = Specific Energy at optimum cutting, kWh/m^3
- σ_C = Uniaxial Compressive Strength, MPa
- σ_t = Brazilian Tensile Strength, MPa
- E_{sta}= Static Elasticity Modulus, GPa
- E_{dyn} = Dynamic Elasticity Modulus, GPa
- SHRV= N 24 Schmidt Hammer Rebound Value

Su and Akcin (2011) carried out a research on peak cutting force estimation using discrete element method. They used three dimensional Particle Flow Analysis code

(PFC3D) and observed some formulations related with Evans, Göktan, Roxborough's theory and laboratory experiments. The equations can be found in Table 2.2.

Table 2.2 : Peak mean cutter force estimation formulas [6].

Unrelieved Cutting
FC'^{lab}= 4.1289 + 4.0537 FC'^{PFC3D}
FC'^{Evans}= 0.3393 + 0.5059 FC'^{PFC3D}
$FC'^{Roxb\&Liu}$= 0.323 + 0.7538 FC'^{PFC3D}
FC'^{Goktan}= 0.2407 + 0.9756 FC'^{PFC3D}

Tiryaki et al. (2010) used multiple linear and nonlinear regression analysis to predict mean cutting force (MCF) acting on a conical cutter. Their formulations are listed in Table 2.3.

Table 2.3 : MCF estimation formulas [7].

Mean Cutting Force Estimation
MCF= -3.93 -(0.01s)+ (0.39d)+ (0.52ρ) + (0.04σ_C)- (0.2σ_t) + (0.02E_{dyn}) + (0.04 SH)
MCF= -1.93 + (0.36d) + (0.04σ_C) + (0.03E_{dyn})
MCF= 0.001$s^{\ 0.11} d^{0.98}\ \rho^{0.72}\ \sigma_C^{0.46}\ \ \sigma_t^{-0.34}\ \ Edyn^{0.17}\ \ SHRV^{1.01}$
MCF= 0.01$d^{1.08}\ \ \sigma_C^{0.32}\ Edyn^{0.29}\ SHRV^{0.52}$

Where;

- s= spacing
- d= depth of cut
- ρ= density
- σ_C= compressive strength
- σ_t= tensile strength
- E_{dyn}= Dynamic elasticity modulus
- SHRV= N 24 Schmidt Hammer Rebound Value

2.2 The Effect of Tool Parameters on the Cutting Force of Conical Cutters

2.2.1 Skew and attack angles

Hurt and Evans (1980) carried out a research on the effect of skew and attack angles for the cutting forces. They performed experiments on Grindleford sandstone. The angle of attack varied from 40˚ to 60˚ and the skew angle starting from the zero and increasing with a span of 5˚. They pointed out that depth of cut and spacing between the tool was 20 and 40 mm respectively. They concluded that angle of skew up to 30˚ with a 45˚ attack angle had no clear effect on cutting forces. It can be seen that increasing angle of attack will cause decrease on rake angle and definetely increase the back clereance angle. They also showed that angle of attack between 40 and 50˚ with zero skew angle is decreasing the forces, but angles between 50 to 60˚ is causing counter view. In the Figures 2.4 and 2.5 effect of attack and skew angle can be seen. They stated that cutting action of point attack tools has two functions, first is breaking the rock ahead of the cutting tool and second called profiling which is clearing the path through the remaining material [8].

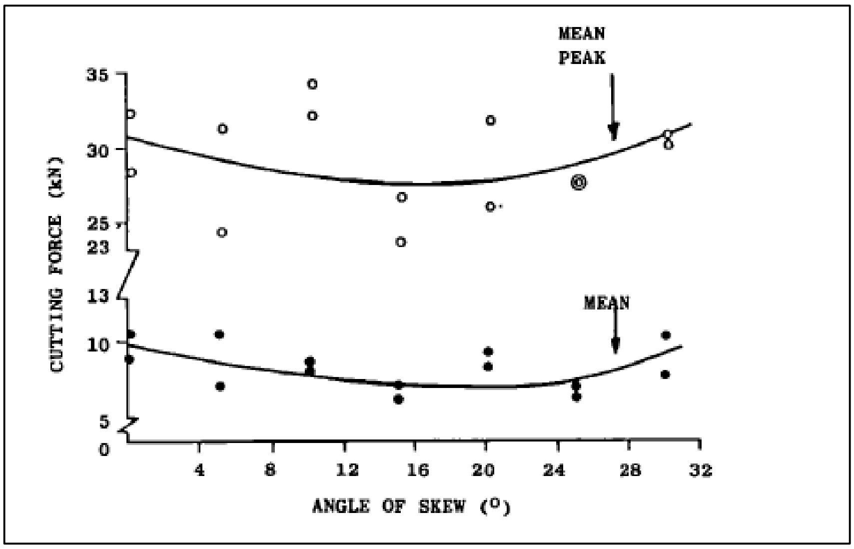

Figure 2.4 : Effect of angle of skew on the cutting force [8].

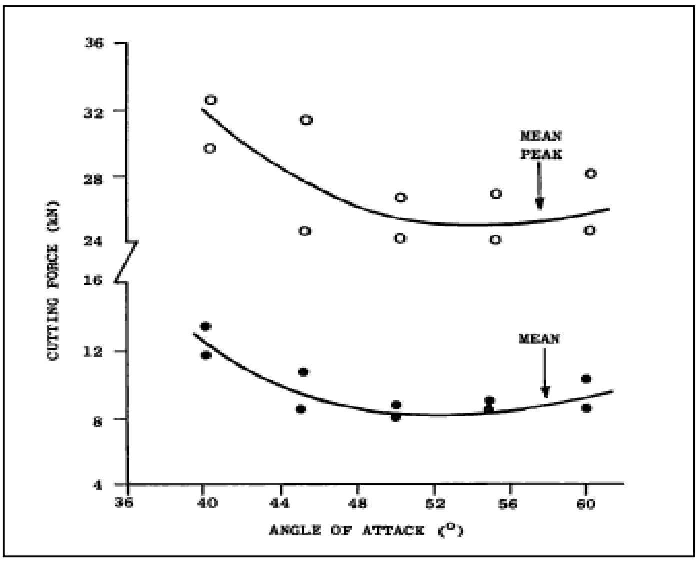

Figure 2.5 : Effect of attack angle on the cutting force [8].

Mostafavi et al. (2011) studied on effect of attack angle on the pick performance. They made their research both experimentaly and numerically. For the experimental and numerical analysis they used a linear cutting machine and a finite element program respectively. They found that attack angle of 55° gave the smallest specific energy for sandstone. Finally, they pointed out the ratio of cutting force to normal force kept minimum at attack angle of 45° with this way tool life will be longer than expected [9].

2.2.2 Tip diameter

Lıu et al (2009) made a research on the effect of carbide tip diameter on the cutting forces. They used a device called cutting testbed coal and rock (CTCR) and three picks having length of 84 mm, cone angle of 75° and carbide tip diameters of 8, 10, 12 mm. They pointed out increasing carbide tip diameter is causing increase on the force acting on the pick [10].

2.3 Cutting Force of Chisel Cutters

In Figure 2.6 a chisel cutter is given. Independent and dependent parameters are as follows [11].

Independent parameters:

- d= depth of cut

- w= width of tool
- α= rake angle
- β= clearance angle
- s= cutter spacing

Dependent variables:

- FC= cutting force
- FN= normal force
- θ= Breakout angle
- SE= specific energy

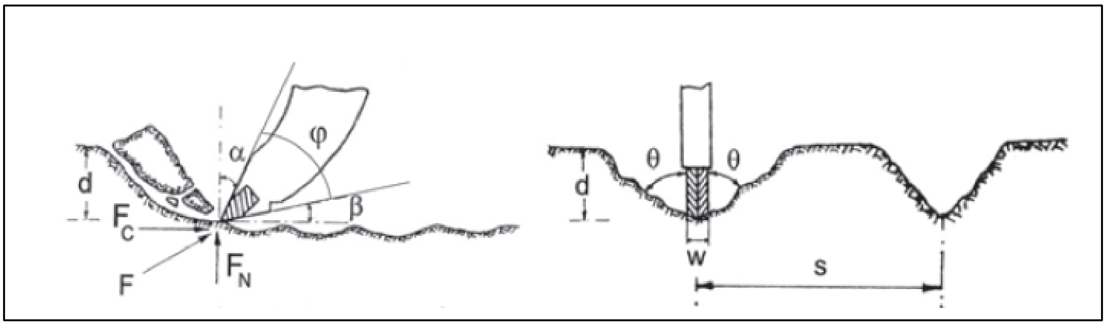

Figure 2.6 : Chisel cutters with design parameters and acting forces [12].

Evans and Pomeroy (1966) defined a theoretical model based on tensile strength of the rock. The formulation is given in Equation 2.4 [11].

$$F'C= \frac{2\ \sigma_t\ d\ w \sin\frac{1}{2}\left(\frac{\Pi}{2}-\alpha\right)}{1-\ \sin\frac{1}{2}\left(\frac{\Pi}{2}-\alpha\right)} \qquad \textbf{(2.4)}$$

Where;

- F'C= peak cutting force
- d= depth of cut
- σ_T= tensile strength
- α= rake angle
- w= width of the tool

Nishimatsu (1972) defined a model predicting peak cutting forces acting on a chisel cutter based on shear strength. This formulation is given in Equation 2.5 [13].

$$F'C= \frac{2\ \sigma_S\ d\ w\ \cos(\psi-\alpha)\cos(i)}{(n+1)\ [\ 1-\sin(i+\psi-\alpha)]} \qquad \textbf{(2.5)}$$

Where;

- F'C= peak cutting force
- d= depth of cut
- σ_S= shear strength
- α= rake angle
- w= width of the tool
- ψ= friction angle between rock and cutter
- i= rock internal friction angle
- n= stress factor (12-(α/5))

2.4 Effect of Tool Parameters on the Cutting Forces of Chisel Picks

2.4.1 Rake angle

Increasing rake angle will cause decrease on the forces but at a certain point high rake angles are effecting tool strength. For this reason rake angle can be taken between -10 and 20 degrees. In Figure 2.7 effect of rake angle on the cutting forces and specific energy are given. Depth of cut and tool width are 20 and 30 mm respectively in this study [12].

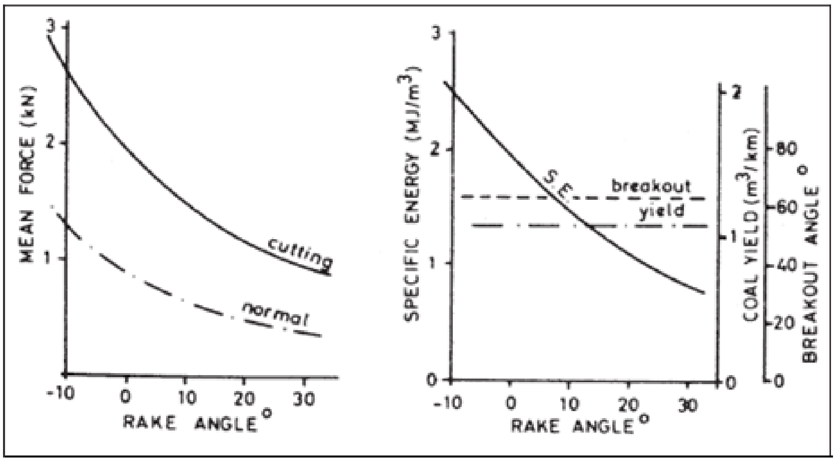

Figure 2.7 : Effect of rake angle on cutting force and specific energy [12].

2.4.2 Clearance angle

Generally clereance angle is kept at 5 degrees where minimum cutter forces and specific energy takes place. Negative clearance angle is causing increase on the forces and dust generation. The effect of clearance angle on the cutting performance is given in Figure 2.8 [12].

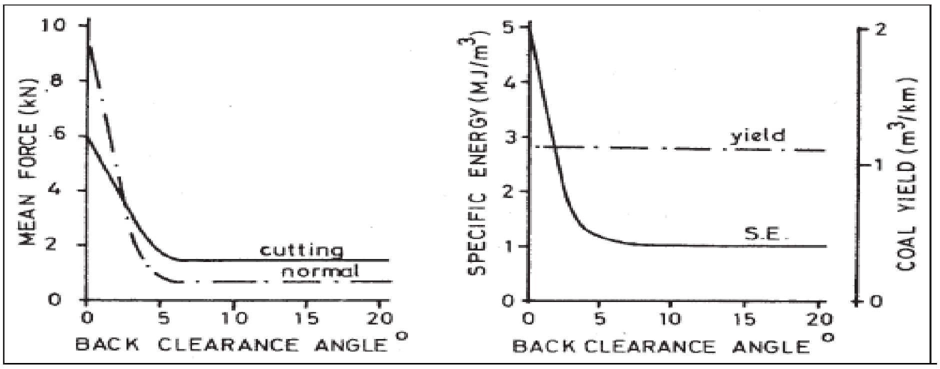

Figure 2.8 : Effect of clearance angle on the cutting performance [12].

2.4.3 Tool width

Increasing tool width is effecting cutter forces and yield linearly. In the Figure 2.9 effect of tool width on the cutting performance is given [12].

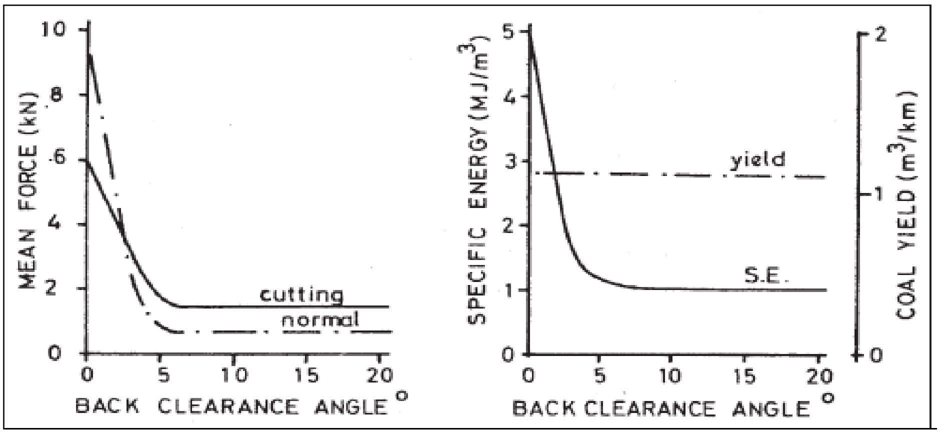

Figure 2.9 : Effect of tool width on the cutting performance [12].

2.5 Specific Energy

Specific energy can be defined as energy needed to excavate unit volume of rock. In terms of kWh/m^3 or MJ/m^3. In the mechanized excavation machineries specific energy is the key factor for an efficient cutting.

2.5.1 Specific energy defined by Hughes (1972)

Hughes (1972) state a specific energy formulation that can relate with compressive strength and elasticity modulus. In this paper, elasticity modulus taken roughly 350 times of compressive strength. The formulation is given in Equation 2.6 [14].

$$SE=\frac{\sigma_c^2}{2E} \tag{2.6}$$

Where;

- SE= Specific energy
- σ_C= compressive strength
- E= Elasticity modulus

2.5.2 Destruction work defined by Thuro and Spaun (1996)

Thuro and Spaun (1996) stated a specific energy model using the area under the stress strain curve. They stated that area under this model gives the destruction work (kJ/m^3) for the rock type. The model is given in Figure 2.10 [15].

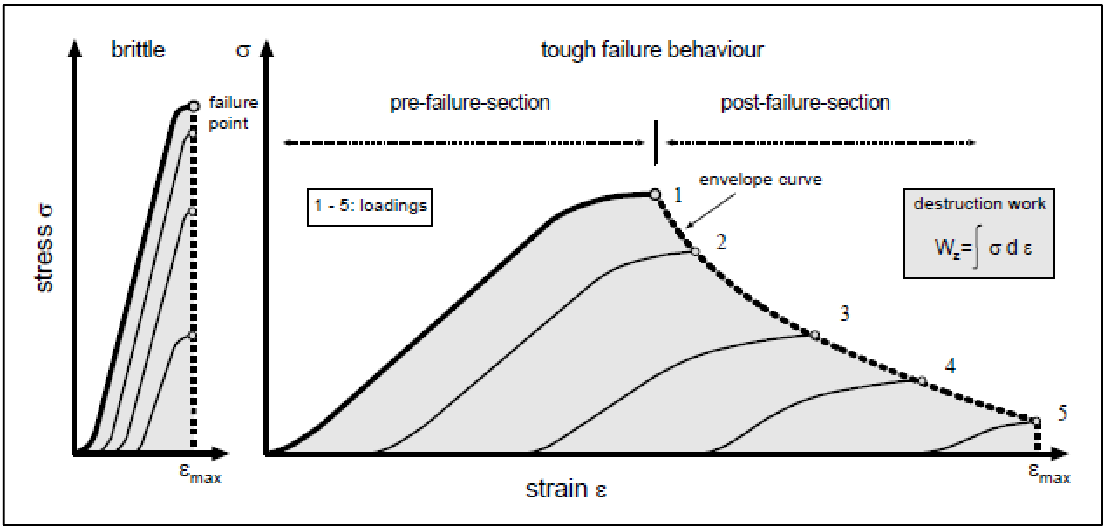

Figure 2.10 : Destruction work under the stress strain graph [10].

2.5.3 Specific energy defined by Bilgin et al. (2006)

Bilgin et al. (2006) made a research with real life conical cutters using 22 different rock types having uniaxial compressive strengths of 10 to 170 MPa to find which mechanical rock properties affecting the specific energy. The formulations are given in Equations 2.7 to 2.11 [5].

$$SE_{opt}=0.083\ \sigma_C+1.424 \quad \textbf{(2.7)}$$

$$SE_{opt}=1.259\ \sigma_t+1.424 \quad \textbf{(2.8)}$$

$$SE_{opt}=0.3912\ e^{0.058\ SHRV} \quad \textbf{(2.9)}$$

$$SE_{opt}=0.984\ E_{dyn}^{0.542} \quad \textbf{(2.10)}$$

$$SE_{opt}=2.424\ E_{sta}^{0.414} \quad \textbf{(2.11)}$$

2.5.4 Specific energy defined by Balci et al. (2004)

Balci et al (2004) defined optimum specific energy derived from full scale cutting tests using conical picks and correlated with the rock properties. In this study depth of cuts set for the experiments are 5 and 9 mm. The formulations are given below in Equations 2.12 to 2.23 [16].

For depth of cut 5 mm;

$$SE_{opt}=0.37*\ \sigma_C^{0.86} \quad \textbf{(2.12)}$$

$$SE_{opt}=3.36*\ \sigma_T^{0.72} \quad \textbf{(2.13)}$$

$$SE_{opt}=3.55*\ E_{sta}^{0.71} \quad \textbf{(2.14)}$$

$$SE_{opt}=3.55*\ E_{dyn}^{0.59} \quad \textbf{(2.15)}$$

$$SE_{opt}=0.77*\ e^{0.59\ SHRV} \quad \textbf{(2.16)}$$

$$SE_{opt}=1.16*\ (\sigma_C*\sigma_T)^{0.40} \quad \textbf{(2.17)}$$

For depth of cut 9 mm;

$$SE_{opt}=0.41*\ \sigma_C^{0.67} \quad \textbf{(2.18)}$$

$$SE_{opt}=2.19*\ \sigma_T^{0.62} \quad \textbf{(2.19)}$$

$$SE_{opt}=2.68*\ E_{sta}^{0.40} \quad \textbf{(2.20)}$$

$$SE_{opt}=1.55*\ E_{dyn}^{0.50} \quad \textbf{(2.21)}$$

$$SE_{opt}=0.46*\ e^{0.06\ SHRV} \quad \textbf{(2.22)}$$

$$SE_{opt}=0.92*\ (\sigma_C*\sigma_T)^{0.34} \quad \textbf{(2.23)}$$

2.5.5 Specific energy defined by Tumac et al. (2007)

Tumac et al. (2007) defined optimum specific energy based on shore hardness test (SH1, SH2 and deformation coefficient (K)). The formulations are given in Equations 2.24 to 2.26 [17].

$$SE_{opt}=0.23*SH1 - 2.01 \quad \textbf{(2.24)}$$

$$SE_{opt}=0.17*SH2 - 3.95 \quad \textbf{(2.25)}$$

$$SE_{opt}=243.01*\ K^{-0.92} \quad \textbf{(2.26)}$$

2.6 Laboratory Experiments Used in Mechanized Excavation

There are currently two main laboratory experiments named full scale linear cutting machine (LCM) and small scale core cutting machine (SLCM) in ITU laboratories. They are widely accepted for the selection of mechanized machineries.

2.6.1 Full scale linear cutting machine

The LCM is using for rock cutting tests with real cutters to measure cutting forces. It can host 1.0 x 0.7 x 0.7 m rock samples. There are some adjustable parameters like depth of cut and spacing. The forces acting on a cutter is measured by a data acquisition system located in the machinery. This system can record normal, cutting and side forces [18]. The LCM can be seen in Figure 2.11.

Specific energy and instantaneous cutting rate can be found from the following formulations given below in Equations 2.27 and 2.28. According to Rostami et al (1994) energy transfer ratio, k is 0.8 - 0.9 for TBMs and 0.4 - 0.6 for roadheaders [19].

$$SE=\frac{FC}{Q} \quad \textbf{(2.27)}$$

$$ICR = k^* \frac{P}{SE} \quad \textbf{(2.28)}$$

Where;

- SE= Specific Energy
- FC= Cutting Force
- Q= Yield per unit length of cut
- ICR= Instantaneous Cutting Rate
- P= Power
- k= energy transfer ratio

Figure 2.11 : LCM located at Istanbul Technical University.

2.6.2 Small scale core cutting machine

Small scale core cutting machine (SLCM) is a shaping machine used for understand cuttability characteristics of the rock samples. The machine can host a core samples or rectangular blocks in the dimensions of 20 x 10 x 10 cm. The sample has been cut by a tungsten carbide pick having tool width 12.7 mm, clearance angle of 5˚ and rake angle of -5˚. Forces acting on the tool and specific energy can be calculated after the test [20]. In Figure 2.12 a photo of SLCM is given.

Figure 2.12 : SLCM located at ITU.

2.7 Roadheader Performance Prediction

Roadheaders are widely used in mining and tunneling projects in soft to hard rocks. There are mainly two types of roadheaders which are transverse and axial. These types can be seen in Figures 2.13. Due to challenges in the industry there are various performance prediction models have been developed. The classification of these machines according to their weight summarized in Table 2.4. Some advantages of roadheaders can be classified as follows [11].

- Roadheaders are partial face machines which provide selective mining
- Cutterhead inspection can be done easily due to accessibility of the face
- Due to their low weight, moving is easier than other mechanical miners
- Relatively they are cheaper than other methods
- Roadheaders can be used in excavation of any kind of opening
- They can work at 15 degrees gradient and sharp turnings are easier than the other types.

Table 2.4 : Classification of Roadheaders [11].

Roadheader Class	Roadheader Weight (ton)	Cutterhead Power (kW)	Max. Cross Section Area (m^2)	Max. UCS (MPa)
Light	8-40	50-170	25	60-80
Medium	40-70	160-230	30	80-100
Heavy	70-110	250-300	40	100-120
Extra Heavy	>110	350-400	45	120-140

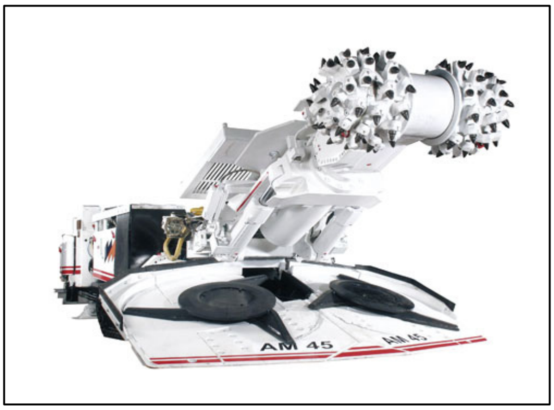

Figure 2.13 : Axial type (up) and transverse type (down) roadheaders.

2.7.1 Performance prediction model stated by McFeat Smith and Fowell (1979)

McFeat Smith and Fowell (1979) emphasized charts for medium and heavy weight roadheader performance rely on SLCM experiments. These charts and the nomogram developed can be found in table 2.5, 2.6 and Figure 2.14 respectively [21].

Table 2.5 : Performance Predicton for light weight roadheaders.

Laboratory Specific Energy (MJ/m^3)	Cutting Performance Light Weight Machines
20	Machines can only cut these rocks at economic rates if they occur in thin bands (less than 0.3m). Short term replacement of machine components may be required due to substantial cutting vibrations. Specialist advice should be obtained and modifications for cutting hard rock may help.
15	Poor cutting performance. Excavation may be have to be assisted by blasting for rocks at top en of scale. Shattered inserts should be expected. Regular replacement of slightly worn picks will improve energy requirements and reduce component wear. Point attack tools may be more beneficial and low speed cutting motors and side stells will improve stability. Upper limit of weight stability.
12	Moderate poor cutting performance. Shattered pick inserts can still be expected, although less common. For abrasive rocks picks must be inspected frequently as sharp picks will increase performance.
8	Moderate to good cutting performance with very low wear of machine components. Picks must be inspected and changed regularly, particularly when excavating abrasive rocks. Drag picks well adapted to these rocks if face geometry suitable.
5	Machines well suited to these rocks . Good adcance rates can be expected. Mudstones in lower end of category may be ripped rather than cut very high cutting rates can be achieved. Regular inspection and replacement of worn picks still advantageous.

Table 2.6 : Performance Predicion for medium weight roadheaders.

Laboratory Specific Energy (MJ/m^3)	Cutting Performance Medium Weight Machines
32	Machines can cut only thin bands of these rocks and tool wear will be exceptionally high. Short term damage to machine can be expected. Machines must be capable of adaption for hard rock cutting conditions.
25	Poor cutting performance particularly in massive faces. Pick wear critical and cutting will improve by frequent inspection. Machines with modifications for cutting hard rock will reduce risk of failure. Point attack picks are essential.
17	Moderate cutting performance too good at bottom of category. Picks should be inspected and changed regularly particularly when excavating abrasive rocks. Consistent cutting rates can be programmed for.
8	Machines well suited to these rocks and rapid advance rates can be anticipated. Many mudstones in this category can be ripped rather than cut and progress rates will be enhanced by a large capacity mucking system. Regular inspeciton and replacement of tools still advantageous.

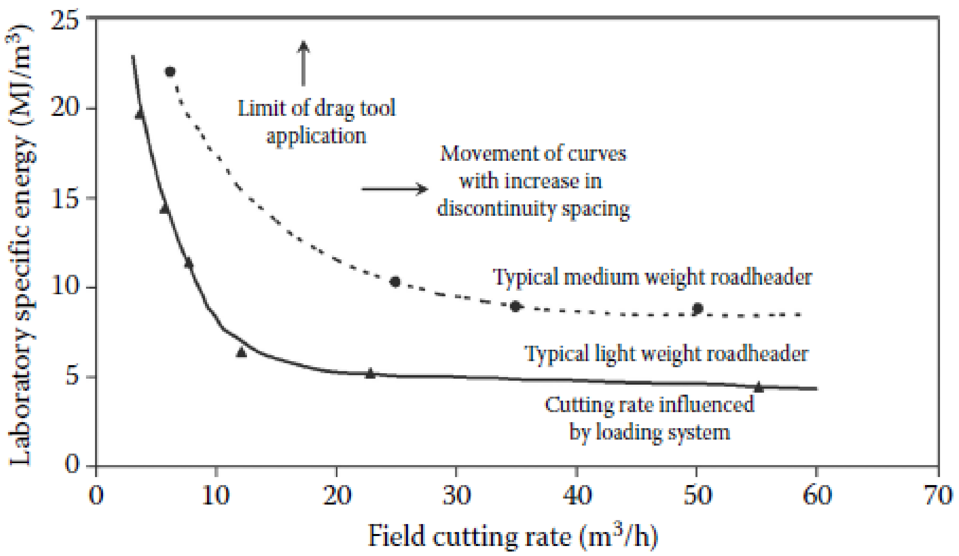

Figure 2.14 : Nomogram developed for roadheader performance.

2.7.2 Performance prediction model stated by Gehring (1989)

Gehring (1989) stated a model 230 kW axial and 250 kW transverse roadheaders related with the uniaxial compressive strength (UCS). The formulations are given in Equations of 2.29 and 2.30 [22].

$$\mathrm{ICR} = \frac{719}{\mathrm{UCS}^{0.78}} \text{ for transverse type} \tag{2.29}$$

$$\mathrm{ICR} = \frac{1739}{\mathrm{UCS}^{1.13}} \text{ for axial type} \tag{2.30}$$

2.7.3 Performance prediction model stated by Bilgin et al. (1990)

Bilgin et al. (1990) pointed out a model based on rock mass cuttability index which uses rock quality designation (RQD) and UCS for roadheaders. In order to predict instanteous cutting rate, RMCI and cutting power of the machinery are used. The relations are given in Equations 2.31 and 2.32 [23].

$$\mathrm{RMCI}=\mathrm{UCS}*\left(\frac{\mathrm{RQD}}{100}\right)^{2/3} \tag{2.31}$$

$$\mathrm{ICR}=0.28*\mathrm{P}*(0.974)^{\mathrm{RMCI}} \tag{2.32}$$

2.7.4 Performance prediction model stated by Rostami et al. (1994)

Rostami et al. (1994) showed that instantaneous cutting rate can be found from ratio of installed power to optimum spesific energy obtained from rock cutting tests. They also stated that k factor is between 0.45 and 0.55 for roadheaders. The model is given in Equation 2.33 [24].

$$ICR=k*\frac{P}{SE_{opt}} \quad \textbf{(2.33)}$$

2.7.5 Performace prediction model stated by Copur et al. (1998)

Copur et al. (1998) defined an empirical model that uses roadheader penetration index related to UCS, roadheader weight (W), and cutterhead power. This model mainly developed for evaporatic rock types excavated by transverse type roadheaders. The relationships are given in Equations 2.34 and 2.35 [25].

$$RPI=P*\frac{W}{UCS} \quad \textbf{(2.34)}$$

$$ICR=27.511*e^{0.0023*RPI} \quad \textbf{(2.35)}$$

2.7.6 Performance prediction model stated by Thuro and Plininger (1999)

Thuro and Plininger (1999) stated a model based on UCS for 132 kW roadheader, even the correlation coefficent (r^2=0.62) for this work is low according to performance prediction. They also stated a relationship which uses destruction work with roadheader performance, in this model correlation coeffient is higher than the other one (r^2=0.89) The models are given in Equations 2.36 and 2.37 [15, 26].

$$ICR=75.7 - 14.3* \ln (UCS) \quad \textbf{(2.36)}$$

$$ICR=107.6 - 19.5* \ln (W_z) \quad \textbf{(2.37)}$$

2.7.7 Performance prediction model stated by Balci et al. (2004)

Balci et al. (2004) developed a model predicting optimum specific energy using 23 rock samples taken from different mine sites in Turkey. Later, they stated following Equations 2.38 and 2.39 can be used in roadheader performance prediction for 5 and 9 mm depth of cut [16].

$$\text{For d=5mm, ICR} = 0.8 * \frac{P}{0.37*UCS^{0.86}} \quad \textbf{(2.38)}$$

$$\text{For d=9mm, ICR} = 0.8 * \frac{P}{0.41*UCS^{0.67}} \quad \textbf{(2.39)}$$

2.7.8 Performance prediction model stated by Tumac et al. (2007)

Tumac et al. (2007) made a research on roadheader performance prediction based on Shore Hardness (SH1, SH2) and deformation coefficent. After reading the SH1 value 15 to 20 more readings done for SH2. Deformation coefficent calculated from their relative error. The formulations in this study are given in Equations 2.40 – 2.42 [17].

$$ICR = 81.21 * SH1^{-0.78} \quad \textbf{(2.40)}$$

$$ICR = 258.43 * SH2^{-0.982} \quad \textbf{(2.41)}$$

$$ICR = 0.06 * K + 1.08 \quad \textbf{(2.42)}$$

2.7.9 Performance prediction model stated by Ocak et al. (2007)

Ocak et al. (2007) made a research on roadheaders used in Kadikoy-Kartal metro tunnels. The model is based on uniaxial compressive strength and net cutting rate. Formulation obtained from this research is given in Equation 2.43 [27].

$$ICR = 510588 * UCS^{-2.1799} \quad \textbf{(2.43)}$$

2.8 Optimum Spacing for Picks for Effective Cutting

Specific energy is inversely proportional to the depth of cut. There is an optimum ratio for spacing to depth of cut which gives the lowest specific energy. In Figure 2.15 the spacing to depth of cut ratio and its effect on specific energy can be seen. Firstly, when the spacing is too close the rock is over crushed. Secondly, when spacing has its optimum value chipping will occur. Lastly, when spacing is too high coring will occur. Besides, Bilgin et al (2006) stated that optimum spacing to depth of cut ratio is around 1-5 for pick cutters [5].

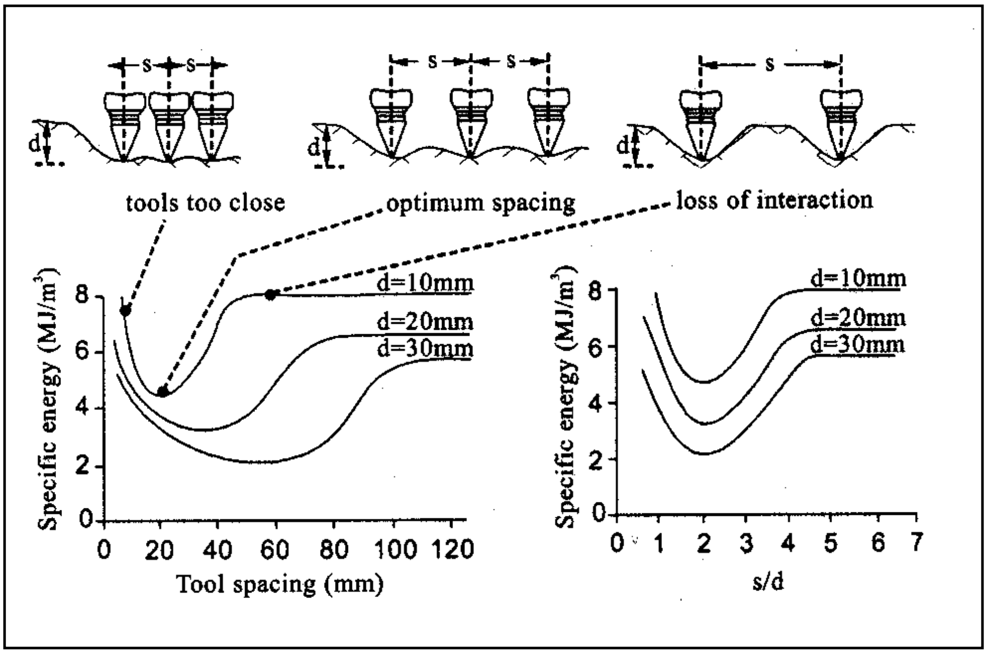

Figure 2.15 : Spacing to depth of cut ratio and its effect on specific energy.

2.9 Bit Wear Classifications and Reseach Done

According to Thuro and Plinninger (1998) there are 7 types of bit wear. They made reseach on four diffrent tunnels excavated by roadheaders and classify the bit wears given below [28].

- Tip wear
- Asymmetrical wear
- Steel wear
- Tip damage
- Total tip removal
- Total wear out
- Steel shank damage

Bilgin et al. (2005) also classify bit wear in Kucuksu tunnel and they found there are mainly four types of cutter wear. These are given below. In Figure 2.16 cutter wear classification can be found [29].

- Symmetrical wear
- Asymmetrical wear
- Breakage of the tungsten carbide tip
- Breakage of the tip shaft

Figure 2.16 : Cutter wear classification in Kucuksu Tunnel.

3. EXPERIMENTAL STUDIES

3.1 Physical and Mechanical Properties of Rocks

In this study six different rock types are subjected to the experiments for concical cutter 2 and 9 rocks are used for conical cutter 1 and chisel pick. These are Beige Marble, Sandstone, Limestone, Kufeki Limestone and Travertine, which is located in the rock cutting laboratory for scientific research. Travertine (DT), Finike Limra and Kavaklıdere Beyaz were taken from project 112 M 860. Green Sandstone was taken from Amasya - Suluova basin in order to make research on roadheader performance.

Experiments performed on these rocks to understand their mechanical and physical behavior are uniaxial compressive strength, Brazilian tensile strength, natural unit weight, static elasticity modulus, P and S wave velocities, Schimdt hammer and Shore hardness. All experiments done by ISRM or ASTM standarts referenced to Ulusay et al (2011) [30].

3.1.1 Specimen preparation

Samples taken from the field firstly cut by saw given in Figure 3.1. After, specimens were used either in rock cutting tests or rock mechanics experiments. Also, for rock mechanics experiments core samples taken from rock samples.

Figure 3.1 : Saw used in preparation of rock samples.

3.1.2 Natural unit weight

Density of the rocks are determined by measuring their weight with electronic precision balance and their volume are calculated by using a caliper. After that natural unit weight of the samples determined by Equation 3.1 given below.

$$D=\frac{m}{V} \tag{3.1}$$

Where;

D= Density of the rock

m= mass of the rock

V= volume of the rock

3.1.3 Uniaxial compressive strength

This experiment is used to understand compressive strength of rocks. NX cores (54.7 mm diameter) having their length to diameter ratio 2.5 to 3 are used in this experiment. The loading rate of the machine was 0.5 and 1 kN per second. Compressive strength at the failure point can be determined from following equation.

$$\sigma_c = \frac{F}{A} \tag{3.2}$$

Where;

- σ_c = Compressive strength of the specimen
- $F =$ Force measured at failure point
- $A =$ Area of the cylindrical specimen

3.1.4 Brazilian (indirect) tensile strength

This experiment used to found out tensile strength of rocks. NX cores which has length to diameter ratio around 0.5 to 1 are used while performing the experiments. Loading rate was 0.2 kN/sec. Tensile strength of the rocks can be found from the equation given below. In Figure 3.2 the machine is given for the experiments of UCS and BTS.

Figure 3.2 : Hydraulic press used for the UCS and BTS experiment.

$$\sigma_T = \frac{2*F}{\Pi*D*t} \quad \textbf{(3.3)}$$

Where;

- σ_T= tensile strength of the rock
- F = force measured at the failure point
- D = Diameter of the sample
- t = thickness of the sample

3.1.5 Determination of p and s waves

This experiment is used in determination of pressure (P) and shear (S) waves on a rock sample. These waves are explained in detail in figure 3.3. With this values dynamic young modulus and dynamic poisons' ratio can be calculated. Dynamic values usually cannot match with the static values obtained from laboratory experiments and generally they are higher than static ones. In figure 3.4 the machine used in this experiment is given. Experiments are performed on the samples that are used in uniaxial compressive strength tests. Calculations done according to Equations 3.3-3.6 given below.

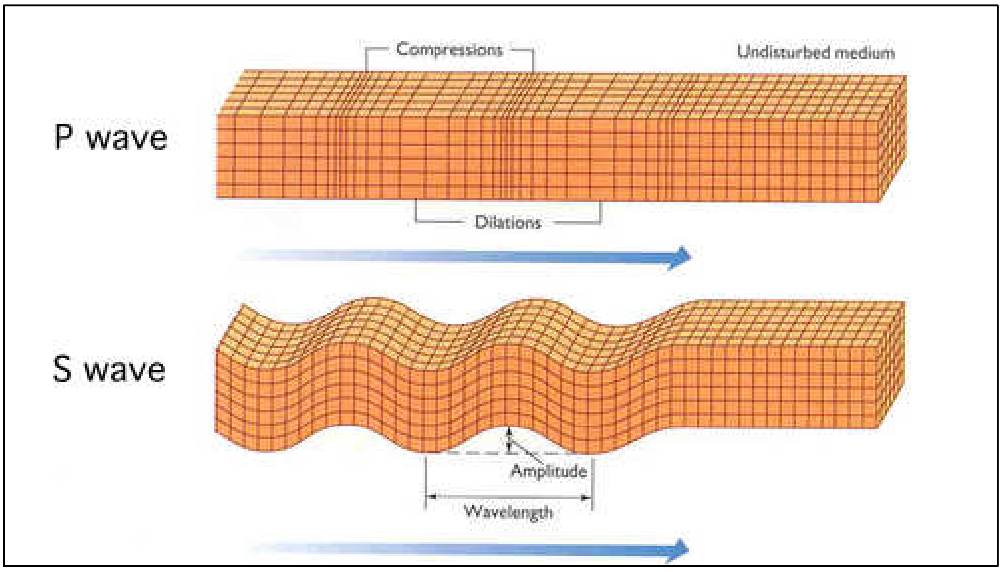

Figure 3.3 : Explanition of P and S wave

Figure 3.4 : Machine used in determination of P and S waves.

$$V_p=\frac{L}{t_p} \tag{3.4}$$

$$V_s=\frac{L}{t_s} \tag{3.5}$$

$$E_{dyn}=p*V_s^2\,\frac{3V_p^2-4V_s^2}{V_p^2-V_s^2} \tag{3.6}$$

$$v_{dyn} = \frac{V_p^2 - 2V_s^2}{2(V_p^2 - V_s^2)} \quad \textbf{(3.7)}$$

Where;

- E_{dyn}= dynamic elasticity modulus
- p= density of rock sample
- V_p= pressure wave velocity (m/s)
- V_s= shear wave velocity (m/s)
- L = Length of the specimen (mm)
- t_p = P wave propagation time (ms)
- t_s =S wave propagation time (ms)

3.1.6 Determination of elasticity modulus and poisson's ratio

This experiment procedure is used in plotting of stress strain graphs of a given rock in uniaxial compressive condition. Axial and diametrical deformations are measured while performing the experiment and calculations done by Equations given below.

$$\varepsilon_a = \frac{\Delta L}{l_0} \quad \textbf{(3.8)}$$

$$\varepsilon_d = \frac{\Delta D}{D_0} \quad \textbf{(3.9)}$$

$$E = \frac{\Delta \sigma}{\Delta \varepsilon_0} \quad \textbf{(3.10)}$$

$$v = \varepsilon_d / -\varepsilon_a \quad \textbf{(3.11)}$$

Where;

- E= static elasticity modulus
- v= static poison's ratio
- ε_a = axial deformation
- ΔL = change in length of the specimen
- l_0= initial height of the specimen
- ε_d= diametrical deformation
- ΔD= change in the diameter of the specimen
- D_0= initial diameter of the specimen
- σ= stress

3.1.7 Schmidt hammer

In this experiment Schmidt hammer rebound value determined by using an L-9 type Schmidt Hammer which is given in Figure 3.5. First, hammer is calibrated using an anvil, afterwards 10 at least readings are taken from the block samples.

Figure 3.5 : L-9 type Schmidt Hammer used in the experiment.

3.1.8 Shore scleroscope

In this experiment C-2 type shore scleroscope equipment is used to find out shore hardness value of the rocks. Experiments performed on a flat surface of core or block samples. 20 readings are taken from each sample and average of them used as shore hardness value. In Figure 3.6 C-2 type equipment is given.

Figure 3.6 : C-2 type shore scleroscope.

3.1.9 Results of rock mechanics experiments

Results of rock mechanics experiments are given in Table 3.1.

Table 3.1 : Rock Mechanics Experiment Results

Sample	Beige Marble	Limestone	Travertine	Sandstone	K. Limestone	G. Sandstone	Travertine (DT)	Finike Limra	K. Beyaz
Density ±sd(g/cm3)	2.7 ± 0.01	2.68 ± 0.01	1.92 ± 0.06	2.8 ±0.01	2.16 ± 0.02	2.5 ± 0.03	2.14	2.22	2.67
UCS ±sd (MPa)	160.7± 10	70.2 ± 12.5	9.1 ± 1	120.6 ± 21.5	15.6 ± 3.3	11.26	11	52.6	79.3
BTS ±sd(MPa)	7.82 ± 1.82	7.73 ± 1.33	3.17 ± 0.26	11.94 ± 1.32	1.14 ± 0.16	1.5	4.8	4.4	6.4
Esta±sd(GPa)	22.61 ± 8.55	14.93 ± 3.12	3.96 ± 2.39	21.79 ± 9.51	4.87 ± 0.84	1.8	3.2	18.8	28.1
Edyn ±sd(GPa)	85.46 ± 20.81	71.16 ± 6.52	24.57 ± 2.84	97.30 ± 6.72	21.64 ± 2.4	16.7	37.2	37	61.8
νdyn	0.35	0.34	0.31	0.33	0.35	0.33	0.24	0.21	0.22
νsta	-	-	-	-	-	0.38	0.22	0.26	0.27
Schmidt H.	63.3	56.7	41.4	61.8	20.3	26.7	40.1	39	65.5
Shore H.	64.25	53.95	51.2	64.1	16.55	31.75	26.6	27.9	58

3.2 Rock Cutting Tests

A PLCM is developed for the measurement of orthogonal forces acting on a cutter. In this thesis two conical picks and one chisel pick used for rock cutting tests. These cutters are well defined in the next section. After measuring the forces with a data acquisition system specific energy calculated as given below.

$$SE=\frac{FC}{Q} \qquad \textbf{(3.12)}$$

Cutting force and normal force are related with the torque and thrust capabilities of a mechanical excavator. Specific energy is also connected with the net cutting rates. This can be defined as optimum specific energy means higher production rates [31].

3.2.1 Portable linear cutting machine test equipment and procedures

Within the project TUBITAK 112M859 a PLCM is designed. The machine can accomadate block samples of 10*10*15 cm with a clamp or concreted in a metal box. In this new design all mini scale cutters can be used in the experiments (discs, conical and chisel cutters). The cutter is attached to the dynamometer with a tool holder. Experiments are performed at 3 cm/s cutting speed and forces are measured with a data logger system. Before performing the experiments surface of the rock trimmed as flat with the cutters. All experiments are replicated 3 or 4 times in order to minimizing the possiblity of making mistake. The main advantagse of this experiment procedure are that its quite easy and fast to obtain results than the real life linear cutting machine. It is less time consuming and do not need manual labour. On the other hand, the disadvantages are experiments can not be done with real life cutters and usage of big blocks that represent the rock mass is not possible. In Figure 3.7 a photo of the machine can be found.

Figure 3.7 : PLCM designed within the project.

First of all specimens are prepared dimensions of 10 x 10 x 15 cm and concreted in metal cases. After the curing of concrete, specimens are subjected to the rock cutting experiments. In the figure 3.8 this process can be seen.

Figure 3.8 : Specimen preperation for rock cutting tests.

Data acquisition done by using a 4 leg data logger. In this system data acquisition rate and cutting speed are 1000 Hz and 3 cm/s respectively. In figure 3.9 acquisition equipment can be found. In Figure 3.10 an example of cutter forces obtained from experiments are given.

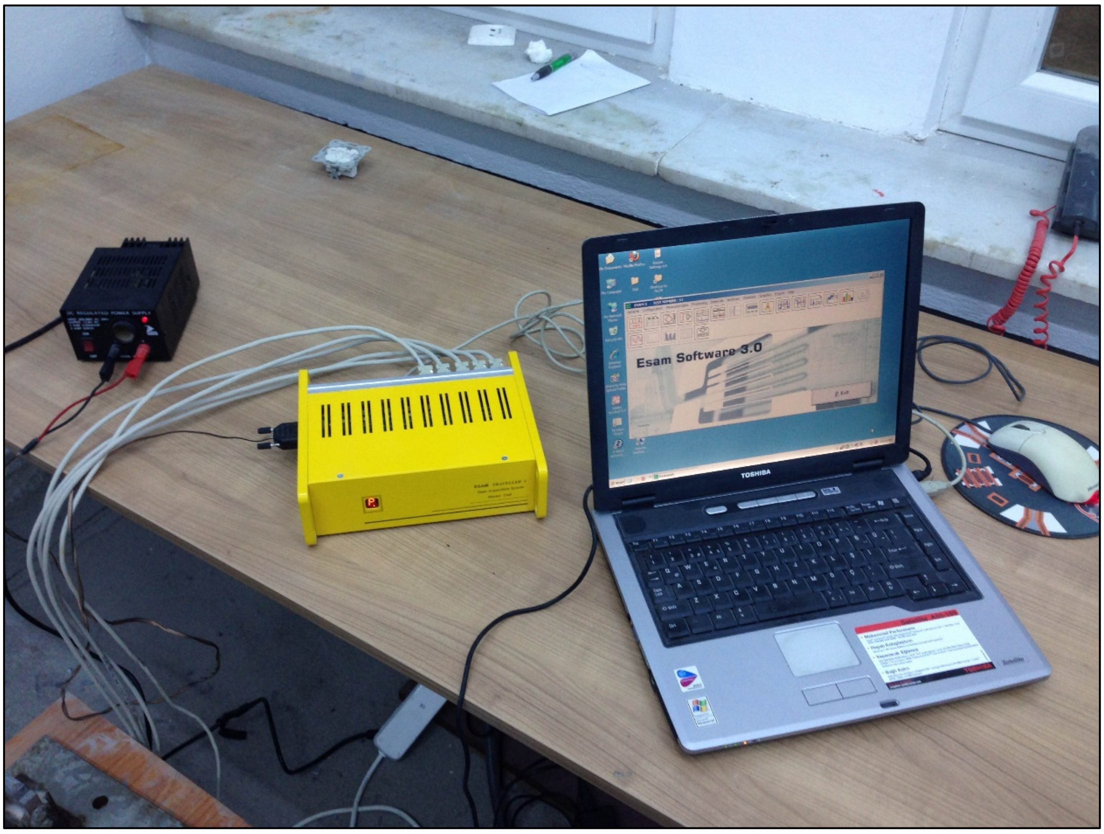

Figure 3.9 : Data acquisition system.

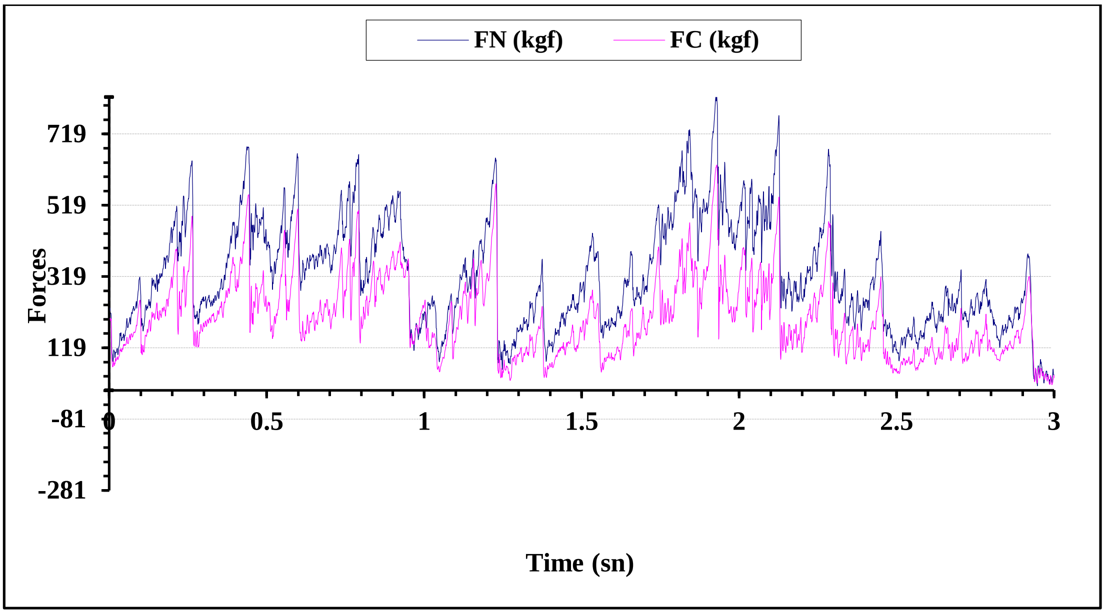

Figure 3.10 : An example of cutter forces obtained from the experiments.

3 different cutters are used in this study which named as conical cutter 1, conical cutter 2, and chisel cutter. Conical cutter 1 has a 60° tip angle, 45° angle of attack and 15° clearance angle. Conical cutter 2 has its tip, attack and clearance angles 85, 45 and 2.5° degrees respectively. Besides, chisel cutter has 12.7 mm wide, -5° of rake angle and 5° of clearance angle. These cutters' photographic views can be found in Figures 3.11 to 3.13.

Figure 3.11 : Photographic view of conical cutter 1.

Figure 3.12 : Photographic view of conical cutter 2.

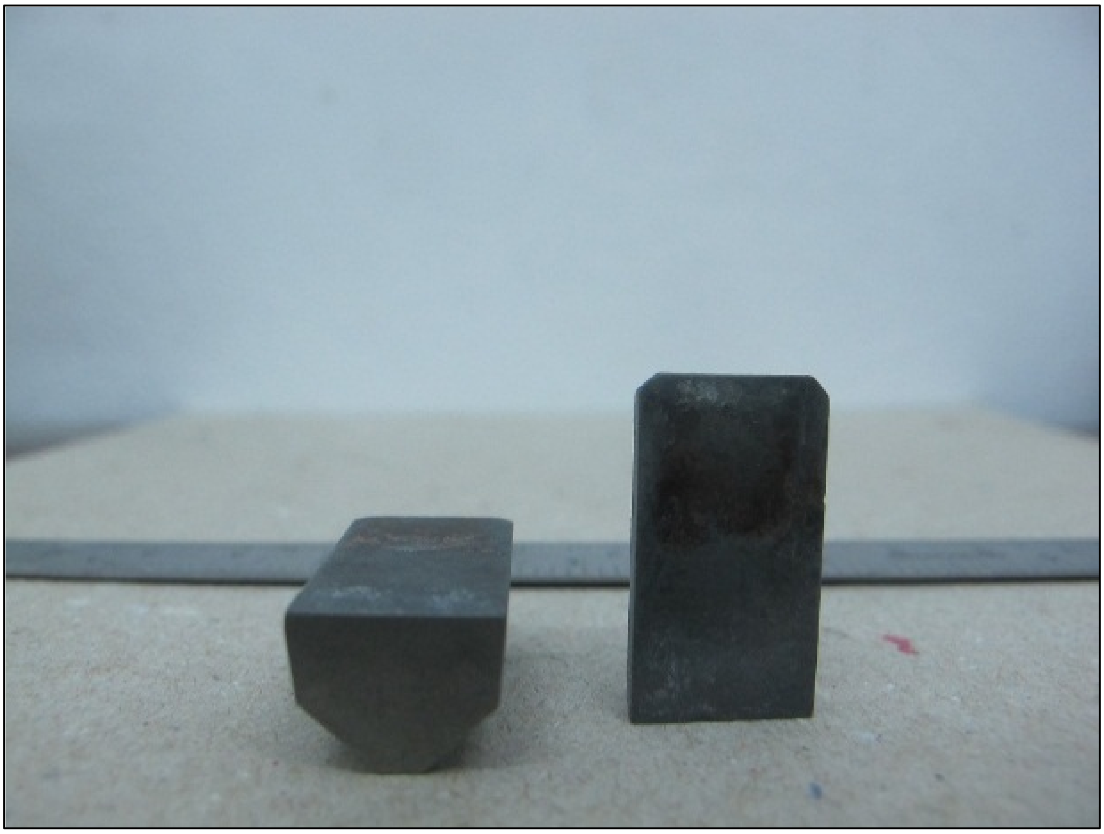

Figure 3.13 : Photographic view of chisel cutter

3.2.2 Portable linear cutting test parameters

Experiments performed on the various rock types which are beige marble, limestone, sandstone, travertine and kufeki limestone to understand the relationships conical and chisel cutters used. Also green sandstone is used for field verification of PLCM developed. Additionaly, extra three rock types were used with chisel and conical cutter 1 and subjected to the rock cutting experiments within the project 112 M 860 which are Travertine (DT), Finike Limra and Kavaklıdere Beyaz.

First of all, rock types from 112 M 860 are tested with same depth of cuts using two cutters. After, 6 specimens are tested with chisel cutter with 3 different depth of cuts which are 2.5, 3.5 and 5 mm. Then, with conical cutter 1 only 5 mm depth of cut used to develop an index value. 3 different spacings are used in this cutter to find the optimum spacing to depth of cut ratio. Lastly, with conical cutter 2 only unrelieved and optimum spacing to depth of cut ratio performed which is obtained from conical cutter 1. Experiment program is given in Table 3.2.

Table 3.2 : Experiment program used in this study.

	Chisel		Conical 1		Conical 2	
Sample Name	s (mm)	d(mm)	s (mm)	d (mm)	s (mm)	d (mm)
Beige Marble	unr	1.5, 2.5, 3.5, 5	unr, 10,15,20	5	unr,15	5
Limestone	unr	2.5, 3.5, 5	unr, 10,15,20	5	unr,15	5
Travertine	unr	2.5, 3.5, 5	unr, 10,15,20	5	unr,15	5
Sandstone	unr	2.5, 3.5, 5	unr, 10,15,20	5	unr,15	5
K. Limestone	unr	2.5, 3.5, 5	unr, 10,15,20	5	unr,15,20	5
G. Sandstone	unr	2.5, 3.5, 5	unr, 10,15,20	5	unr,15	5
Travertine (DT)	unr	2, 3.5, 5	unr	2, 3.5, 5	-	-
Finike Limra	unr	2, 3.5, 5	unr	2, 3.5, 5	-	-
K. Beyaz	unr	2, 3.5, 5	unr	2, 3.5, 5	-	-

3.2.3 Results of orthogonal forces

While performing the experiments forces acting on the picks are measured by a data logger. Orthogonal forces, which are normal, cutting and side forces acting on a pick. The results of these forces can be found in Tables 3.3 - 3.6.

Table 3.3 : Results of orthogonal forces for chisel cutter.

Sample Name	d (mm)	FN (kgf)	F'N (kgf)	FC (kgf)	F'C (kgf)	FS (kgf)	F'S (kgf)
Beige Marble	1.5	311.8	728.2	195.7	522.1	4.8	25.7
	2.5	430.5	1137.7	288.3	993.1	4.9	32.9
	3.5	521.5	1500.8	388.3	1400.5	10.1	52.8
	5	870.4	2525.5	739.3	2707.1	17.1	97.5
Limestone	2.5	222.1	596.0	202.7	585.4	8.9	43.1
	3.5	239.7	837.7	234.0	936.8	12.8	47.8
	5	363.6	1102.6	384.1	1340.7	24.9	103.9
Travertine	2.5	126.1	373.4	117.8	392.6	3.4	19.3
	3.5	146.0	386.5	162.6	507.2	5.6	22.5
	5	245.5	628.6	300.7	808.3	3.2	32.9
Sandstone	2.5	562.8	1423.9	354.9	951.2	8.1	51.8
	3.5	663.6	1909.5	417.8	1445.6	9.2	74.2
	5	869.9	2414.7	594.9	2082.0	8.9	74.0
K. Limestone	2.5	45.1	109.9	27.4	98.2	3.1	12.3
	3.5	42.8	103.1	38.3	112.4	3.7	13.3
	5	68.4	163.9	66.2	186.0	4.4	17.2
G. Sandstone	2.5	55.8	110.9	43.5	110.4	3.9	12.1
	3.5	72.4	176.8	66.6	194.6	4.5	14.7
	5	117.1	314.3	138.8	331.9	6.5	21.8
Travertine (DT)	2	54.5	163.6	52.6	168.4	1.5	12.9
	3.5	108.5	293.9	124.3	399.2	3.6	20.2
	5	170.2	630.3	226.8	826.8	9.3	44.8
Finike Limra	2	63.5	250.9	62.1	234.1	1.4	16.0
	3.5	133.4	463.6	169.0	609.0	4.9	33.8
	5	270.6	949.4	387.9	1497.9	3.4	80.9
K. Beyaz	2	810.7	1451.9	402.9	714.7	13.8	47.5
	3.5	1124.8	2093.3	708.3	1477.4	15.7	76.4
	5	1450.7	2979.8	998.8	2484.7	17.0	86.8

Table 3.4 : Results of orthogonal forces for conical cutter 1 (112 M 860).

Sample Name	d (mm)	FN (kgf)	F'N (kgf)	FC (kgf)	F'C (kgf)	FS (kgf)	F'S (kgf)
Travertine (DT)	2	42.9	201.7	45.3	174.7	-1.0	31.6
	3.5	90.2	337.0	80.2	323.6	4.0	58.8
	5	108.3	520.9	122.0	508.2	16.7	150.4
Finike Limra	2	38.9	126.3	29.3	100.4	2.8	12.7
	3.5	60.2	186.3	53.7	184.3	4.3	26.8
	5	92.4	337.0	90.5	355.3	4.9	76.4
K. Beyaz	2	230.5	463.8	109.7	219.9	3.0	45.2
	3.5	381.4	819.1	190.0	457.4	10.5	118.2
	5	691.3	1705.3	374.7	1002.9	-18.5	132.6

Table 3.5 : Results of orthogonal forces for conical cutter 1.

Sample Name	s (mm)	FN (kgf)	F'N (kgf)	FC (kgf)	F'C (kgf)	FS (kgf)	F'S (kgf)
Beige Marble	unr	396.4	1088.4	250.9	795.2	61.5	348.2
	10	324.6	807.0	220.0	651.2	130.5	385.6
	15	296.6	991.0	187.1	745.4	-40.7	78.9
	20	489.0	1341.0	267.8	923.8	113.2	450.2
Limestone	unr	316.1	1014.6	238.5	850.1	-14.6	148.3
	10	219.0	625.7	157.4	484.9	-60.9	44.3
	15	273.9	770.2	190.5	605.8	-68.7	45.5
	20	459.5	1069.0	301.8	772.8	-69.5	61.0
Travertine	unr	209.3	747.3	180.7	691.1	-16.8	85.7
	10	183.3	611.0	152.9	529.9	-54.3	10.0
	15	214.4	751.1	166.2	661.6	-60.1	41.5
	20	144.2	433.9	181.6	507.8	58.4	209.3
Sandstone	unr	586.8	2029.0	412.9	1526.6	64.8	309.0
	10	431.0	1397.5	316.3	1042.3	176.1	506.6
	15	497.8	1456.7	376.5	1180.7	138.8	410.5
	20	706.0	1869.8	540.0	1442.3	-177.0	221.1
K. Limestone	unr	60.8	323.4	60.2	290.0	2.5	52.2
	10	33.7	157.6	47.4	172.1	21.3	70.1
	15	80.1	307.5	68.2	284.5	13.3	80.2
	20	19.9	76.7	25.8	77.8	-8.4	9.4
G. Sandstone	unr	73.4	183.0	61.4	184.6	2.1	36.5
	10	39.7	125.8	40.8	129.1	23.6	69.9
	15	44.7	138.4	38.3	133.1	21.3	68.2
	20	83.6	224.6	85.6	237.0	-19.8	16.5

Table 3.6 : Results of orthogonal forces for conical cutter 2.

Sample Name	s (mm)	FN (kgf)	F'N (kgf)	FC (kgf)	F'C (kgf)	FS (kgf)	F'S (kgf)
Beige Marble	unr	1322.0	3395.4	894.9	2584.9	83.1	607.5
	15	687.2	1560.6	503.0	1191.0	-203.7	19.0
Limestone	unr	927.8	2140.8	781.9	1904.2	160.4	617.2
	15	692.3	1458.4	538.5	1268.0	-231.8	62.1
Travertine	unr	316.8	1139.2	345.7	1192.1	51.3	261.6
	15	174.9	492.3	213.0	652.0	91.6	243.8
Sandstone	unr	1557.3	4267.0	1158.7	3020.5	-109.6	652.3
	15	789.2	2460.1	611.3	2040.8	-288.2	14.3
K. Limestone	unr	84.0	167.9	88.5	170.5	7.6	38.7
	15	43.6	112.1	55.4	129.0	-8.1	11.5
	20	60.7	142.6	60.9	147.9	-11.2	30.6
G. Sandstone	unr	184.3	504.5	157.3	477.8	22.2	127.5
	15	132.6	328.4	118.3	308.3	18.1	106.5

Experiments are performed with different depth of cut only with chisel cutter to understand data logger can withstand the forces acting on the pick or not. For different depth of cuts experiment performed on chisel cutter showed that cutter forces are increasing with increasing depth of cut. In the Figures 3.14 to 3.22 this relationship can be seen.

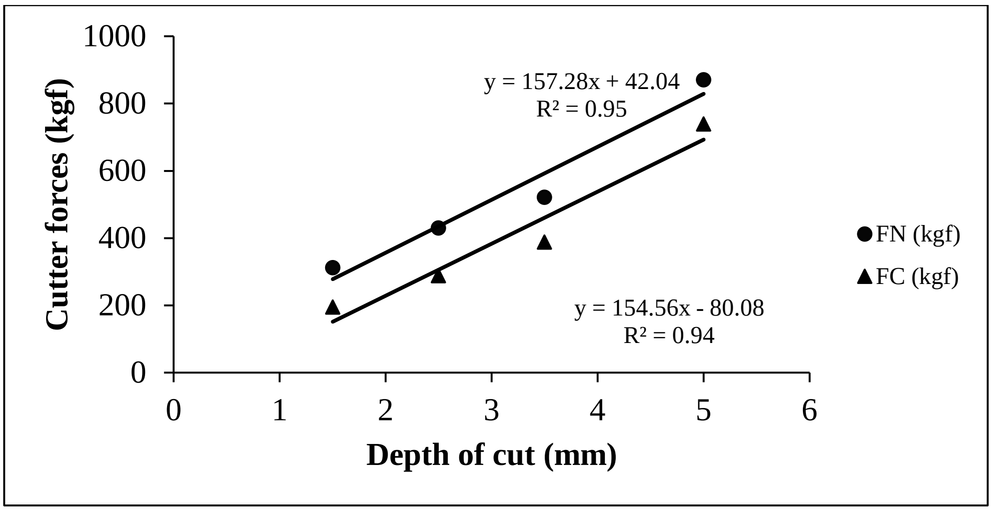

Figure 3.14 : Relationship between depth of cut and cutter forces for Beige Marble.

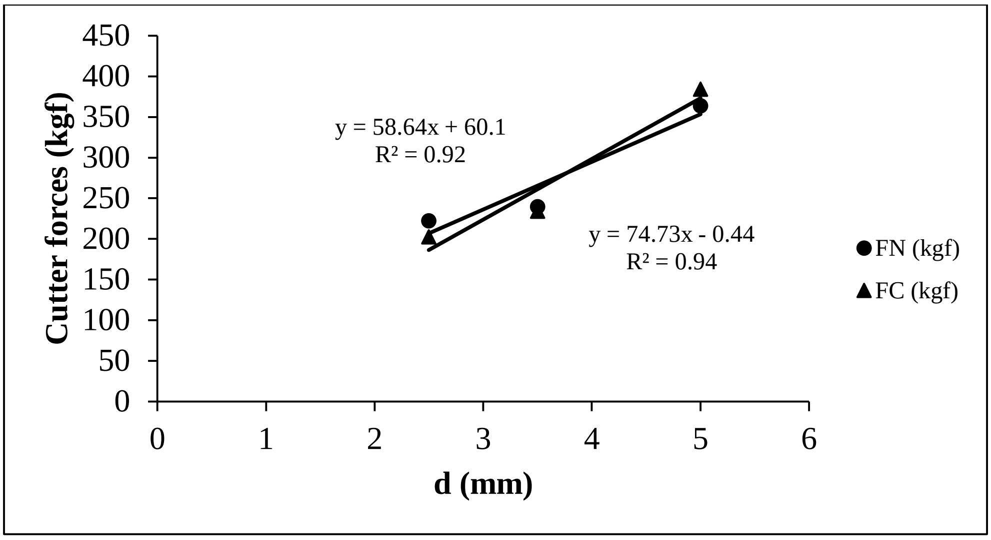

Figure 3.15 : Relationship between depth of cut and cutter forces for Limestone.

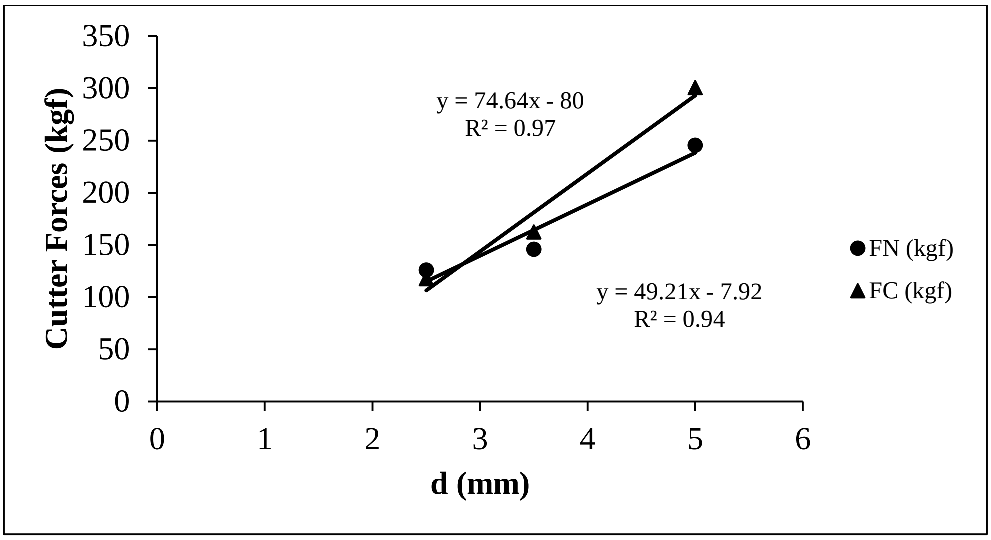

Figure 3.16 : Relationship between depth of cut and cutter forces for Travertine.

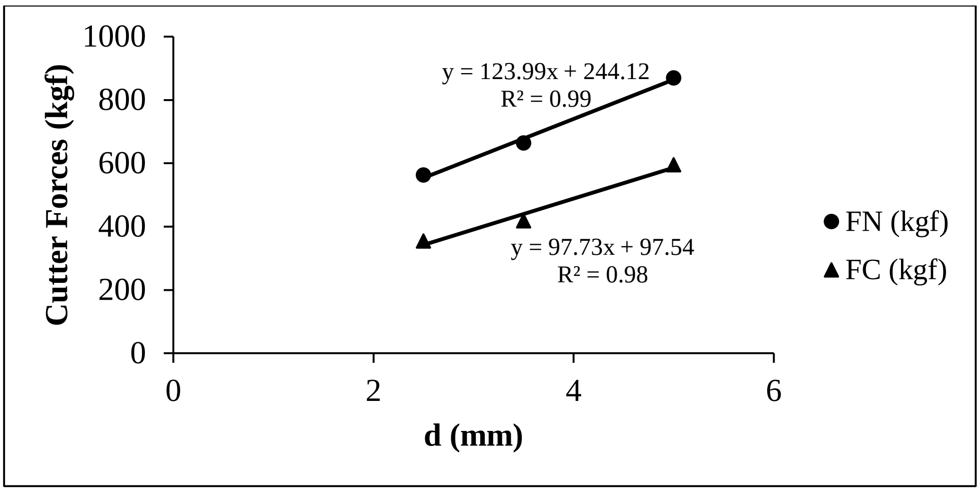

Figure 3.17 : Relationship between depth of cut and cutter forces for Sandstone.

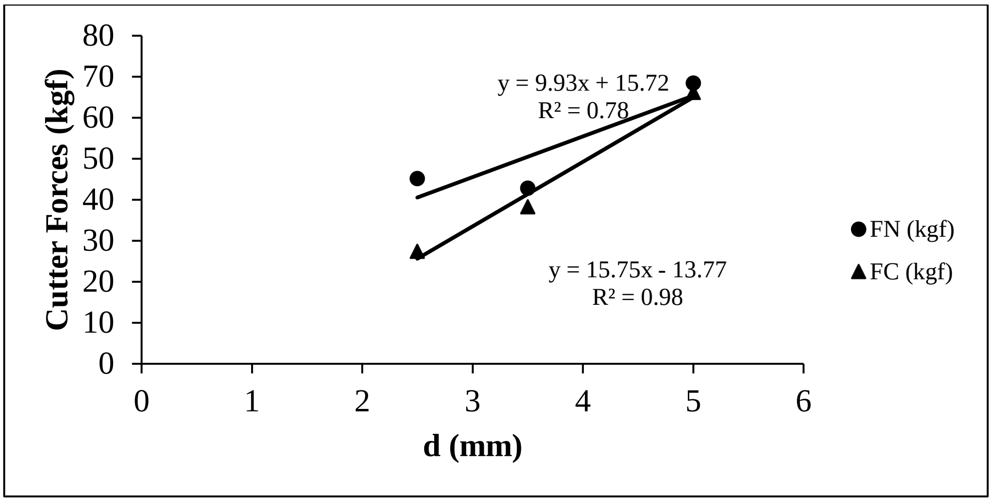

Figure 3.18 : Relationship between depth of cut and cutter forces for K. Limestone.

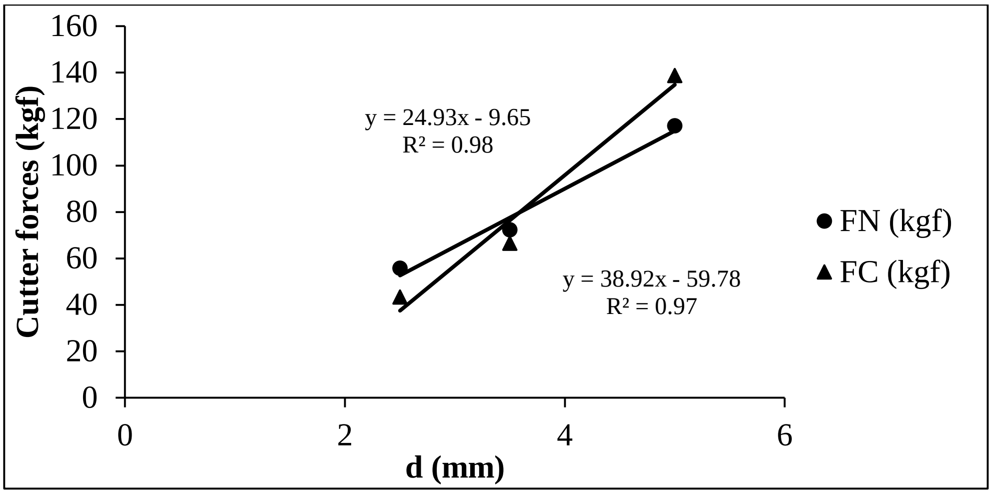

Figure 3.19 : Relationship between depth of cut and cutter forces for G. Sandstone.

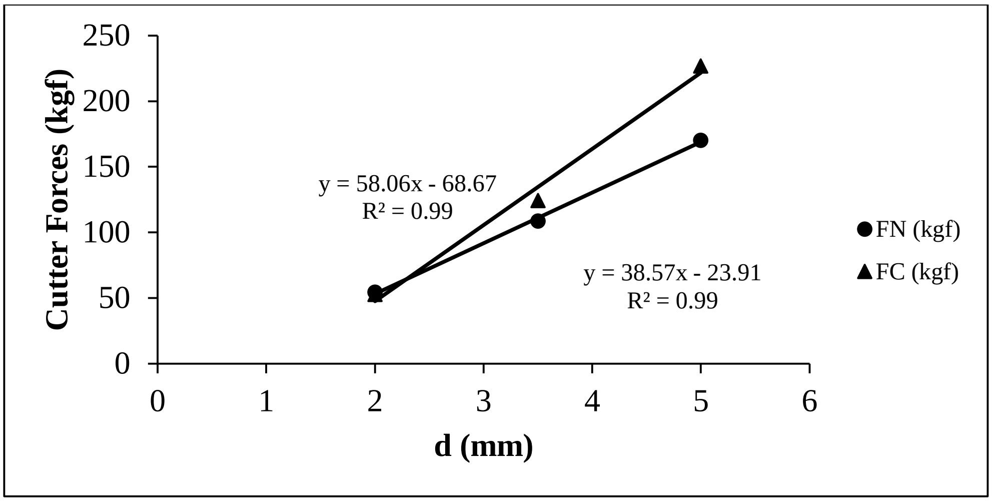

Figure 3.20 : Relationship between depth of cut and cutter forces forTravertine (DT)

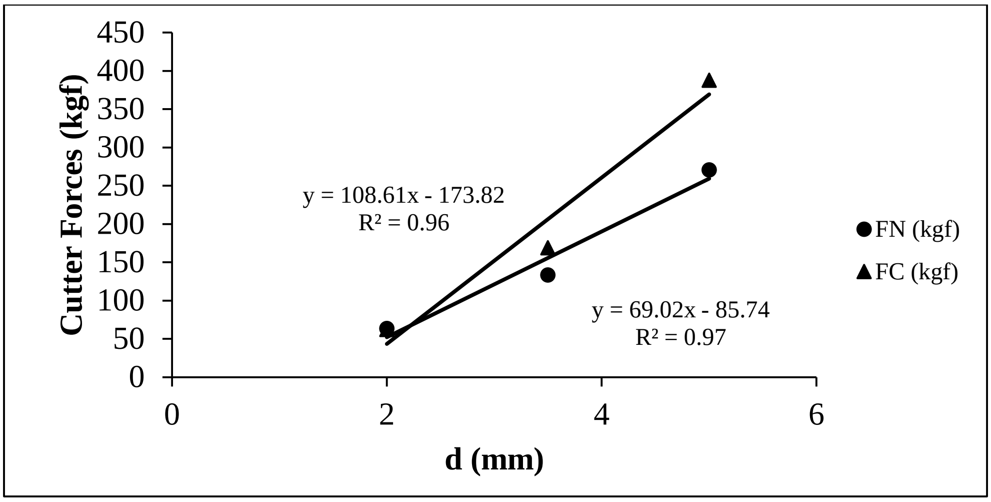

Figure 3.21 : Relationship between depth of cut and cutter forces for Finike Limra

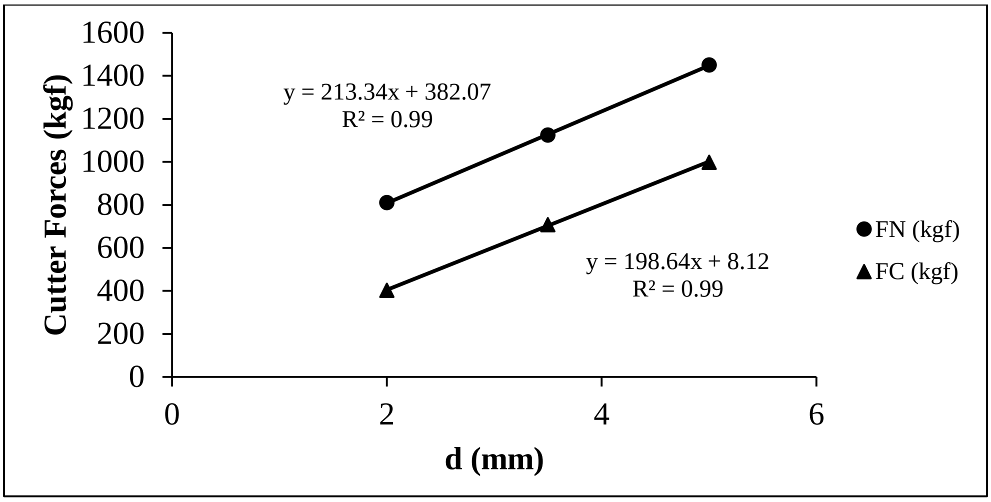

Figure 3.22 : Relationship between depth of cut and cutter forces for K. Beyaz

3.2.4 Results of specific energy

After performing the test, the muck obtained form the experiments are collected and for each test specific energies are calculated in terms of MJ/m^3 and kWh/m^3. The results can be found in Tables 3.7-3.10.

Table 3.7 : SE results for chisel cutter

Sample Name	d (mm)	SE (MJ/m^3)	SE (kWh/m^3)
Beige Marble	1.5	80.89	22.47
	2.5	72.94	20.26
	3.5	60.40	16.78
	5	58.44	16.23
Limestone	2.5	59.78	16.60
	3.5	41.47	11.52
	5	37.44	10.40
Travertine	2.5	27.23	7.56
	3.5	26.91	7.48
	5	25.17	6.99
Sandstone	2.5	92.50	25.69
	3.5	71.93	19.98
	5	54.56	15.15
K. Limestone	2.5	9.21	2.56
	3.5	7.84	2.18
	5	7.71	2.14
G. Sandstone	2.5	12.78	3.55
	3.5	10.19	2.83
	5	9.79	2.72
Travertine (DT)	2	16.76	4.66
	3.5	14.03	3.90
	5	10.94	3.04
Finike Limra	2	22.38	6.22
	3.5	18.97	5.27
	5	17.75	4.93
K. Beyaz	2	158.96	44.16
	3.5	132.88	36.91
	5	102.42	28.45

Table 3.8 : SE results for conical cutter 1 for 5 mm depth of cut

Sample Name	s (mm)	SE (MJ/m^3)	SE (kWh/m^3)
Beige Marble	unr	47.06	13.07
	10	36.66	10.18
	15	24.65	6.85
	20	27.39	7.61
Limestone	unr	36.10	10.03
	10	26.90	7.47
	15	20.29	5.63
	20	26.78	7.44
Travertine	unr	19.42	5.39
	10	26.79	7.44
	15	17.05	4.74
	20	21.54	5.98
Sandstone	unr	99.34	27.59
	10	68.26	18.96
	15	55.31	15.36
	20	76.74	21.32
K. Limestone	unr	8.50	2.36
	10	9.85	2.74
	15	8.96	2.49
	20	3.38	0.94
G. Sandstone	unr	7.82	2.17
	10	6.70	1.86
	15	4.36	1.21
	20	10.37	2.88

Table 3.9 : SE results for conical cutter 1 (112 M 860)

Sample Name	d (mm)	SE (MJ/m^3)	SE (kWh/m^3)
Travertine (DT)	2	45.91	12.75
	3.5	34.37	9.55
	5	19.92	5.53
Finike Limra	2	28.15	7.82
	3.5	19.61	5.45
	5	11.55	3.21
K. Beyaz	2	232.91	64.70
	3.5	140.33	38.98
	5	90.76	25.21

Table 3.10 : SE results for conical cutter 2 for 5 mm depth of cut

Sample Name	s (mm)	SE (MJ/m^3)	SE (kWh/m^3)
Beige Marble	unr	103.40	28.72
	15	48.14	13.37
Limestone	unr	75.55	20.99
	15	53.09	14.75
Travertine	unr	34.61	9.61
	15	21.12	5.87
Sandstone	unr	136.94	38.04
	15	84.10	23.36
K. Limestone	unr	9.96	2.77
	15	8.59	2.39
	20	6.25	1.74
G. Sandstone	unr	18.45	5.13
	15	14.34	3.98

Only with chisel cutter experiments are carried out with different depth of cuts. Specific energy is inversely proportional to the depth of cut and in the Figures 3.23-3.31 a prove of this theory can be seen for chisel cutter.

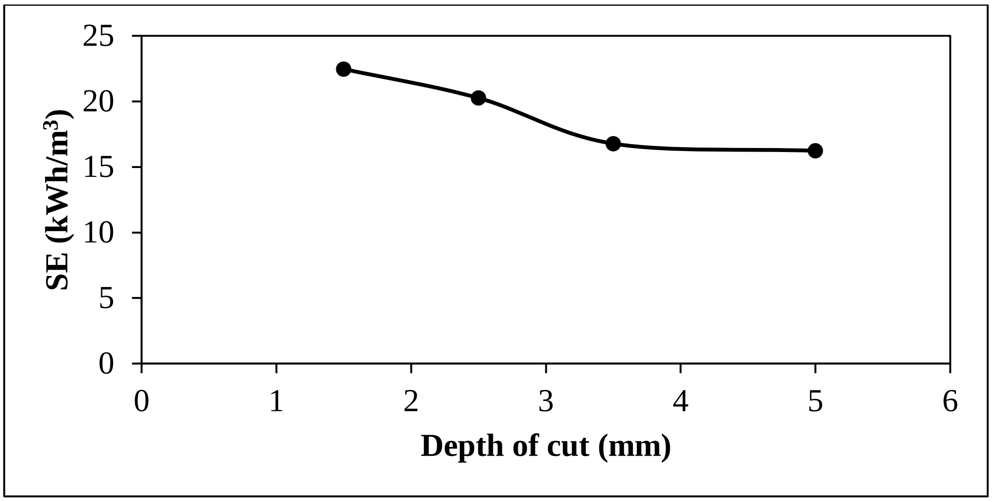

Figure 3.23 : Relationship between SE and Depth of cut for Beige Marble

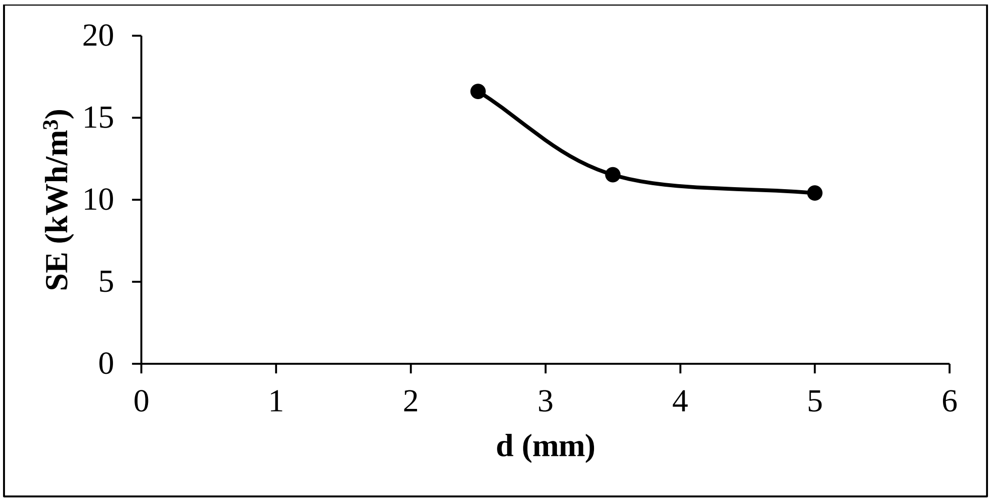

Figure 3.24 : Relationship between SE and Depth of cut for Limestone

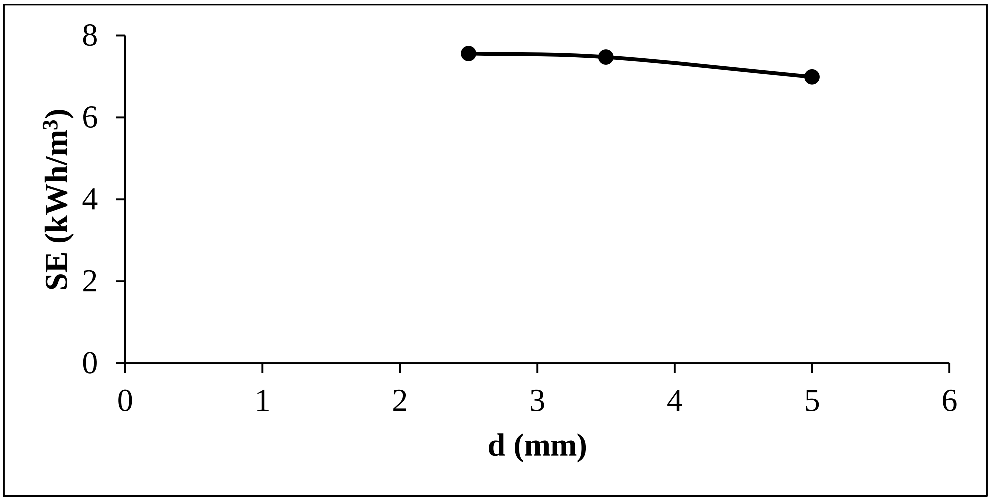

Figure 3.25 : Relationship between SE and Depth of cut for Travertine

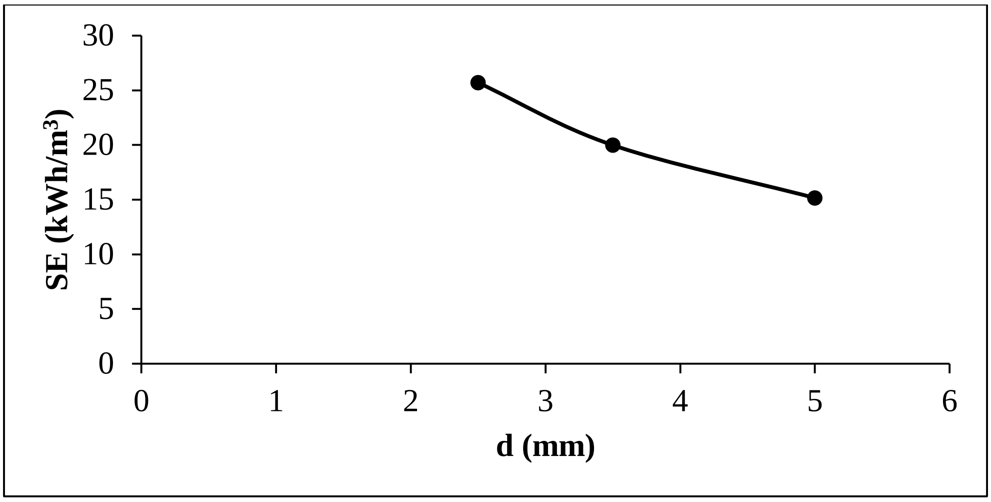

Figure 3.26 : Relationship between SE and Depth of cut for Sandstone

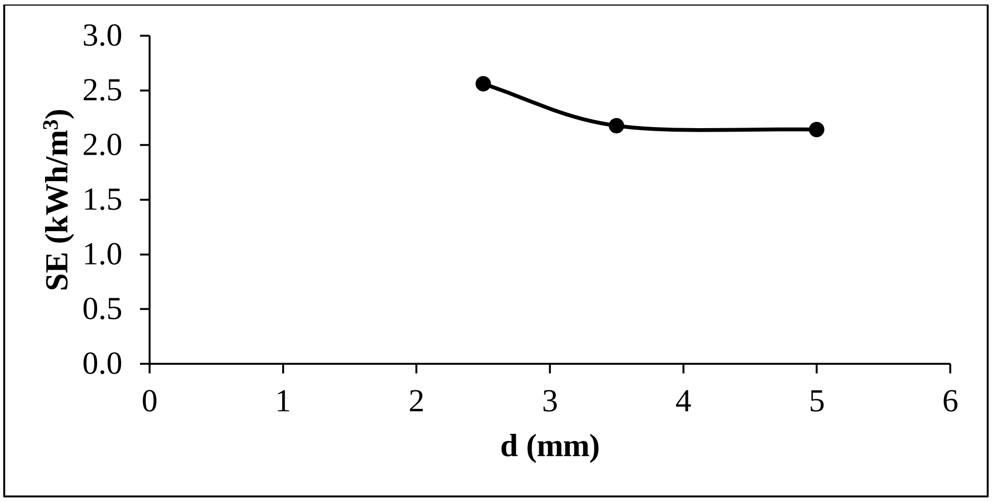

Figure 3.27 : Relationship between SE and Depth of cut for Kufeki Limestone

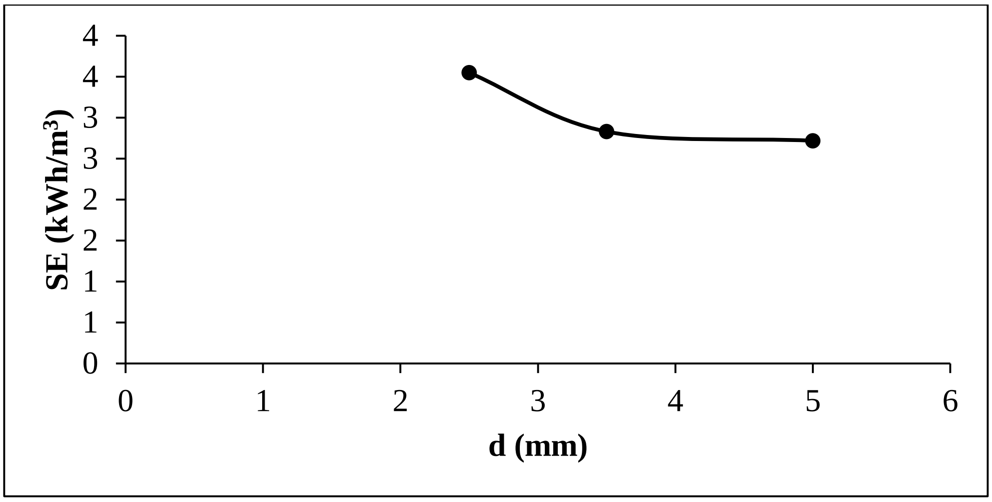

Figure 3.28 : Relationship between SE and Depth of cut for Green Sandstone

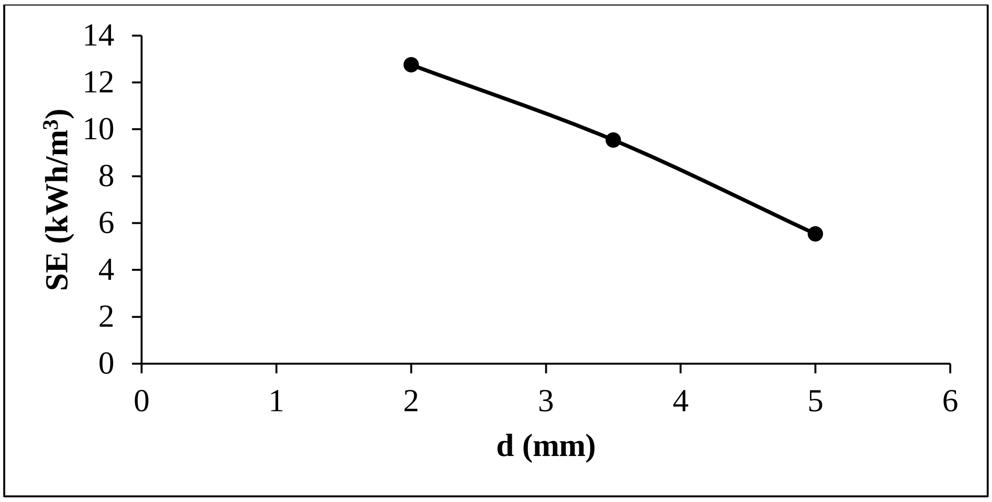

Figure 3.29 : Relationship between SE and Depth of cut for Travertine (DT)

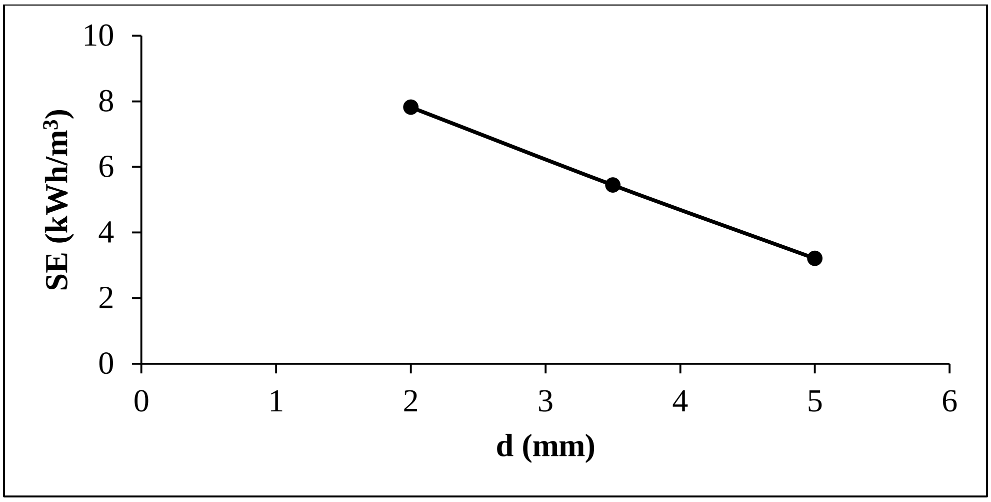

Figure 3.30 : Relationship between SE and Depth of cut for Finike Limra

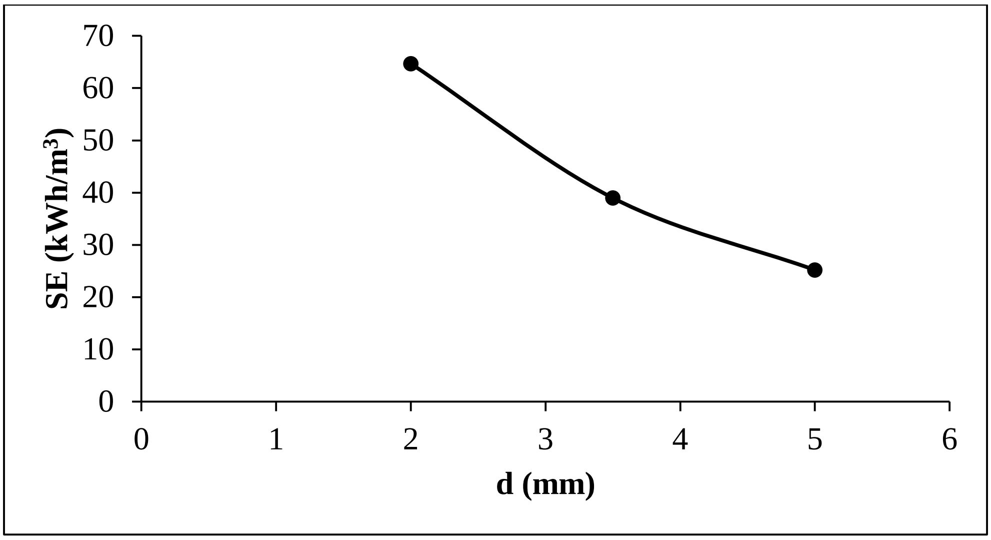

Figure 3.31 : Relationship between SE and Depth of cut for Kavaklıdere Beyaz

3.2.5 Optimum spacing to depth of cut ratio with conical cutter 1

Experiments performed with conical cutter 1 has optimum spacing to depth of cut ratio. For 6 rock samples spacings of 10, 15, 20 mm are performed and their optimum ratios are found. In the Figures 3.32-3.37 these relationships can be seen.

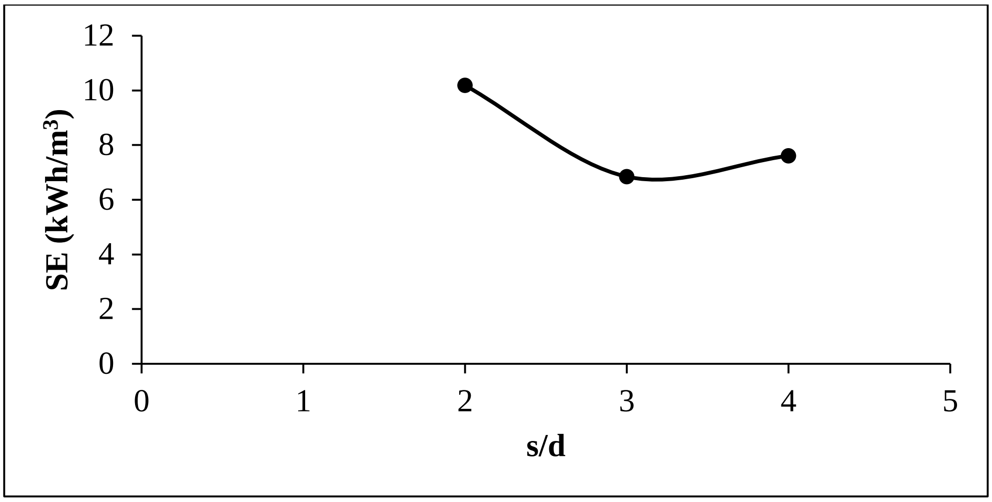

Figure 3.32 : Optimum spacing to depth of cut ratio for beige marble

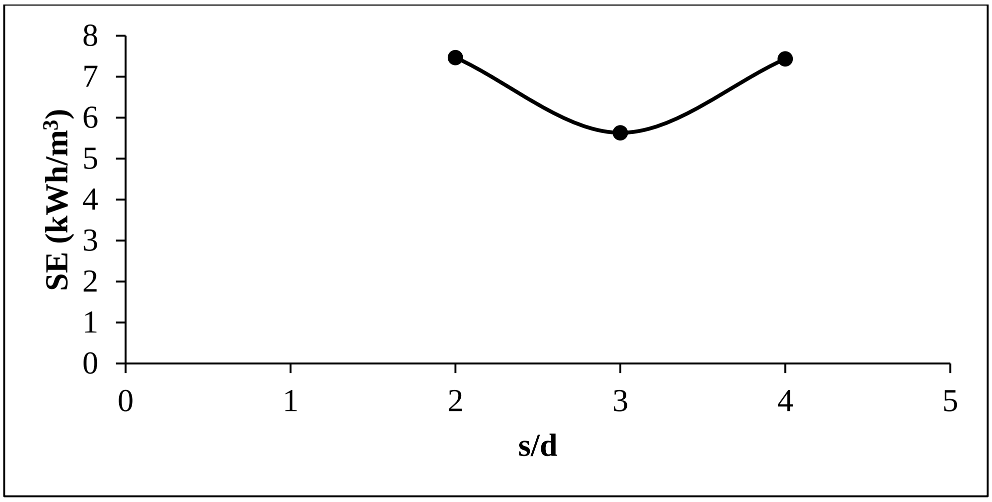

Figure 3.33 : Optimum spacing to depth of cut ratio for limestone

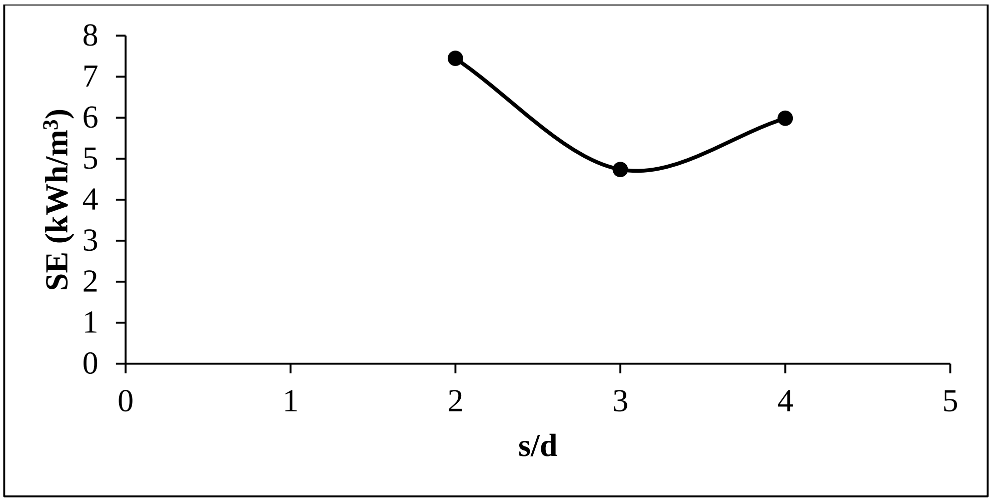

Figure 3.34 : Optimum spacing to depth of cut ratio for travertine

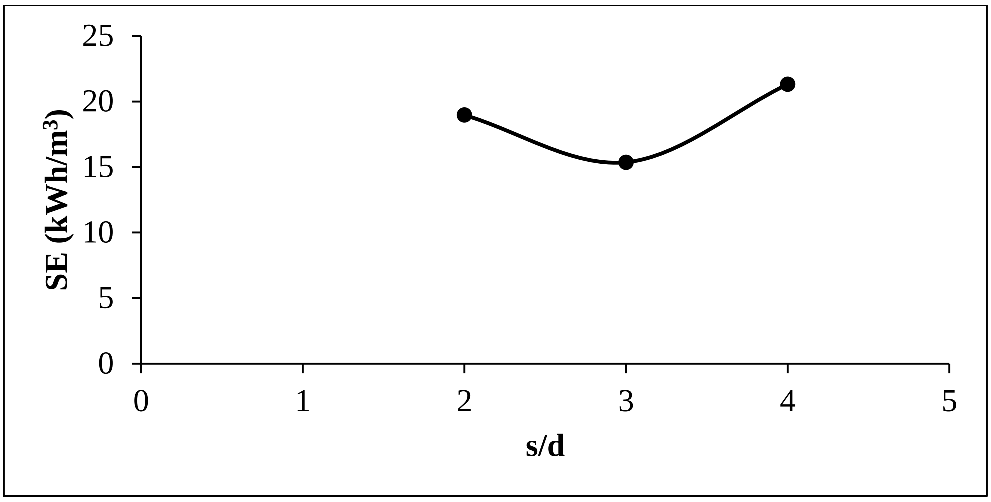

Figure 3.35 : Optimum spacing to depth of cut ratio for sandstone

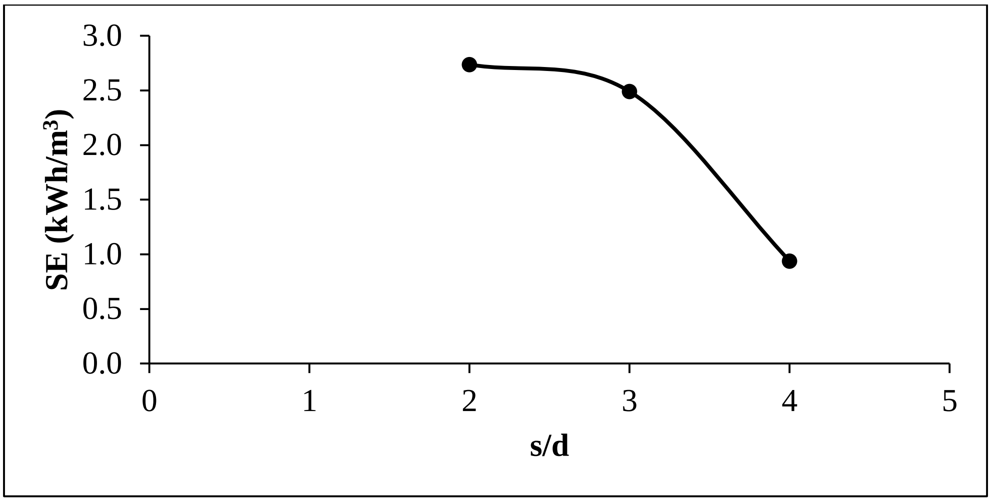

Figure 3.36 : Optimum spacing to depth of cut ratio for kufeki limestone

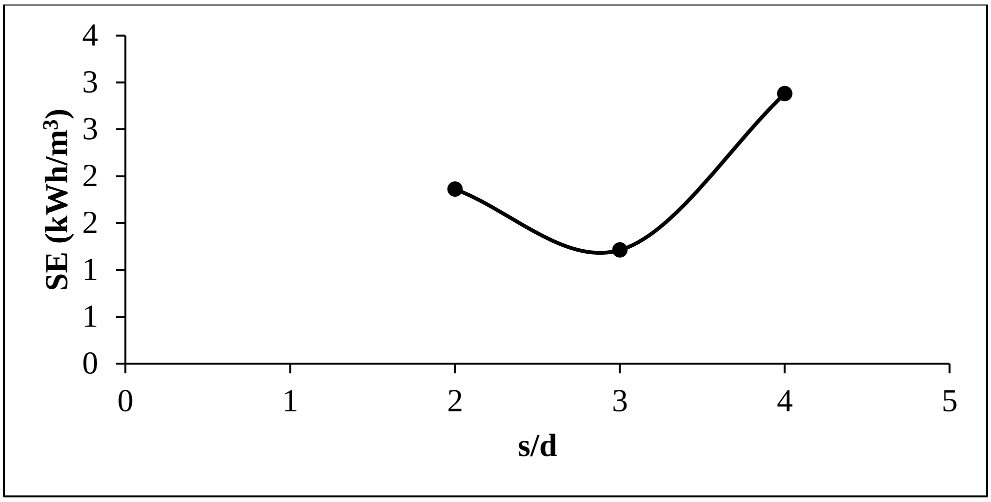

Figure 3.37 : Optimum spacing to depth of cut ratio for green sandstone

Experiments are performed in different samples with diffierent cutters and some photos taken from the experiment surfaces are given in the Figure 3.38 and 3.39 below.

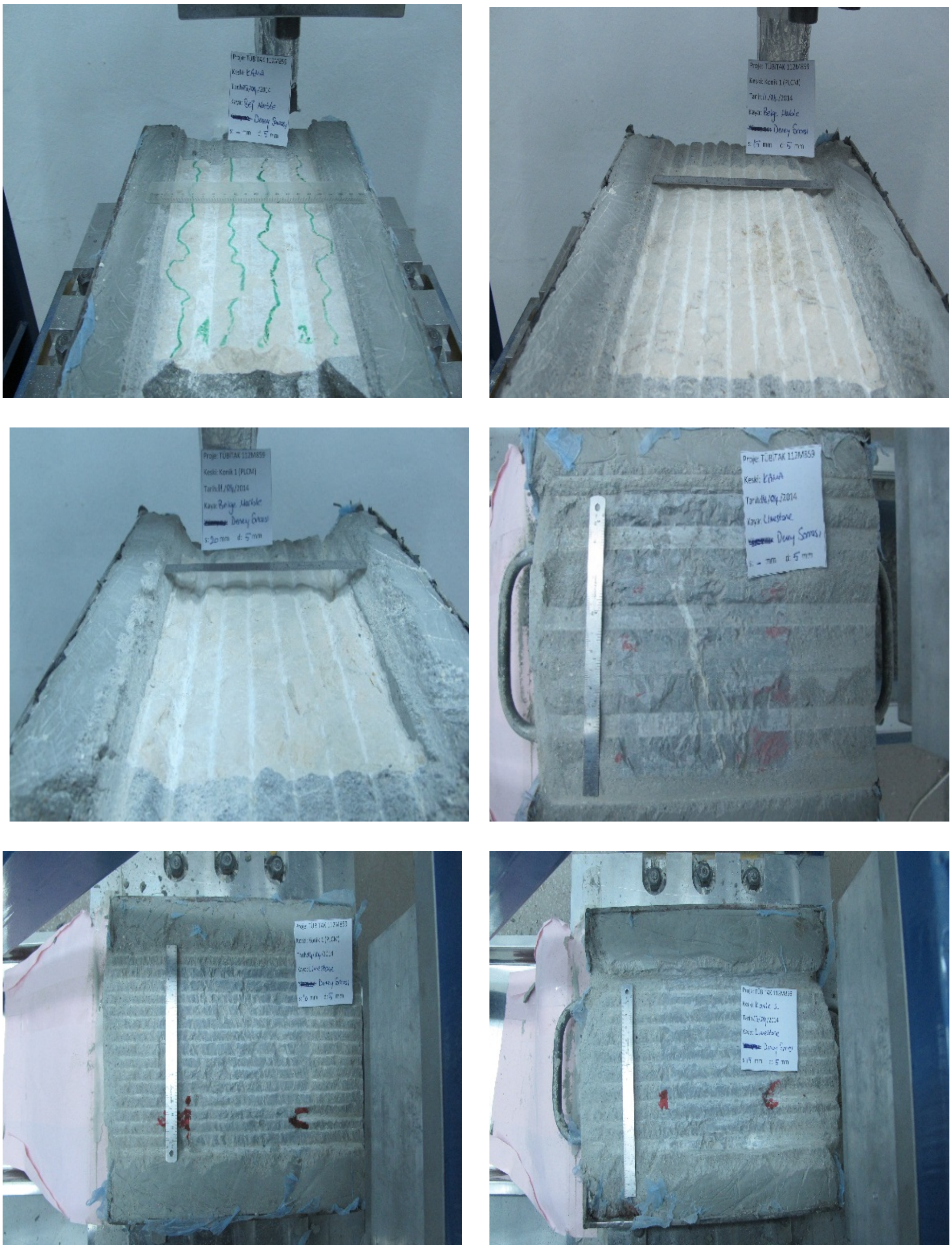

Figure 3.38 : Photos taken from beige marble and limestone.

Figure 3.39 : Photos taken from sandstone, g. sandstone and travertine samples.

3.2.6 Results of sieve analysis

Sieve analysis is performed on the muck samples collected from rock cutting tests. For each set collected samples subjected to sieve analysis using a vibrating screen. Coarness index which can be defined as sum of the cumulative weight percentages retained on the each sieve is found for each experiment. This dimensionless number gives researchers an idea about rock cutting process in the field and laboratory. Tuncdemir et al. stated that coarness index values are at their peak point in optimum cutting condition and lowest specific energy [32]. Results of the sieve analysis tests are given in the Tables 3.11-3.14.

Table 3.11 : Sieve analysis results for chisel pick

Sample Name	d (mm)	CI (chisel)
Beige Marble	1.5	569
	2.5	642
	3.5	644
	5	643
Limestone	2.5	535
	3.5	575
	5	601
Travertine	2.5	548
	3.5	564
	5	576
Sandstone	2.5	684
	3.5	742
	5	745
K. Limestone	2.5	412
	3.5	436
	5	457
G. Sandstone	2.5	564
	3.5	605
	5	636
Travertine (DT)	2	-
	3.5	-
	5	-
Finike Limra	2	-
	3.5	-
	5	-
K. Beyaz	2	-
	3.5	-
	5	-

Table 3.12 : Sieve analysis result for conical pick 1

Sample Name	s (mm)	CI (conical 1)
Beige Marble	unr	638
	10	684
	15	740
	20	748
Limestone	unr	674
	10	664
	15	708
	20	735
Travertine	unr	748
	10	717
	15	765
	20	692
Sandstone	unr	705
	10	787
	15	818
	20	820
K. Limestone	unr	650
	10	603
	15	651
	20	651
G. Sandstone	unr	746
	10	693
	15	757
	20	728

Table 3.13 : Sieve analysis result for conical pick 1 (112 M 860)

Sample Name	d (mm)	CI (conical 1)
Travertine (DT)	2	525
	3.5	623
	5	712
Finike Limra	2	566
	3.5	699
	5	740
K. Beyaz	2	334
	3.5	466
	5	570

Table 3.14 : Sieve analysis result for conical pick 2

Sample Name	s (mm)	CI
Beige Marble	unr	673
	15	660
Limestone	unr	610
	15	683
Travertine	unr	665
	15	672
Sandstone	unr	760
	15	764
K. Limestone	unr	532
	15	512
	20	579
G. Sandstone	unr	698
	15	703

4. CORRELATIVE STUDIES

Firstly, rock cutting experiments performed on rock samples are compared in terms of normal force, cutting force and specific energy. Secondly, rock cutting experiments are correlated with mechanical properties of rocks. After results checked with existing literature in order to understand mini scale conical cutters can be used or not.

4.1 Comparison of Cutters

3 different cutters which are defined in the preceding chapter compared with each other in terms of normal force, cutting force, specific energy. The experiments compared in this chapter performed at 5 mm deprh of cut. According to Balci and Bilgin (2007) there is a suitable correlation between specific energy results obtained from chisel and conical picks. In that study, conical cutter has attack and tip angle 56 and 80 degrees respectively. The correlation coeffient of chisel and conical cutter is 0.83 [20]. In this part mini scale conical picks having different specifications are tried with the same chisel cutter used in that study and new correlations are found to select and design a proper mechanical excavator.

4.1.1 Comparison of chisel and conical cutter 1

The results of cutting, normal forces, specific energy and optimum specific energy are compared among each other with these three cutters. In the Figures 4.1-4.4 these relationships can be found. 9 rock samples subjected to linear cutting experiments with the PLCM developed. The results of the linear cutting tests discussed in the chapter 3. For the normal and cutting force, specific energy and optimum specific energy correlation coefficents are 0.90, 0.69, 0.76 and 0.68 respectively.

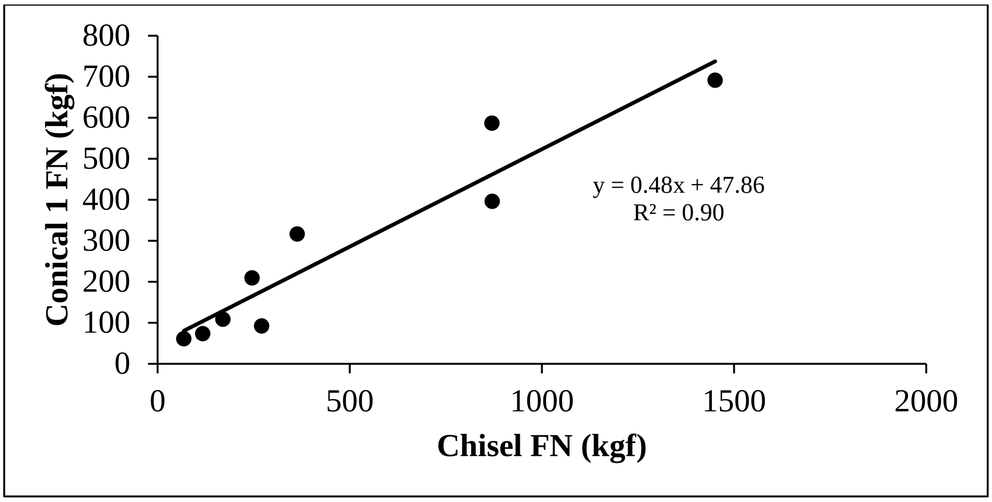

Figure 4.1 : Comparison of normal force for chisel and conical 1.

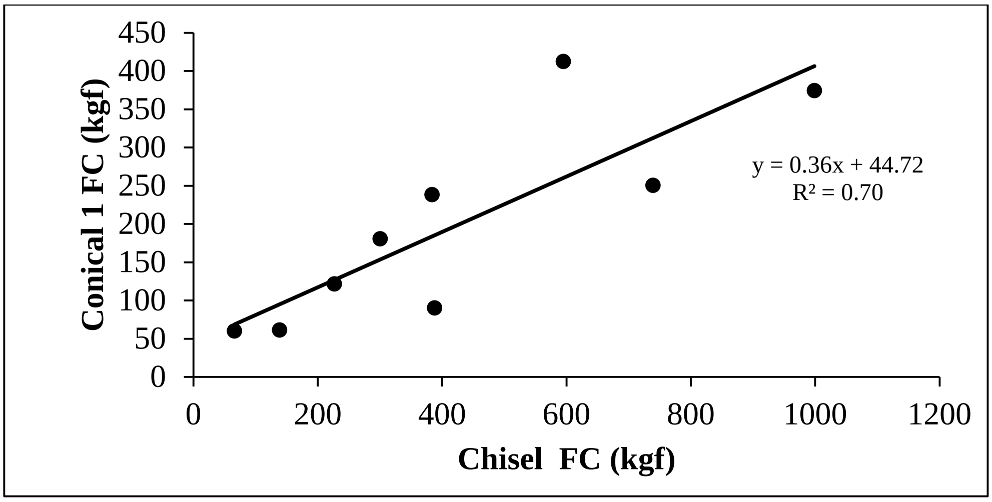

Figure 4.2 : Comparison of cutting force for chisel and conical 1.

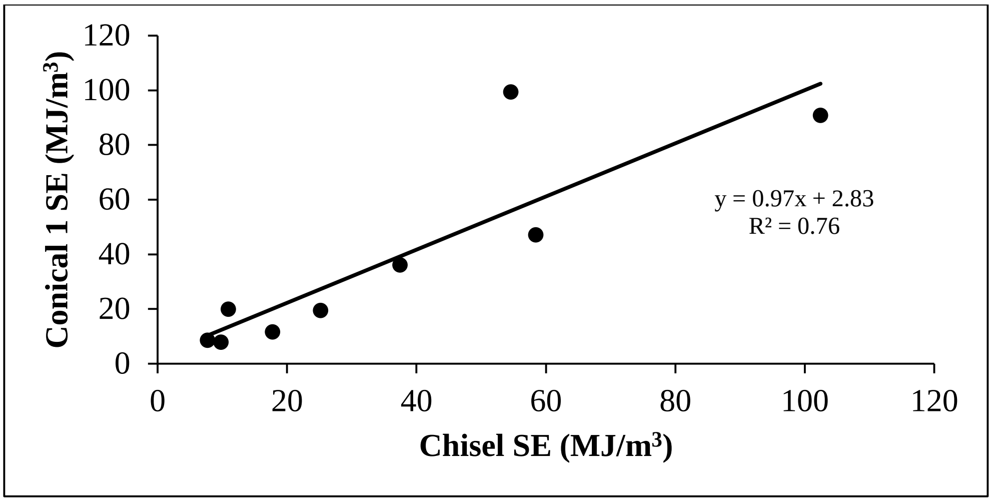

Figure 4.3 : Comparison of specific energy for chisel and conical 1.

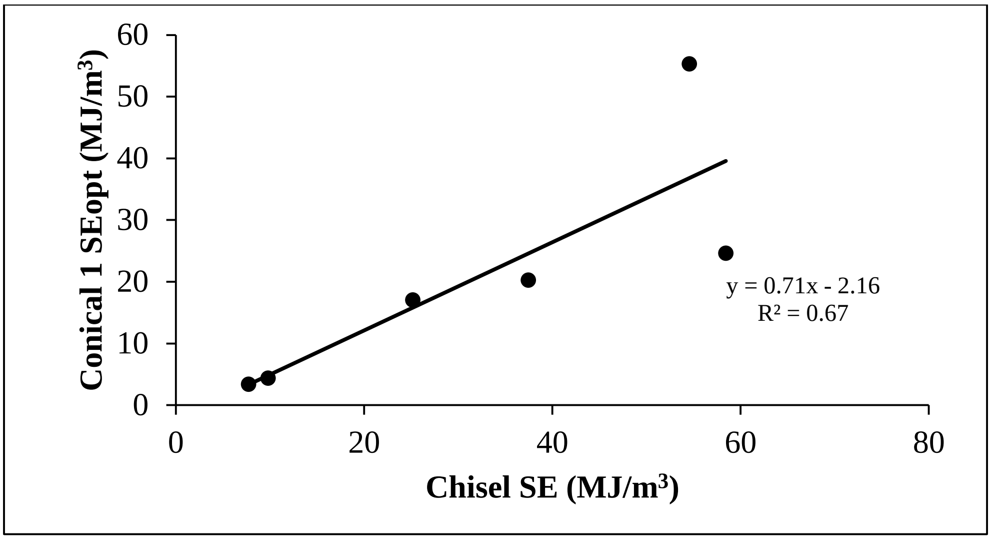

Figure 4.4 : Comparison of specific energy of chisel and SE opt of conical 1.

4.1.2 Comparison of chisel and conical cutter 2

6 rocks defined in chapter 3 used in the experiments with these cutters. Results show that conical cutter 2 gives better correlation than the conical cutter 1. In the Figures 4.5-4.8. normal and cutting force, specific energy and optimum specific energy comparisons can be found. Correlation coefficents found for normal, cutting force, specific energy and optimum specific energy are 0.94, 0.82, 0.91 and 0.77 respectively.

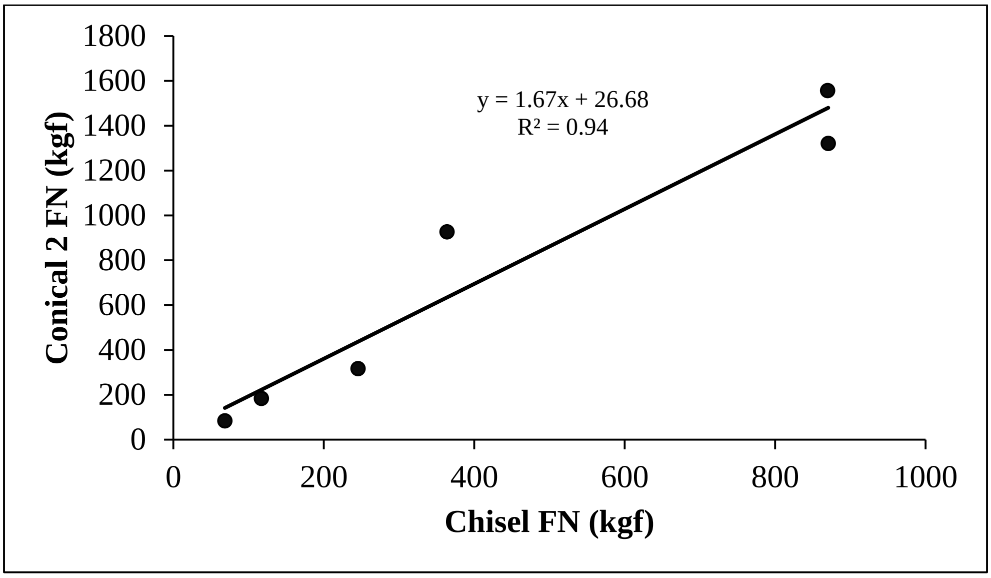

Figure 4.5 : Comparison of normal force for chisel and conical 2.

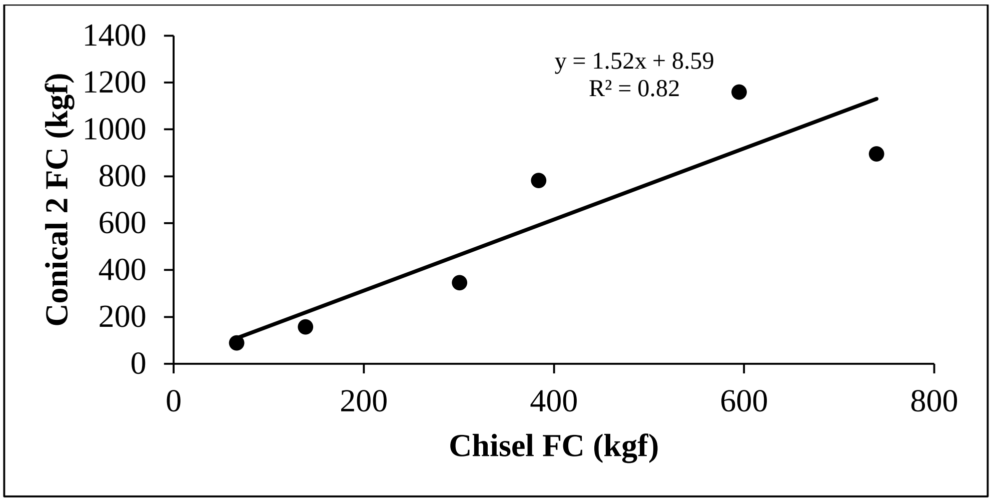

Figure 4.6 : Comparison of cutting force for chisel and conical 2.

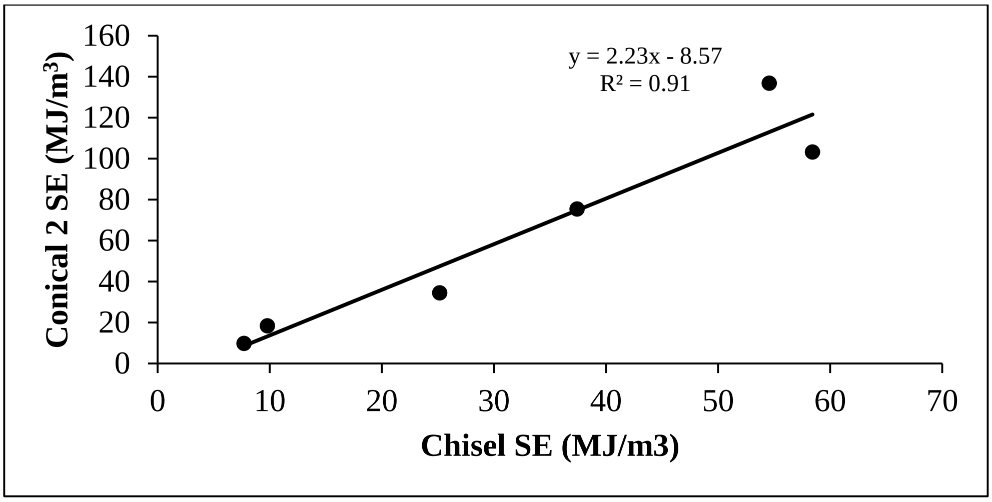

Figure 4.7 : Comparison of specific energy for chisel and conical 2.

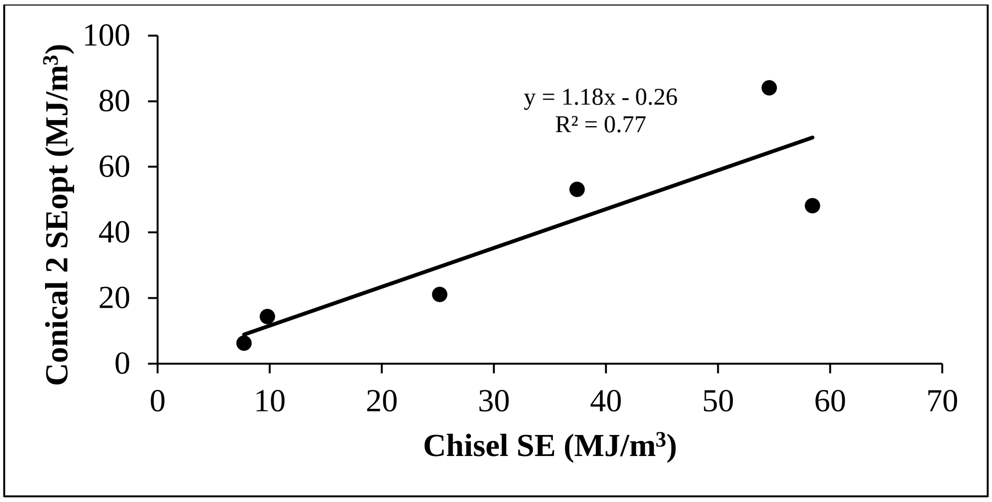

Figure 4.8 : Comparison of specific energy of chisel and SE opt of conical 2.

4.1.3 Comparison of conical 1 and conical 2

This two conical picks have the same attack angle. Tip angles are 60 degrees for conical 1 and 85 degrees for conical 2. 6 rocks subjected to rock cutting experiments to define the relationship between these two picks. As can be seen from the figures FN and FC forces are 2 to 3 times higher in conical cutter 2. In the Figures 4.9-4.12 relationship between normal and cutting force, specific energy and optimum specific energy obtained from spacing to depth of cut ratio can be found.

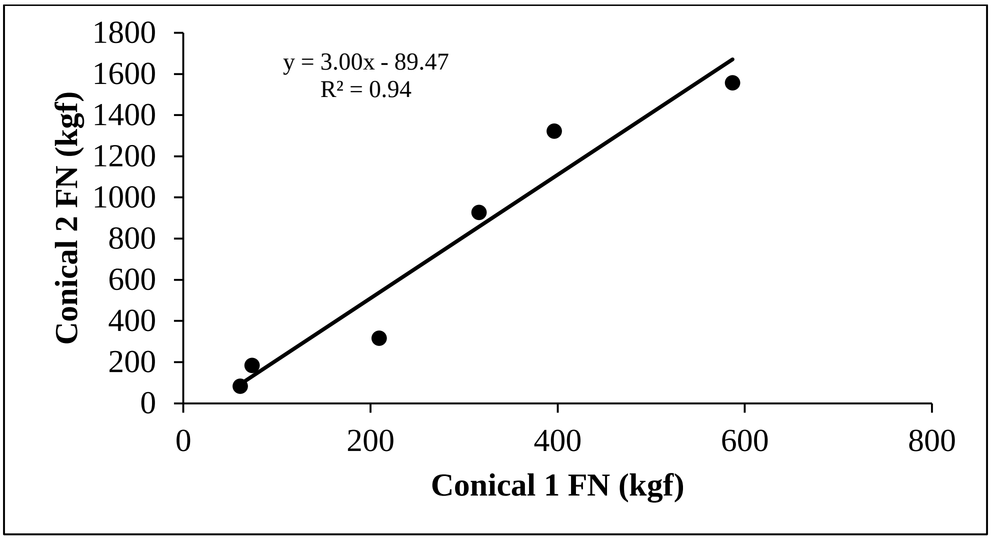

Figure 4.9 : Comparison of normal force for conical 1 and conical 2.

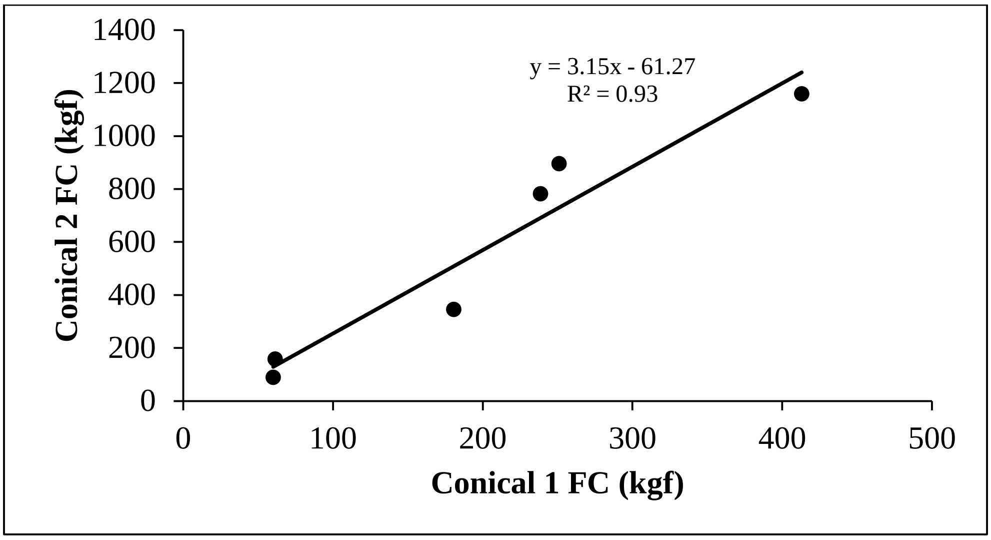

Figure 4.10 : Comparison of cutting force for conical 1 and conical 2

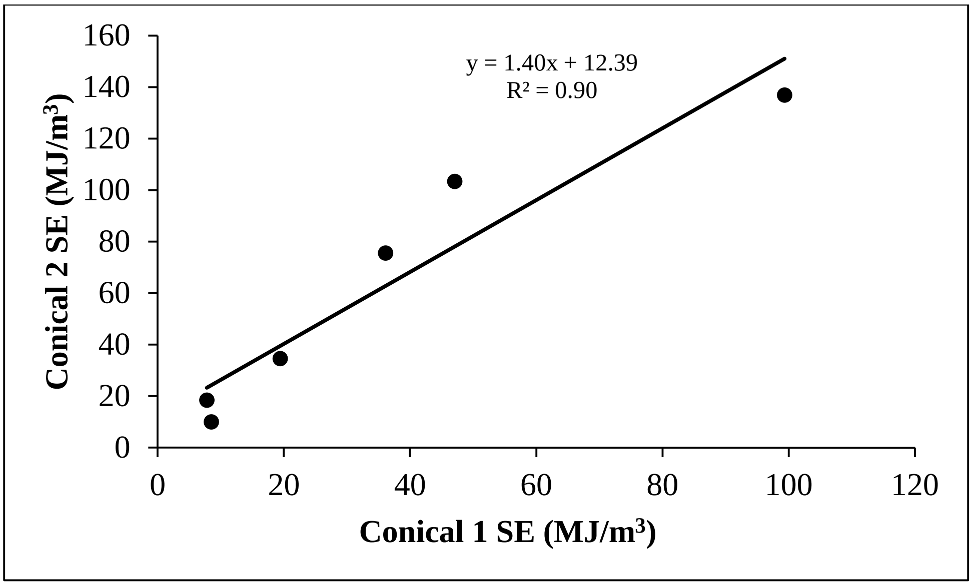

Figure 4.11 : Comparison of specific energy for conical 1 and conical 2

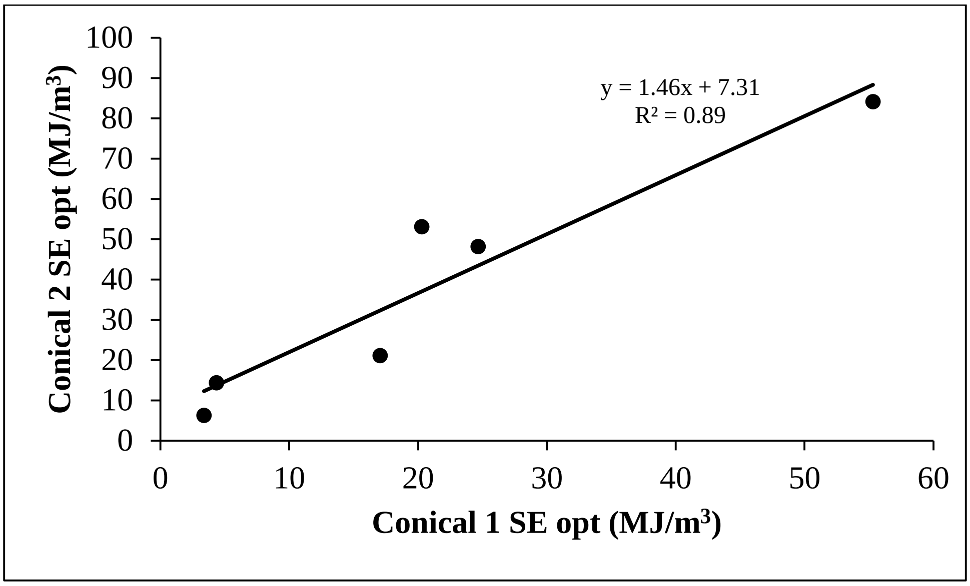

Figure 4.12 : Comparison of optimum specific energy for conical 1 and conical 2

4.2 Correlation of Optimum Specific Energy with Physical Mechanical Properties

Optimum specific energy results obtained from rock cutting tests with mini scale conical cutters are correlated with mechanical properties. According to study Balci et al. (2004) 23 different rock types are subjected to linear cutting tests with real life cutters. This study showed that physical and mechanical properties can be used to predict optimum specific energy obtained from linear cutting tests [16]. In the following Figures 4.13-4.17 correlative study of optimum specific energy and physical and mechanical properties can be seen. Results showed that rock properties can be used reliably to predict optimum specific energy obtained from mini scale conical cutters.

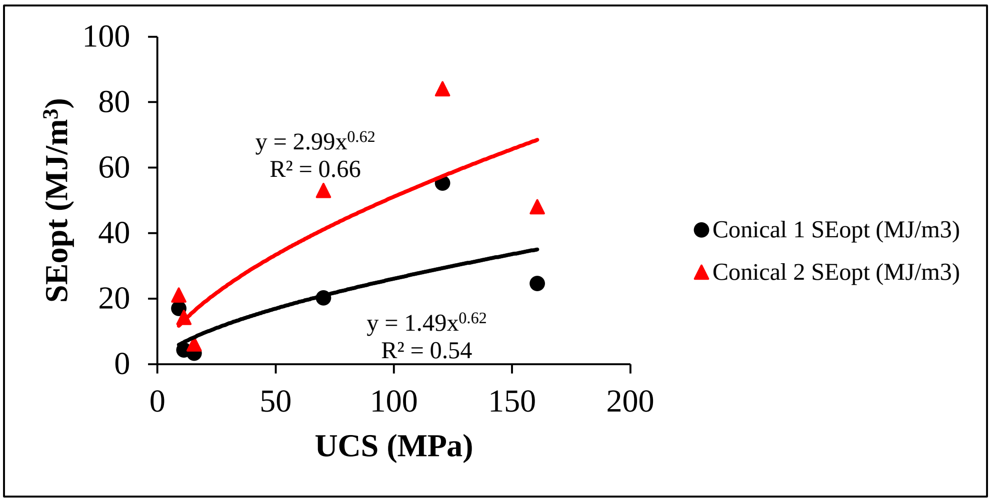

Figure 4.13 : Relationship between SEopt and UCS.

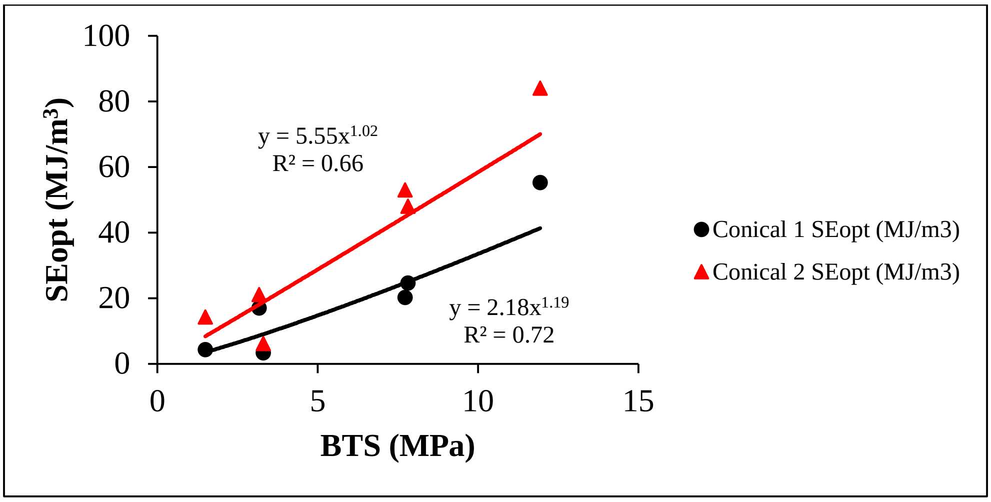

Figure 4.14 : Relationship between SEopt and BTS.

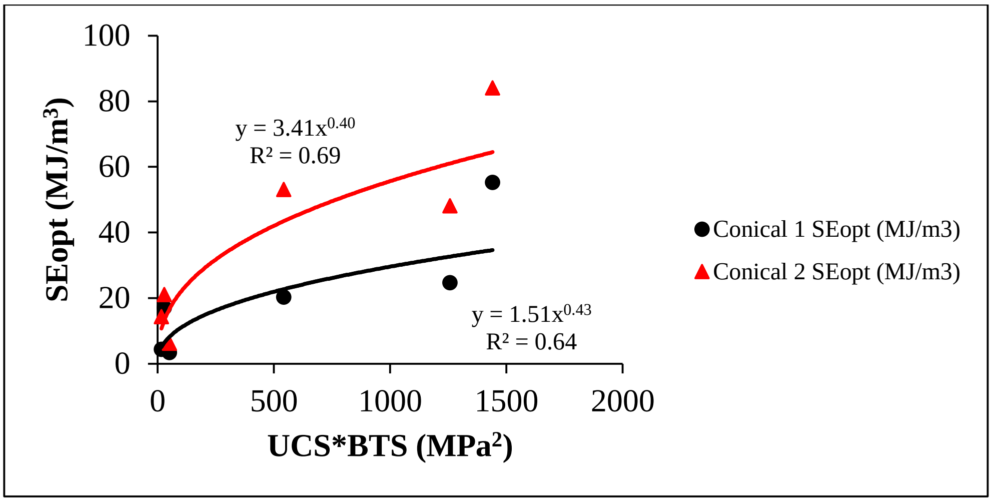

Figure 4.15 : Relationship between SEopt and UCS*BTS.

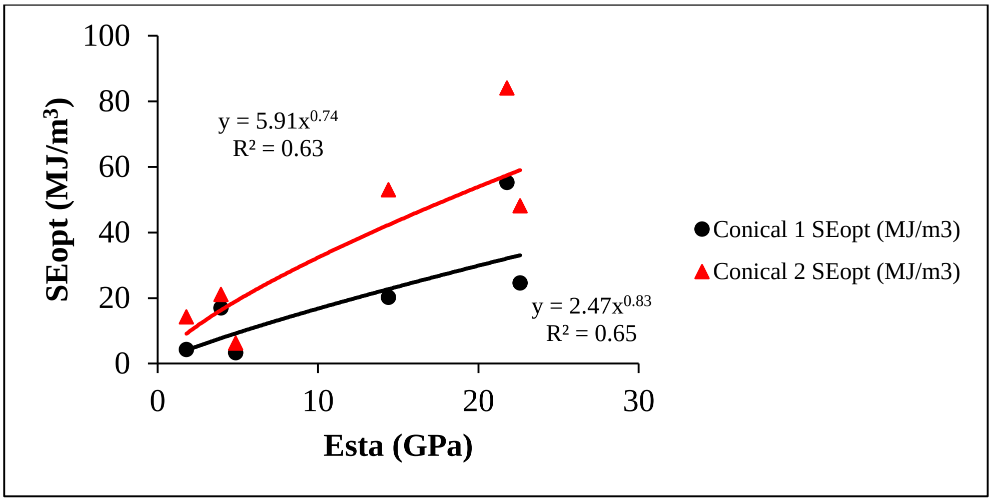

Figure 4.16 : Relationship between SEopt and Esta.

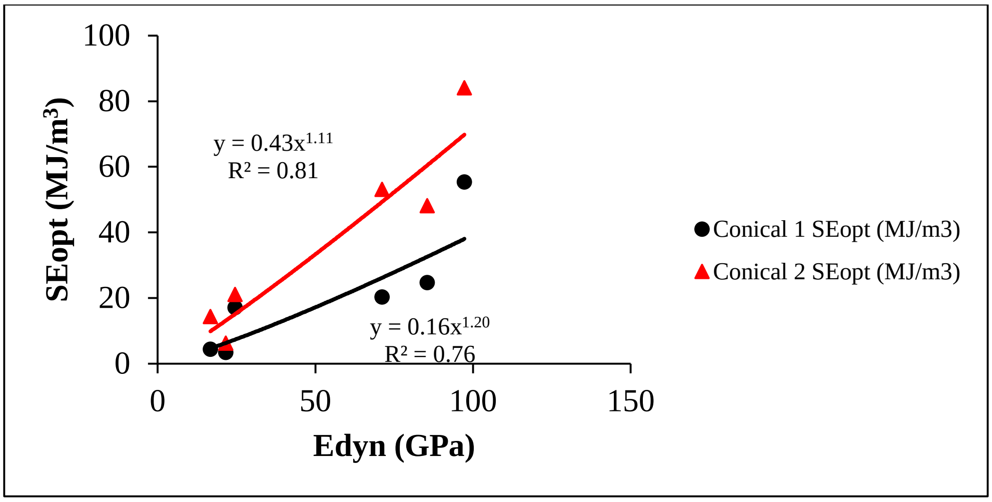

Figure 4.17 : Relationship between SEopt and Edyn.

4.3 Correlation of Physical Mechanical Properties with Cutting Force

Cutting force obtained from the linear cutting tests in unrelieved mode, at 5 mm depth of cut are correlated with physical and mechanical properties. Prediction of cutting force could be done by using only these properties since the cutting force is used in calculation of specific energy. Results obtained from mini scale cutters are quite close results published by Bilgin et al. (2006) [5]. This shows that predicting cutting force from physical and mechanical properties can be done in a proper way using mini scale cutters. These relationships are given in the Figures 4.18 to 4.22 below.

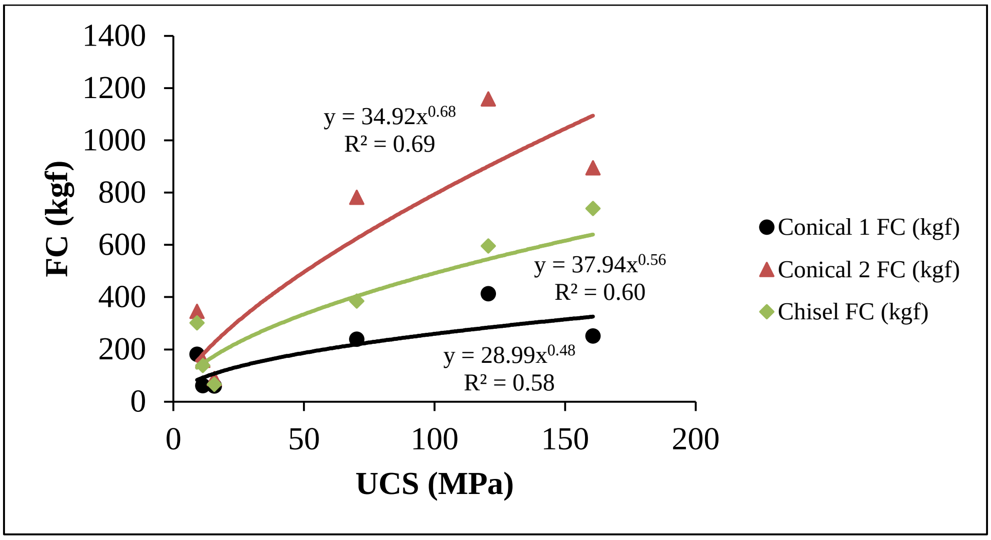

Figure 4.18 : Relationship between UCS and Cutting Force.

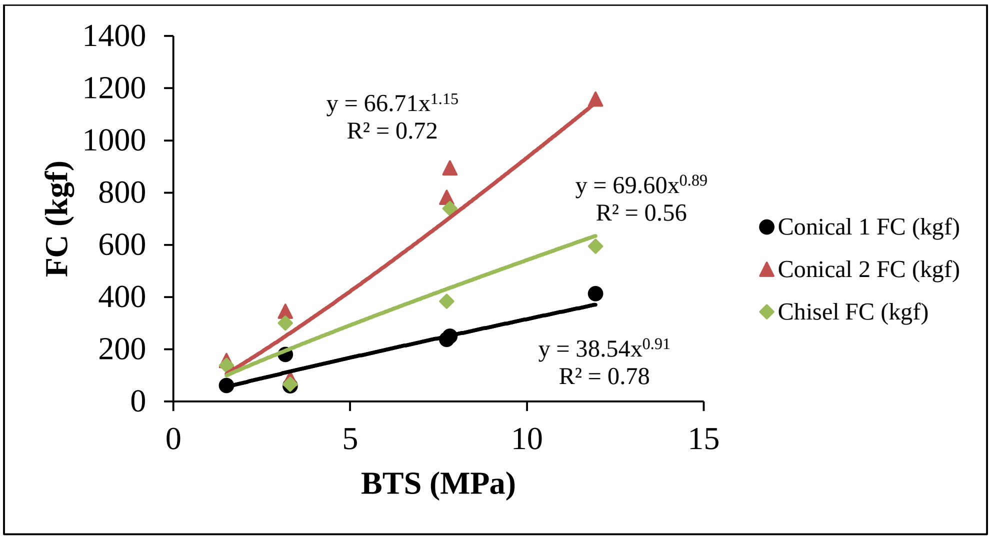

Figure 4.19 : Relationship between BTS and Cutting Force.

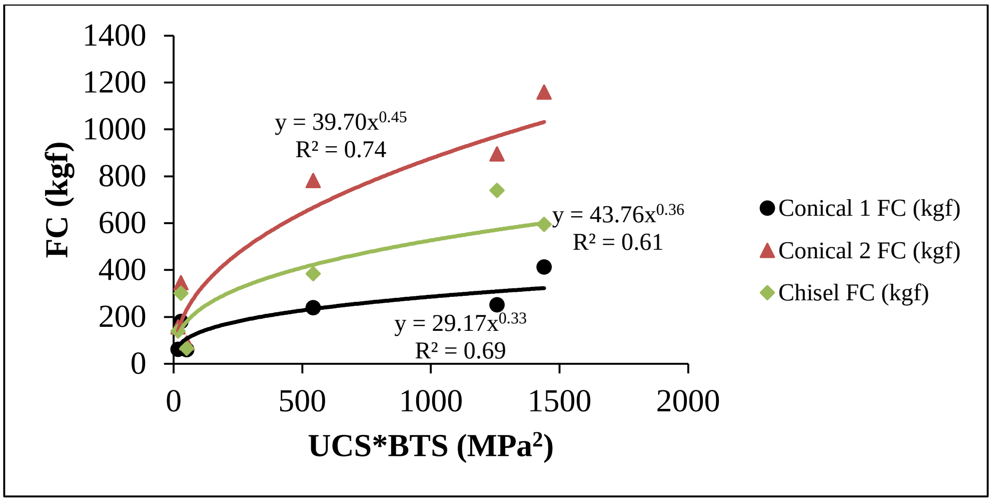

Figure 4.20 : Relationship between UCS*BTS and Cutting Force.

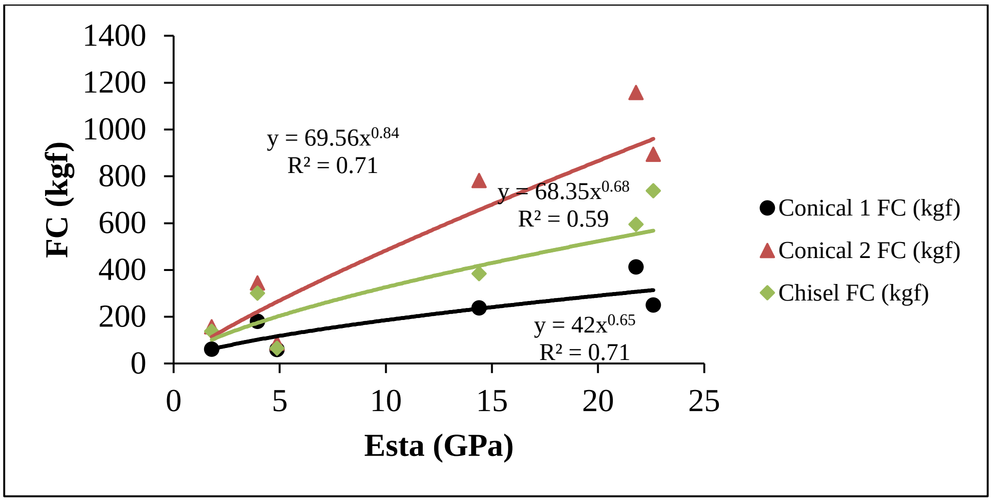

Figure 4.21 : Relationship between Esta and Cutting Force.

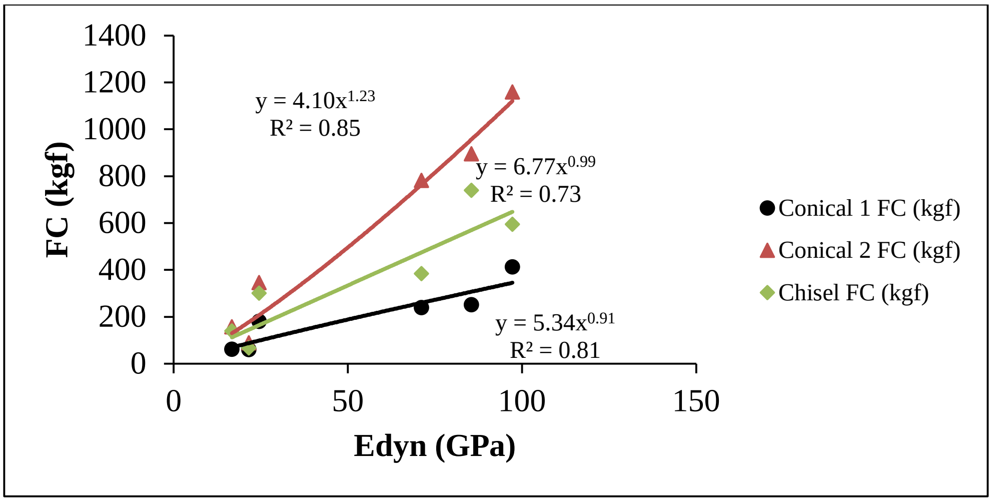

Figure 4.22 : Relationship between Edyn and Cutting Force.

5. FIELD STUDY

Amasya Suluova coal mine owned by PLT mining. According to field study at 25th of February 2014 the company was excavating the main galleries with 16 degrees inclined, through the coal reserve. Two roadheaders were working parallel in both galleries. Green sandstone samples taken from the face and transfered to the laboratory for further research. This chapter explains the relationship between field data and laboratory studies. In Figure 5.1 one of the gallery entrance in the mine can be seen.

Figure 5.1 : Gallery entrance located in Amasya Suluova Mine

5.1 Geology

Geology in Amasya Suluova basin named as Celtek formation. Celtek formation has Eocene aged structures which are mainly yellow, brown and black conglomerates having coal seams inside. Transitions zones of clay stone, marl and sandstone can also be found along the tunnel route [33].

5.2 Roadheaders in Amasya Suluova Coal Mine

Machine specifications for EBZ 75 type roadheader given in table 5.1 and photo of the roadheader can be seen in Figure 5.2.

Table 5.1 : Machine specifications for EBZ 75

Amasya Suluova Roadheader	
Total Weight (ton)	24
Total Power (kW)	135
Cutting Power (kW)	75
Max. Cutting Height (m)	3.5
Max. Cutting Width (m)	4.6
Cutter Type	Conical
Cutter number	36
Cutter head rotation (rpm)	46
Max. Grade ability (degree)	±16

Figure 5.2 : Photographic view of EBZ 75

5.3 Field Performance of Roadheader

Amasya Suluova Coal mine has two inclined ways, which their construction started at the altitude of 643 and 647 meter. Both of them are having 16 degrees grade and 9 m^2 area of opening. Two EBZ 75 type roadheaders excavating through these tunnels. Firstly, company started with conventional methods and afterwards they started to use roadheaders in December 2013. Starting from the January 2014, they are collecting field data of the machineries. From that day machines are mainly excavated grey, brown and green sand and clay stones. Mine visited in 25 February 2014 to measure actual field data and green sand and clay stones taken from the face. Only green sandstone values are given in this work. Due to sticky characteristics of clay and grade in the tunnels they cannot use the gathering arms of the roadheaders. They are taking the muck out using a belt conveyor located near the face. While collecting the muck they are using cutterhead of the machinery to transfer it to the belt conveyor, this causes reduction in the average ICR. That's why, measurements are higher at the field study than the measurements done by company. In the field cutting time for each ring recorded every shift by engineers. To calculate the machine utilization factor and ICR given in Equation 4.1 and 4.2. Measurements taken from the field are given in Table 5.2.

$$\text{MUT}=\frac{\text{Boring Time}}{\text{Shift Time}} \qquad \textbf{(5.1)}$$

$$\text{Field ICR}=\frac{\text{Advance*Area}}{\text{Boring Time}} \qquad \textbf{(5.2)}$$

Where;

- MUT= Machine utilization factor (%)
- Boring time= Time spent for excavation (hours)
- Shift time= Working time in the mine (24 hours)
- Field ICR= Instantaneous cutting rate (m^3/h)
- Area= Area of the tunnel (m^2)

Table 5.2 : Measurement taken at the field in green sandstone.

	Machine 643	Machine 647
Total days of excavation	24	24
Total time spent for excavation (h)	127	148
Machine Utilization (%)	22.05	25.69
Total advance (m)	66	78
Daily Advance (m/day)	2.75	3.25
Average ICR (m^3/h)	4.68	4.74
Max. ICR (m^3/h)	9	9
Measurements done on ICR	8.31	6.35

5.4 Roadheader Performance Prediction Using McFeat Smith and Fowell (1979) Model

McFeat Smith and Fowell developed a field performance prediction chart given in section 2.7.1 [21]. Experiments done with conical cutters are tried to used in that study to predict performance. In the Table 5.3 the results of rock cutting experiments are given for green sandstone and results can be found in figure 5.3.

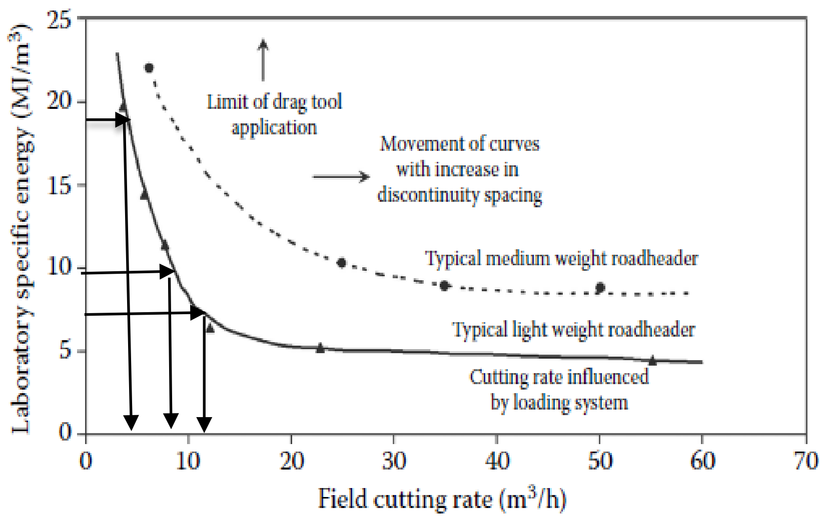

Figure 5.3 : Results of field cutting rate and laboratory specific energy.

5.5 Roadheder Performance Prediction using Gehring (1989) Model

Roadheader performance predicted using Gehring's model according to 230 kW axial machine and linearly interpolation done for estimate the performance for 75 kW. The formulation used for this calculation is given in Equation 2.30.

$$ICR = \frac{1739}{UCS^{1.13}}$$

$$\frac{75}{230} * \frac{1739}{11.26^{1.13}} = 36.76\, m^3/h$$

5.6 Roadheader Performance Prediction using Bilgin et al (1990) Model

In this model RMCI calculated as taking the RQD 100 % and ICR computed as given below. The formulations used for this calculation are given in Equation 2.31 and 2.32.

$$RMCI = UCS * \left(\frac{RQD}{100}\right)^{\frac{2}{3}} = 11.26 * \left(\frac{100}{100}\right)^{\frac{2}{3}} = 11.26\ MPa$$

$$ICR = 0.28 * P * (0.974)^{RMCI} = 0.28 * 100.5 * (0.974)^{11.26} = 20.92\,\frac{\mathrm{m}^3}{\mathrm{h}}$$

5.7 Roadheader Performance Prediction Using Rostami et al (1994) Model

In this model optimum specific energy values are obtained from PLCM results. These results for unrelieved and optimum s/d ratio in terms of kWh/m^3 are given in Table 5.4. In Figure 5.4 SE to optimum s/d can be found for green sandstone. To predict the field performance, formulation developed by Rostami et al. (1994) is used [19]. The formulation used for this calculation is given in Equation 2.33.

$$ICR = k * \frac{P_{ins}}{SE_{opt}}$$

Where;

- P_{ins}= Cutting Power installed (kW)
- SE_{opt}= Optimum specific energy (kWh/m^3)
- $k =$ energy transfer ratio (for roadheaders 0.45-0.55)

Table 5.4 : SE measurements on green sandstone using conical picks

	SE (kWh/m^3)	
s (mm)	Conical cutter 1	Conical cutter 2
unr	2.17	5.13
10	1.86	-
15	1.21	3.98
20	2.88	-

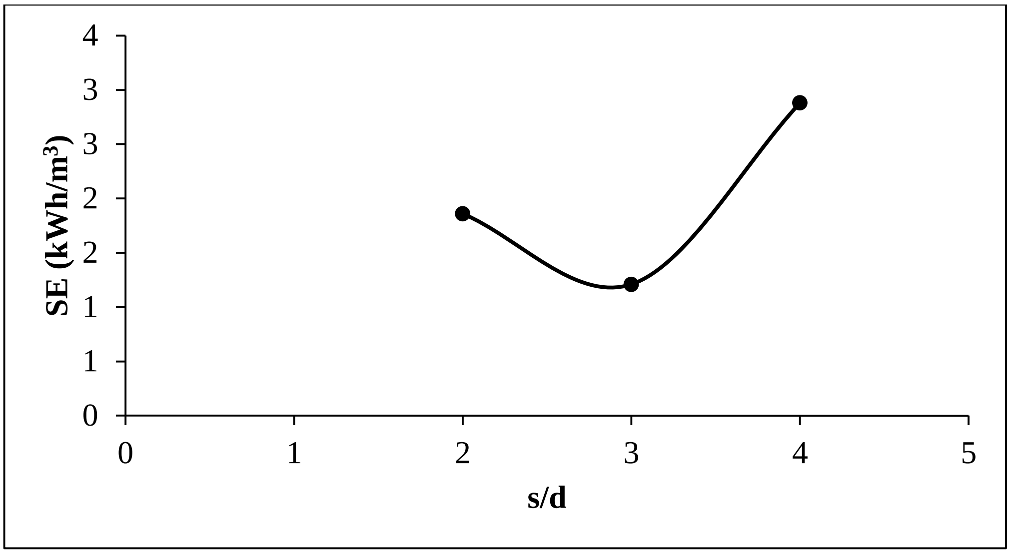

Figure 5.4 : SE to s/d ratio in conical cutter 1.

For conical cutter 1;

$$ICR = 0.45 * \frac{75}{1.21} = 27.89\ m^3/h$$

$$ICR = 0.55 * \frac{75}{1.21} = 34.09\ m^3/h$$

For conical cutter 2;

$$ICR = 0.45 * \frac{75}{3.98} = 8.47\ m^3/h$$

$$ICR = 0.55 * \frac{75}{3.98} = 10.36\ m^3/h$$

5.8 Roadheader Performance Prediction Using Balci et al (2004) Model

Firstly, performance prediction done by predicting optimum specific energy from uniaxial compressive strength of the rock in this model. After, ICR is calculated from the equation given below. The formulation used for this calculation is given in Equation 2.38.

$$ICR = 0.8\ * \frac{P}{0.37 *\ UCS^{0.86}} = 0.8 * \frac{75}{2.97} = 20.21 \frac{m^3}{h}$$

5.9 Performance Prediction Using Tumac et al (2007) Model

Equations developed by Tumac et al contains SH1, SH2 and K values. In this research only SH1 experiment done for the rock types. For this reason, only performance prediction model related to SH1 is calculated. The formulation used for this calculation is given in Equation 2.40.

$$ICR = 81.21 * SH1^{-0.78} = 81.21 * (31.75)^{-0.78} = 5.47\ m^3/h$$

5.10 Comparison of Field, Laboratory and Empirical Studies

In this chapter all of the models prepared by different researchers given in literature survey are computed. As can be seen from the results this empirical, statistical models usually over or underestimates the actual performance. However, usage of these models should be done quite carefully, restrictions and limits must be identified before the computing. Very high or very low predicted values are because of this field study is out of the range of these models. On the other hand usage laboratory and empirical models together gives accurate results. In Table 5.5 all results are given.

Table 5.5 : Field, Laboratory and Empirical Results.

		ICR (m^3/h)	AR (m/h)
Field		6.35-8.31	0.71-0.92
McFeat Smith and Fowell	Conical 1	11	1.22
	Conical 2	5	0.56
Gehring		36.76	4.08
Bilgin et al.		20.92	2.32
Rostami et al.	Conical 1	27.89-34.09	3.09-3.78
	Conical 2	8.47-10.36	0.94-1.15
Balci et al.		20.21	2.25
Tumac et al.		5.47	0.61

Optimum specific energy obtained from PLCM tests used in Rostami et al (1994) model. Laboratory results for conical cutter 1 is between 27.89 and 34.09 m^3/h. However, for conical cutter 2 it is changing between 8.47 and 10.36 m^3/h. From the results conical cutter 2 is closer to actual results but for conical cutter 1 a further study is necessary. For conical cutter 1 performance predicted mainly 4 times more than actual value. This shows that conical cutter 2 can be used to predict roadheader performance with 5 mm depth of cut and optimum s/d ratio.

For the model defined by McFeat Smith and Fowell (1979) experiments performed at 5 mm depth of cut in unrelieved mode. Field performance of roadheaders are quite close to ICR predicted from conical cutter 1 and chisel cutter. On the other hand, conical cutter 2 underestimates the actual field performance. This part shows that conical cutter 1 can be used in the chart developed by McFeat Smith and Fowell.

6. COMPARISON OF THEORETICAL AND EXPERIMENTAL FORCES

6.1 Comparison of Conical Cutter Theoretical and Experimental Forces

Cutting forces measured while performing the experiments and compared with the theoretical conical pick models which are stated by Evans, Goktan and Roxborough [2,3,4]. These formulations are well explained in the part 2.1 and they are all predicting peak cutting force acting on a pick. The theoretical formulations are given in Equation 2.1 to 2.3. In this part only peak cutting forces measured at 5 mm depth of cut in unrelieved condition compared with the models. For conical cutter 1 there are 9 rocks and for conical cutter 2 there are 6 rocks performed at 5 mm depth of cut. First of all there are examples showed that how models used in this study. After, in Tables 6.1-6.2 measured peak cutting forces and theoretical values can be found. In Figures 6.1-6.6 their relationship with the theoretical models can be seen.

Evans' model for Beige Marble

- d= 0.5 cm
- σ_T= 78.2 kg/cm^2
- σ_C= 1607 kg/cm^2
- ϕ= 60 degrees

$$F'C=\frac{16\,\Pi\,d^2\,\sigma_T^2}{\cos^2\left(\frac{\phi}{2}\right)\sigma_C}=\frac{16\,\Pi*0.5^2*78.2^2}{\cos^2\left(\frac{60}{2}\right)*1607}=\frac{16\,\Pi*0.5^2*78.2^2}{0.75*1607}=63.8\text{ kgf}$$

Goktan's model for Beige Marble

- d= 0.5 cm
- σ_T= 78.2 kg/cm^2
- ψ= friction angle between rock and cutter (10°)
- ϕ= 60 degrees

$$F'C=\frac{4\,\Pi\,\sigma_T\,d^2\sin^2\left(\frac{\phi}{2}+\psi\right)}{\cos\left(\frac{\phi}{2}+\psi\right)}=\frac{4\,\Pi*78.2*0.5^2\sin^2\left(\frac{60}{2}+10\right)}{\cos\left(\frac{60}{2}+10\right)}$$

$=\frac{4\ \Pi * 78.2 * 0.5^2 * 0.413}{0.766}$ =132.5 kgf

Roxborough's model for Beige Marble

- d= 0.5 cm
- σ_T= 78.2 kg/cm^2
- σ_C= 1607 kg/cm^2
- ϕ= 60 degrees
- ψ= friction angle between rock and cutter (16°)

$$F'C= \frac{16\ \Pi\ \sigma_C\ d^2\ \sigma_T^2}{\left[2\sigma_T+\left(\sigma_C \cos\left(\frac{\phi}{2}\right)\left(\frac{1+\tan\psi}{\mathrm{Tan}\left(\frac{\psi}{2}\right)}\right)\right)\right]^2} = \frac{16\ \Pi * 1607 * 0.5^2 * 78.2^2}{\left[2*78.2+\left(1607*\cos\left(\frac{60}{2}\right)\left(\frac{1+\tan\psi}{\mathrm{Tan}\left(\frac{\psi}{2}\right)}\right)\right)\right]^2} =$$

$$\frac{16\ \Pi * 1607 * 0.5^2 * 78.2^2}{[2*78.2+(1607*0.866)*9.156]^2} = 0.7 \text{ kgf}$$

Table 6.1 : Peak Cutting force for conical cutter 1 and theoretical models.

Sample Name	F'C (Lab) (kgf)	F'C (Evans) (kgf)	F'C (Goktan) (kgf)	F'C (Rox.) (kgf)
Beige Marble	795.2	63.8	132.5	0.7
Limestone	850.1	142.6	131.0	1.6
Sandstone	1526.6	198.1	202.3	2.2
Kufeki Limestone	290.0	117.0	55.9	1.3
Travertine	691.1	185.0	53.7	1.9
Green Sandstone	184.6	33.5	25.4	0.4
Travertine (DT)	508.2	350.9	81.3	3.4
Finike Limra	355.3	61.7	74.6	0.7
Kavaklıdere Beyaz	1002.9	86.5	108.4	1.0

Table 6.2 : Peak Cutting force for conical cutter 2 and theoretical models.

Sample Name	F'C (lab) (kgf)	F'C (Evans) (kgf)	F'C (Goktan) (kgf)	F'C (Rox.) (kgf)
Beige Marble	2584.9	88.0	254.0	1.0
Limestone	1904.2	196.8	251.1	2.2
Sandstone	3020.5	273.3	387.8	3.1
Kufeki Limestone	170.5	161.4	107.2	1.7
Traverten	1192.1	255.3	103.0	2.5
Green Sandstone	477.8	46.2	48.7	0.5

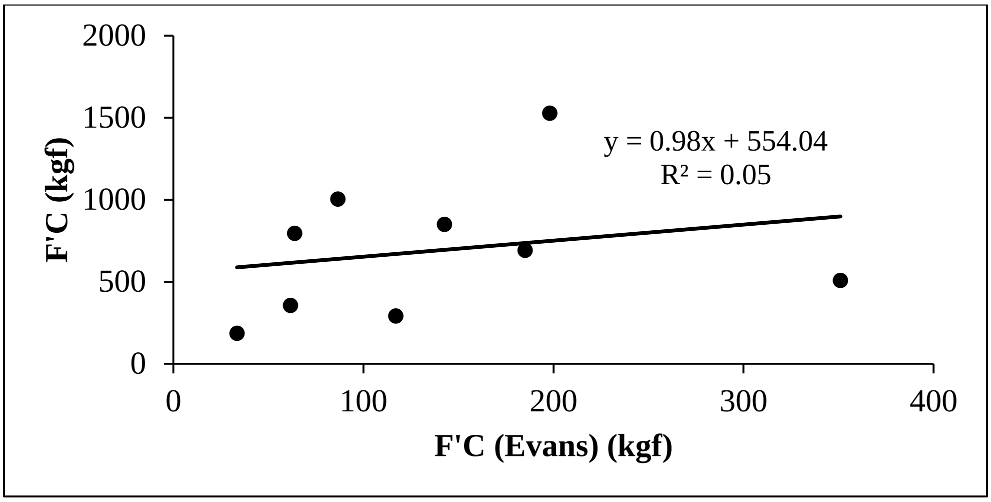

Figure 6.1 : Evans' theory for conical cutter 1.

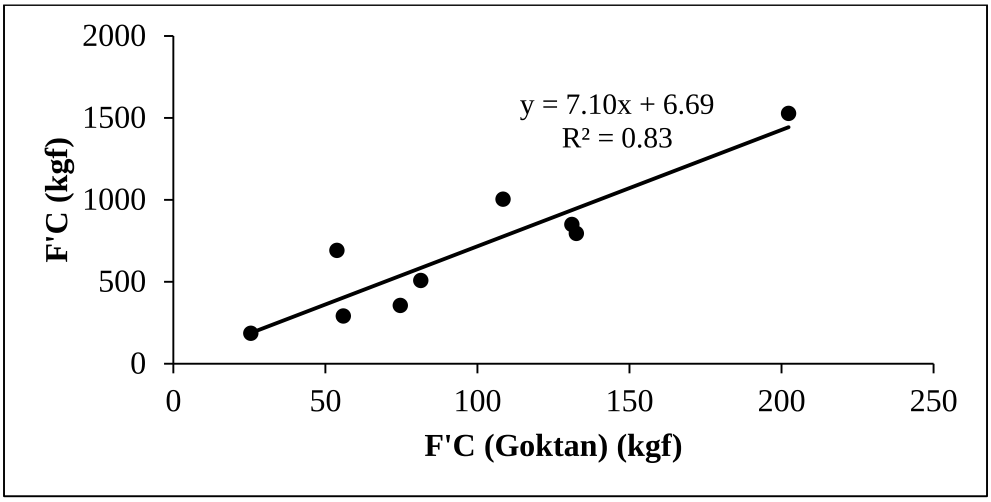

Figure 6.2 : Goktan's theory for conical cutter 1

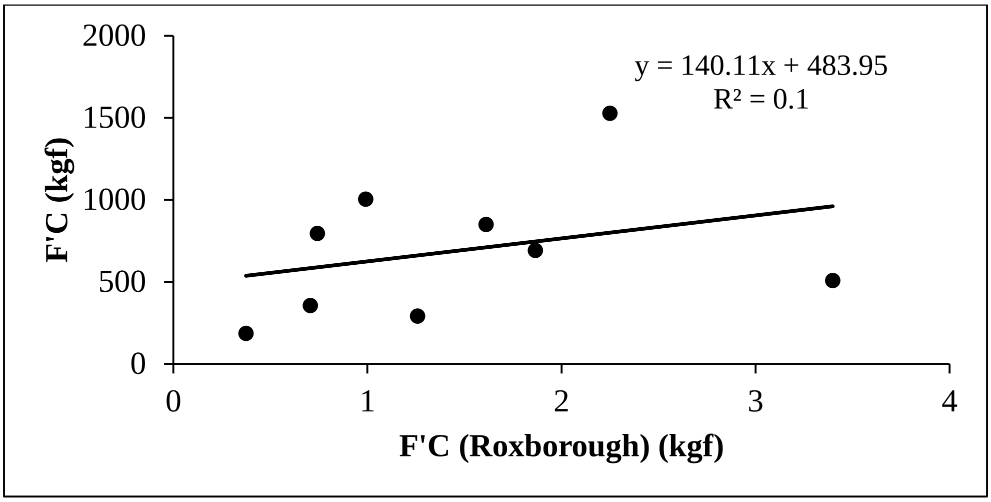

Figure 6.3 : Roxborough's theory for conical cutter 1

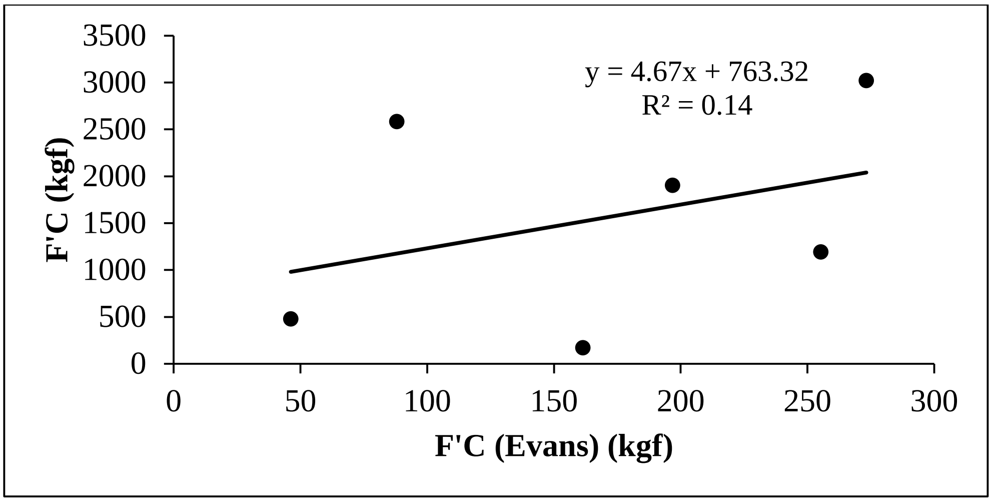

Figure 6.4 : Evans' theory for conical cutter 2.

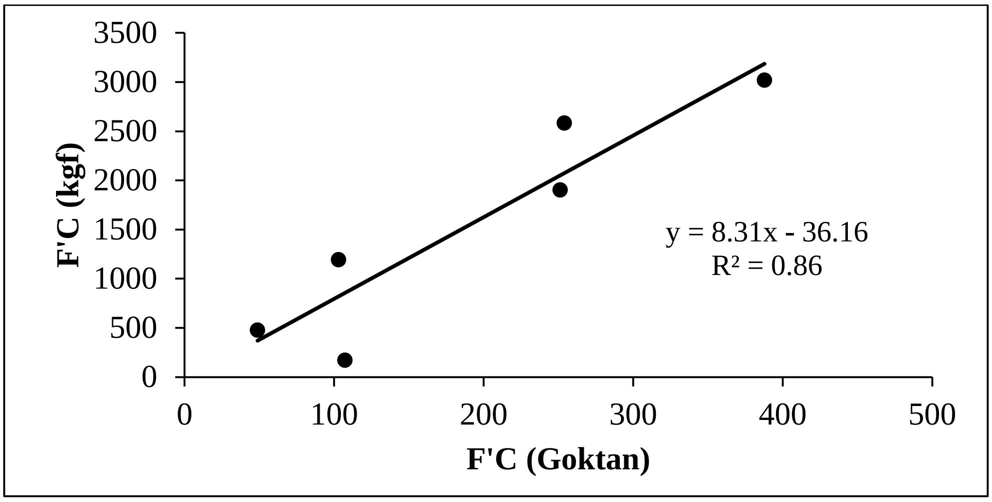

Figure 6.5 : Goktan's theory for conical cutter 2.

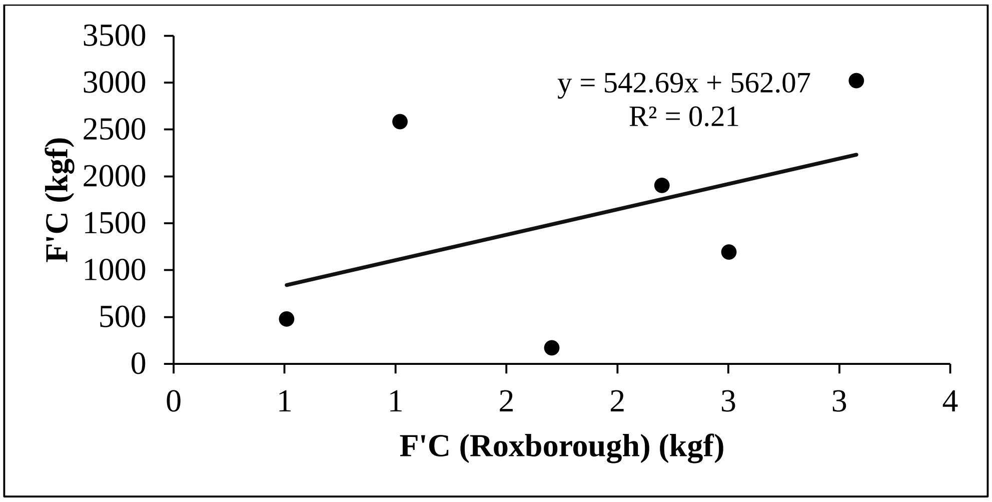

Figure 6.6 : Roxborough's theory for conical cutter 2.

6.2 Comparison of Chisel Cutter Theoretical and Experimental Forces

Linear cutting experiments done in unrelieved mode with chisel cutter and depth of cuts performed were 2.5, 3.5 and 5 mm. Results obtained from the tests are compared with Evans's chisel pick theory in terms of mean peak cutting force. There are 9 rocks performed with this index chisel pick. Results show that there is a reasonable correlation with Evans' theory and experiment results. The formulation used in this part is given in Equation 2.4. An example of calculation of the peak cutting force can be found below. In the Table 6.3 calculated and measured peak mean cutting forces and in figure 6.7 relationship between Evans' theory and laboratory results can be found.

For Beige Marble;

- σ_t= 78.2 kgf/cm^2
- d= 0.5 cm
- w= 1.27 cm
- α= -5 degrees
- Π= 180 degrees

$$F'C = \frac{2\,\sigma_t\, d\, w \sin\frac{1}{2}\left(\frac{\Pi}{2} - \alpha\right)}{1 - \sin\frac{1}{2}\left(\frac{\Pi}{2} - \alpha\right)} = \frac{2 * 78.2 * 0.5 * 1.27 * 0.737}{1 - 0.737} = 278.3 \text{ kgf}$$

Table 6.3 : Peak cutting force for chisel cutter and Evans' model.

Sample Name	F'C (Evans)	F'C (Lab)
Beige Marble	278.3	2707.1
Limestone	275.1	1340.7
Sandstone	424.9	2082
Kufeki Limestone	117.4	186
Travertine	112.8	808.3
Yeşil Kumtaşı	53.4	331.9
Travertine (DT)	170.8	826.8
Finike Limra	156.6	1497.9
Kavaklıdere Beyaz	227.8	2484.7

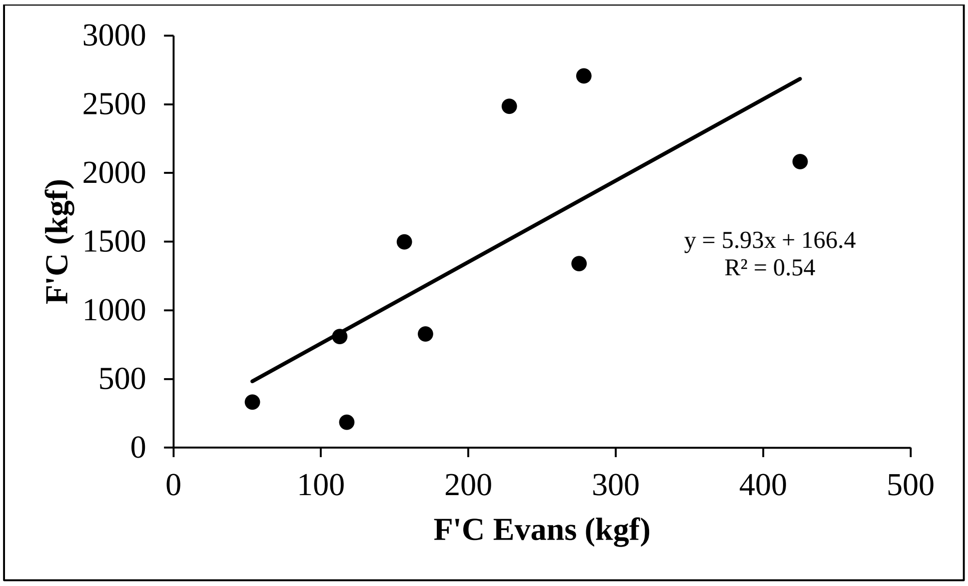

Figure 6.7 : Evans' theory for chisel cutter.

6.3 Results Obtained From the Comparison

In this part theoretical models were compared with the experiment results and for both conical cutters weak correlations are found for models of Evans and Roxborough. However, conical cutter 1 and 2 gave a high correlation coefficients with Goktan's model 0.83 and 0.86 respectively. Statistical equations developed for these relationships are given in Equation 6.1 and 6.2. For the design principles and performance of roadheaders developed for this work can be done by using Goktan's model with a good confidence. After all further study is needed for Goktan's model to use it with a better confidence.

For conical cutter 1;

$$F'C(Lab) = 7.1 * F'C(Goktan) + 6.7 \quad R^2 = 0.83 \qquad (6.1)$$

For conical cutter 2;

$$F'C(Lab) = 8.3 * F'C(Goktan) + 36.2 \quad R^2 = 0.86 \qquad (6.2)$$

In the second part with chisel pick theory and experiment results correlation coefficent 0.54 is found. Experiments correlated with the model were at 5 mm depth of cut and in unrelieved mode.

$$F'\,C(Lab) = 5.93 * F'\,C(Evans) + 166.4 \quad R^2 = 0.54$$

7. COMPARISON OF EMPIRICAL AND EXPERIMENTAL FORCES

7.1 Comparison with Emprical and Experimental Unrelieved Cutting Forces

Bilgin et al (2006) stated emprical relations with phyical and mechanical properties of rocks [5]. These equations are given in Table 2.1. Cutting forces obtained from these equations are correlated with unrelieved experimental cutting forces. In this empirical study a real life conical cutter with a tip angle of 80 degrees used. However, mini scaled conical cutters having 60 and 85 degrees of tip angle. For this reason a correction factor is needed in order to correct differences between the forces. As can be seen from the results conical cutter 2 is giving higher correlation coefficents than conical cutter 1. The best results for both cutter are obtained from equations related with Brazilian Tensile Strength, Dynamic elasticity modulus and Shore hardness values. The relationships between empirical and experimental results are given in Figures 7.1 to 7.5.

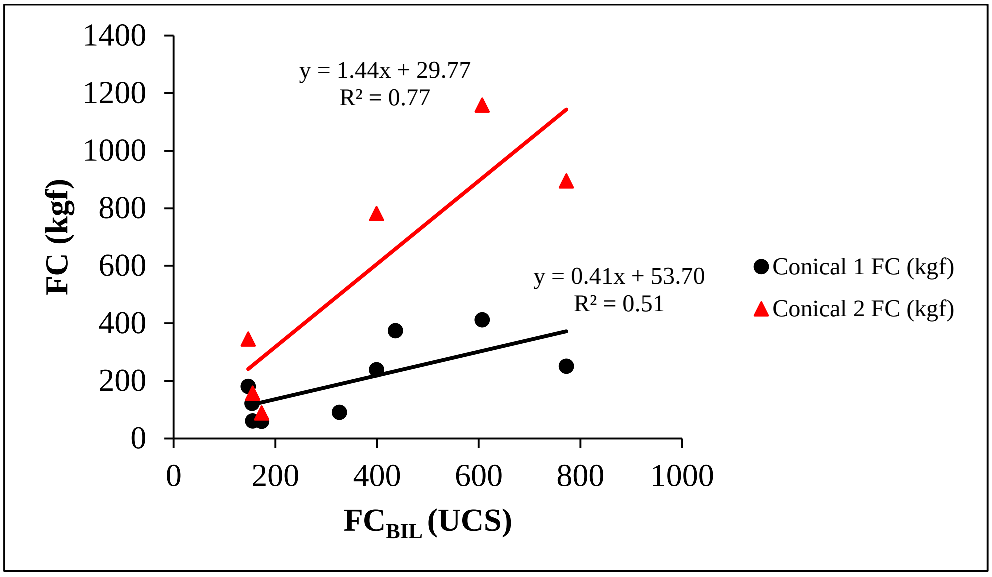

Figure 7.1 : Empirical UCS formulation with unrelieved cutting force.

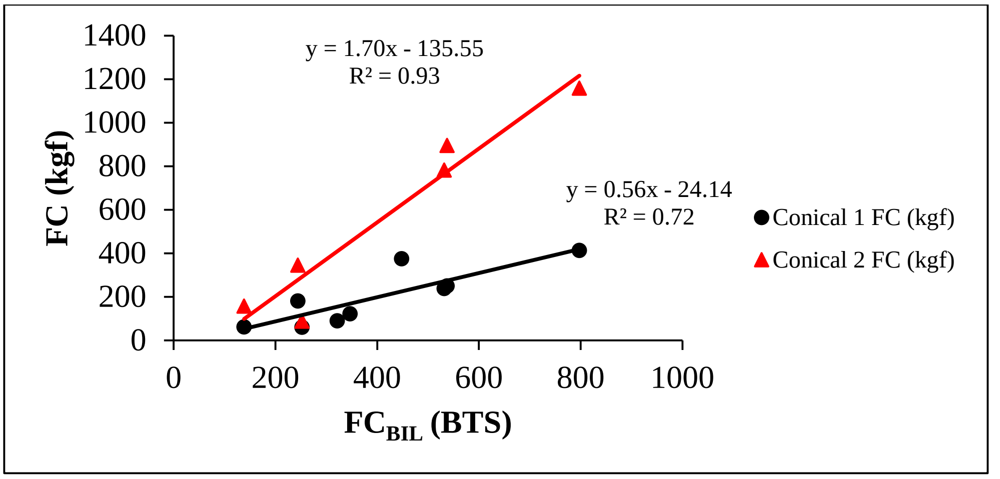

Figure 7.2 : Empirical BTS formulation with unrelieved cutting force.

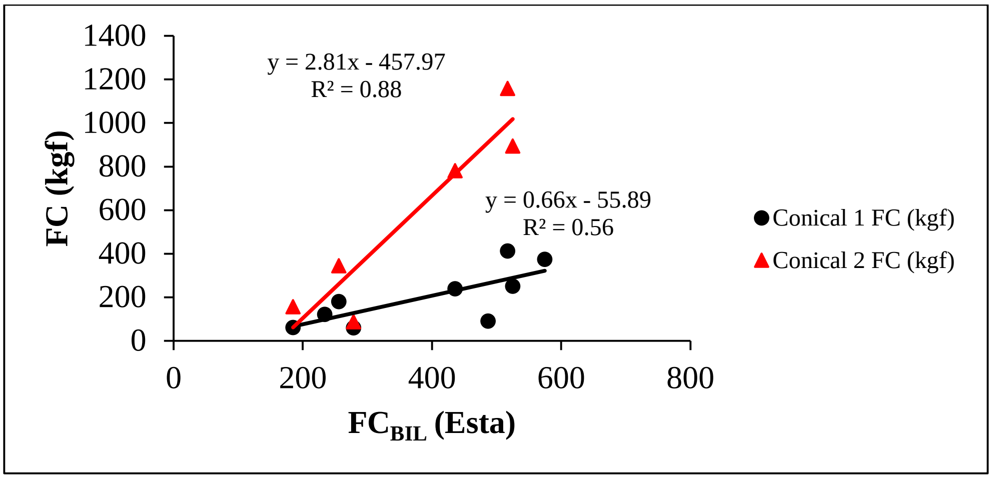

Figure 7.3 : Empirical Esta formulation with unrelieved cutting force.

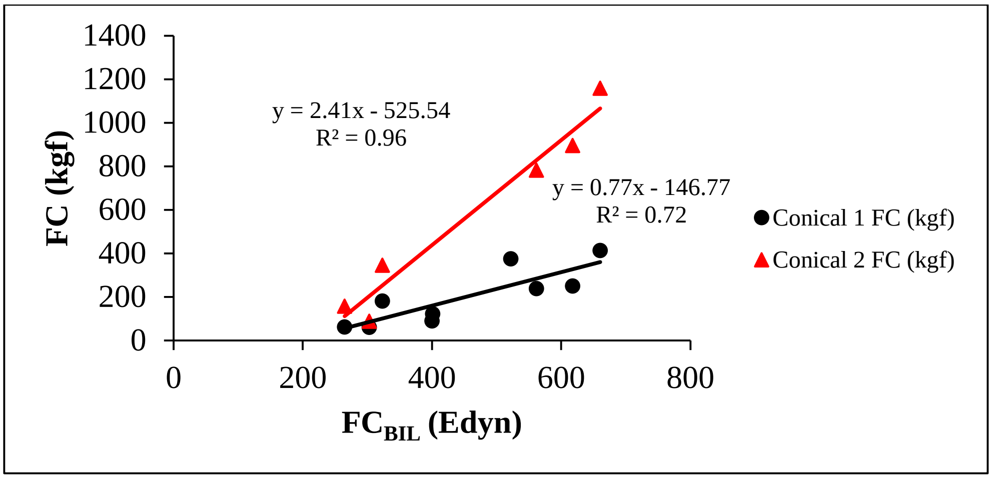

Figure 7.4 : Empirical Edyn formulation with unrelieved cutting force.

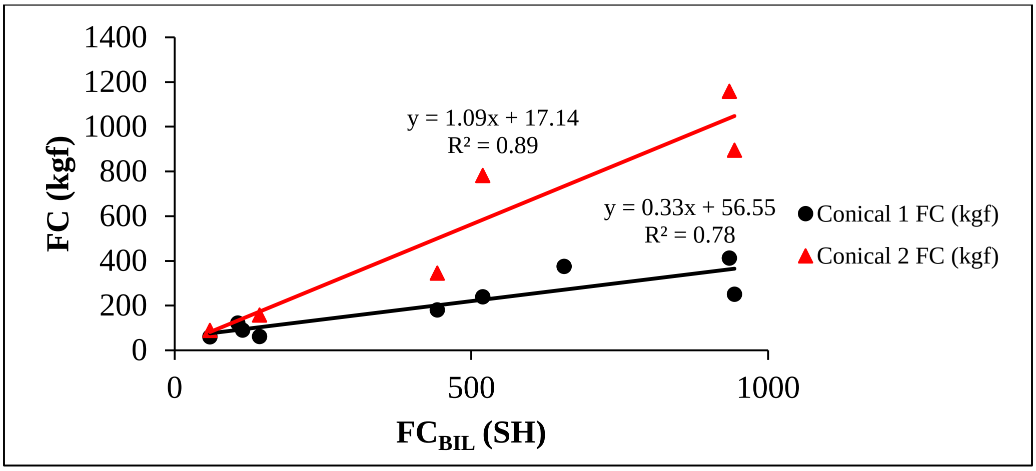

Figure 7.5 : Empirical SH formulation with unrelieved cutting force.

7.2 Comparison with Empirical and Experimental Relieved Cutting Forces

In this chapter cutting forces obtained from relieved cutting tests are correlated with equations stated by Bilgin et al (2006) [5]. The equations used in this study to predict cutting force in relieved mode are given in Table 2.1. The relationships between empirical and experimental results are given in Figures 7.6 to 7.10.

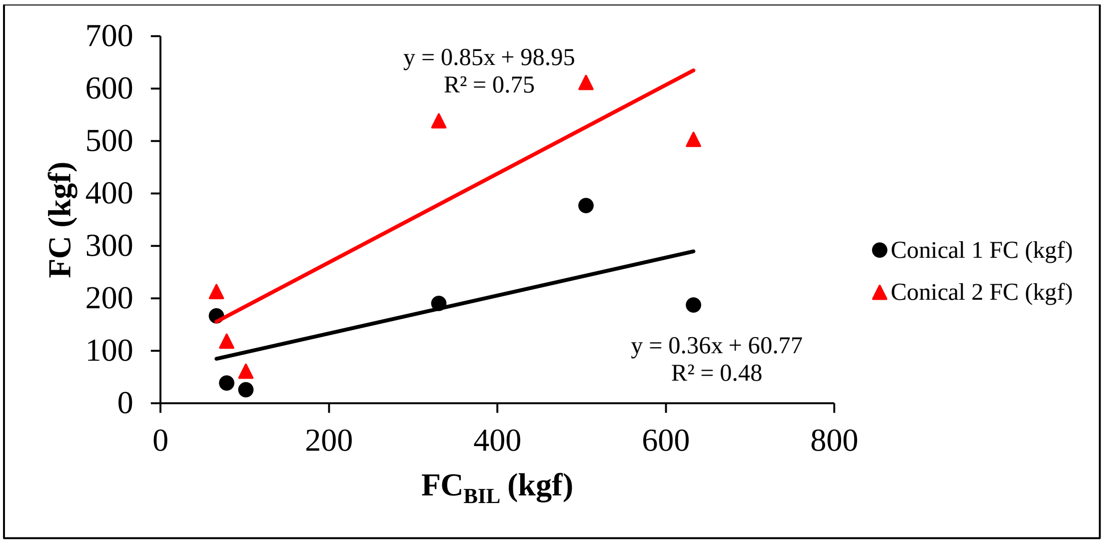

Figure 7.6 : Empirical UCS formulation with relieved cutting force.

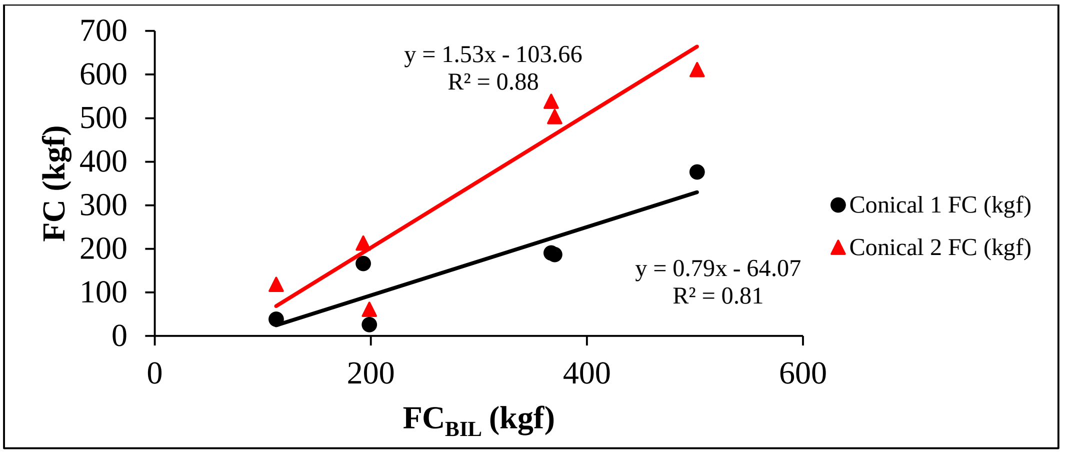

Figure 7.7 : Empirical BTS formulation with relieved cutting force.

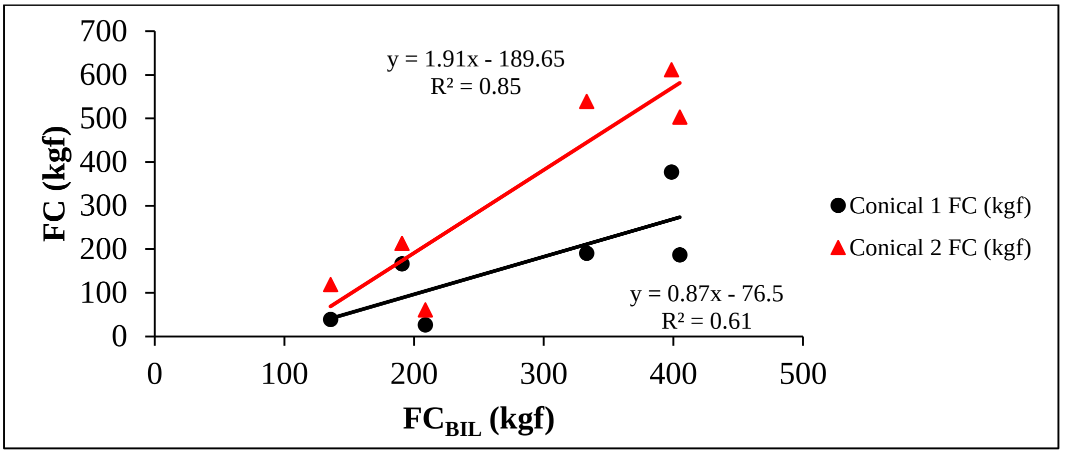

Figure 7.8 : Empirical Esta formulation with relieved cutting force.

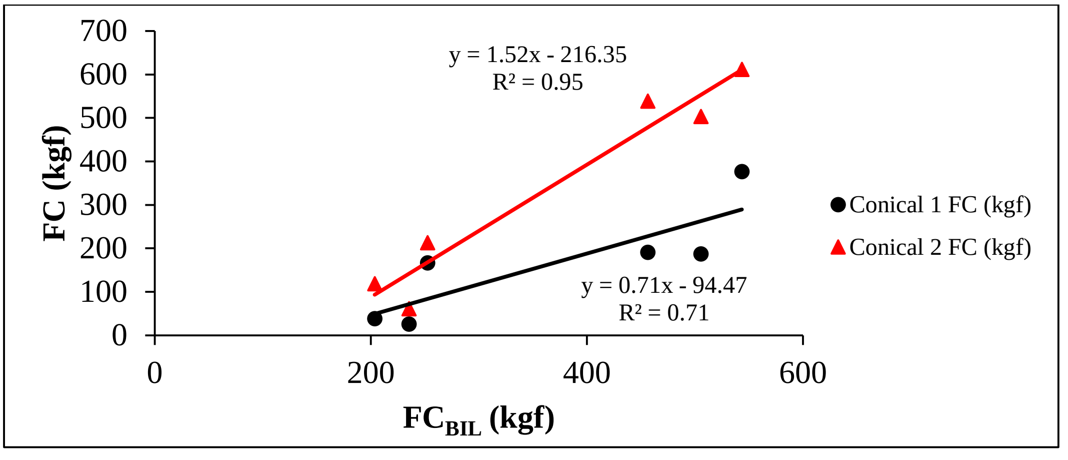

Figure 7.9 : Empirical Edyn formulation with relieved cutting force.

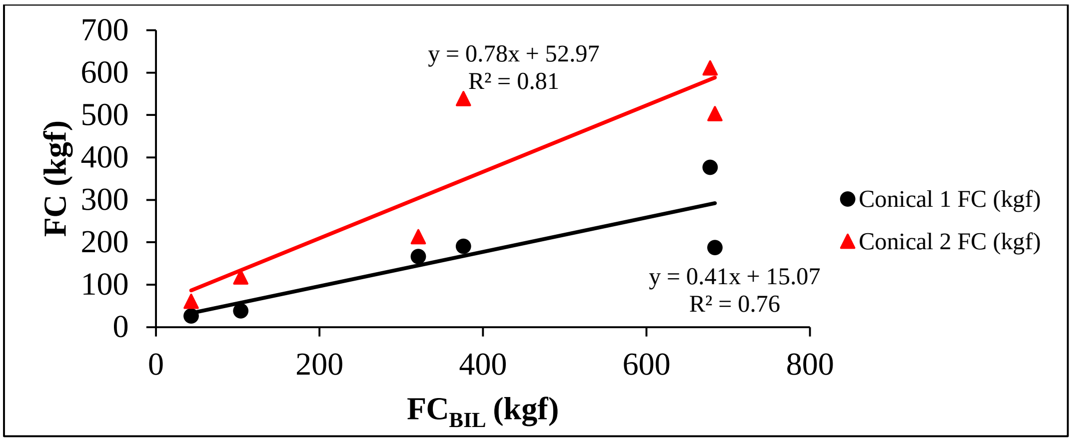

Figure 7.10 : Empirical SH formulation with relieved cutting force.

8. CONCLUSIONS

This thesis is about rock cutting with PLCM using mini scale cutters. In the first part mini scale conical cutters and chisel cutter compared with each other to understand their relations and to use them in roadheader performance prediction. To understand this, rock cutting experiments done with a certain range of mechanical properties. In correlative study part, results are showing that mini scale conical cutters can be used instead of chisel pick in the experiments. Specific energy and cutting force are also compared with mechanical properties and checked with existing literature. The results are quite close to the findings from different researchers.

In the field study part, samples taken from Amasya-Suluova coal mine subjected to the rock mechanics and rock cutting experiments. Besides, actual field performance of the roadheaders compared with the statistical models given in the literature. The closest results obtained from McFeat Smith and Fowell nomogram with conical cutter 1 and Rostami et al model with conical cutter 2. Statistical models usually over or under estimate the performance of the machine due to limits and constraints of the models.

In the theoretical model part three models are used for conical cutters and one model is used for chisel picks. Among these models, Evans, Goktan and Roxborough for conical picks, Goktan's model is giving highest correlation coeffiecent with the experiment results. For chisel picks, Evans' model compared with the laboratory results and reasonable correlation coeffiecent is found.

Finally, empirical models related with mechanical and physical properties checked through the experimental relieved and unrelieved cutting forces. According to results Brazilian tensile strentgth, dynamic elasticity modulus and shore hardness equations are giving the best results. However, it is always better to perform a cutting experiment than using empirical or theoretical models while selecting a mechanical excavator for a given project.

The laboratory studies with PLCM and field studies are continuing to develop a nomogram for roadheaders, as well as to develop models for mechanical miners using disc cutters and chisel tools. After the completion of these studies, linear cutting experiments can be done in a quite easy and faster way than existing experiment types.

REFERENCES

[1] **Kurt K.G., MacAndrew K.M**. (1985) Cutting efficiency and life of rock cutting picks. *Mining Science and Technology, 2,* 139-151.

[2] **Evans I.** (1984) A theory of the cutting force for point attack picks. *International Journal of Mining Engineering*, 2, 63–71.

[3] **Goktan RM.** (1997) A suggested improvement on Evans cutting theory for conical bits. In: Gurgenci H, Hood M, editors. *Proceedings of the fourth international symposium on mine mechanization and automation, Brisbane, Queensland, vol. I.* p. A457–61.

[4] **Roxborough FF, Liu ZC,** (1995) Theoretical considerations on pick shape in rock and coal cutting. In: Golosinski TS, editor. *Proceedings of the sixth underground operator's conference, Kalgoorlie, WA, Australia,* 189–193.

[5] **Bilgin. N., Demircin, M.A., Copur, H., Balci. C., Tuncdemir, H., Akcin, N.** (2006) Dominant rock properties affecting the performance of conical picks and the comparison of some experimental and theoretical results. *International Journal of Rock Mechanics & Mining Sciences, 43,* 139–156.

[6] **Su, O., Akcin, N.A.** (2011) Numerical simulation of rock cutting using the discrete element method. *International Journal of Rock Mechanics & Mining Sciences, 48,* 434–442.

[7] **Tiryaki, B., Boland, J.N., Li, X.S.** (2010) Empirical models to predict mean cutting forces on point-attack pick cutters. *International Journal of Rock Mechanics & Mining Sciences, 47,* 858–864.

[8] **Hurt. K.G., Evans. I.** (1980) A laboratory study of rock cutting using point attack tools. *21st U.S. Symposium on Rock Mechanics*.

[9] **Mostafavi. S. S., Yao. Q. Y., Zhang. L. C., Li. XS., Lunn. J., Melmeth. C**., (2011) Effect of attack angle on the pick performance in linear rock cutting. *45th US Rock Mechanics / Geomechanics Symposium held in San Francisco, CA,* 596

[10] **Lıu. S., Du. C., Cui. X.** (2009) Research on the cutting force of a pick. *Mining Science and Technology, 19,* 514–517.

[11] **Bilgin N., Copur H., Balci C.,** (2014) Mechanical Excavation in Mining and Civil Industries Taylor and Francis Group pp. 367.

[12] **Roxborough F.** (2010) Elements of Machine Mining. *Mineral Council of Australia* p.94.

[13] **Nishimatsu Y.** (1972) The mechanics of the rock cutting. *International Journal of Rock Mechanics & Mining Sciences, 9,* 261–71.

[14] **Hughes H.** (1972) Some aspects of rock machining. *International Journal of Rock Mechanics & Mining Sciences*,9, 205–211.

[15]**Thuro, K., Spaun, G.** (1996) Introducing destruction work as a new rock property of toughness referring to drillability in conventional drill and blast

tunneling. In G. Barla (ed) *Eurock 96 Prediction and performance in rock mechanics and rock engineering 2:* 707-713. Rotterdam, Brookfield, Balkema.

[16] **Balci, C., Demircin, M. A., Copur, H., Tuncdemir, H**., (2004) Estimation of optimum specific energy based on rock properties for assessment of roadheader performance. *The Journal of The South African Institute of Mining and Metallurgy,* December 633-642

[17] **Tumac, D., Bilgin, N., Feridunoglu, C. and Ergin, H**., (2007) Estimation of rock cuttability from shore hardness and compressive strength properties. *Rock Mech. Rock Eng.,* 40 (5), 477–490.

[18] **Balci. C.** (2009) Correlation of rock cutting tests with field performance of a TBM in a highly fractured rock formation: A case study in Kozyatagi-Kadikoy metro tunnel, Turkey. *Tunnelling and Underground Space Technology, 24,* 423–435.

[19] **Rostami, J., Ozdemir, L., Neil, D.M.** (1994) Performance prediction: a key issue in mechanical hard rock mining. *Mining Engineering, 11,* 1263–1267.

[20] **Balci. C., Bilgin. N.** (2007) Correlative study of linear small and full-scale rock cutting tests to select mechanized excavation machines *International Journal of Rock Mechanics & Mining Sciences, 44,* 468–476.

[21] **McFeat Smith, I.,Fowell, R,J.,** 1979. The selection and application of roadheaders for rock tunnelling. *Proc. Rapid Excavation and Tunnelling Conference*, Atlanta, Vol. 1, pp. 261-279.

[22] **Gehring, K.H.,** (1989) A cutting comparison, *Tunnels Tunnelling* November, 27–30.

[23] **Bilgin, N., Seyrek, T., Erdinc, E. and Shahriar, K.,** (1990) Roadheaders clean valuable tips for Istanbul Metro, *Tunnels Tunnell*ing, October, 29–32.

[24] **Rostami, J., Ozdemir, L. and Neil, D.M.,** (1994) Performance prediction: A key issue in mechanical hard rock mining, *Mining Engineering*, November, 1263-1267.

[25] **Copur, H., Ozdemir, L. and Rostami, J.,** (1998) Roadheader Applications in Mining and Tunneling, *Mining Engineering,* 38-42.

[26] **Thuro, K. and Plinninger, R.J.,** (1999) Roadheader excavation performance - geological and geotechnical influences, *The 9th ISRM Congress, Theme 3: Rock dynamics and tectonophysics/ Rock cutting and drilling, Paris,* 1241–1244.

[27]**Ocak, I., Bilgin, N.,** (2010) Comparative studies on the performance of a roadheader, impact hammer and drilling and blasting method in the excavation of metro station tunnels in Istanbul. *Tunnelling and Underground Space Technology, 25,* 181–187

[28] **Thuro, K., Plinninger, R. J.** (1998) Geological limits in roadheader excavation – Four Case Studies. *8 th International IAEG Congress*, 3545-3552.

[29] **Bilgin, N., Tumac, D., Feridunoglu, C., Karakas, A. R., Akgul, M.,** (2005) The performance of a roadheader in high strength rock formations in

Kucuksu tunnel. *31th ITA-AITES World Tunnel Congress, Istanbul, Turkey. Underground Space Use: Analysis of the Past and Lessons for the Future,* 815-820.

[30] **Ulusay R., Gokceoglu C., Binal A.,** (2011) Rock Mechanics Laboratory Experiments (In Turkish) *TMMOB Jeoloji Mühendisleri Odası* pp.167

[31] **Copur, H.,** (2010) Linear stone cutting tests with chisel tools for identification of cutting principles and predicting performance of chain saw machines. *International Journal of Rock Mechanics & Mining Sciences* 47 104–120.

[32]**H. Tuncdemir, N. Bilgin, H. Copur, C. Balci** (2008) Control of rock cutting efficiency by muck size *International Journal of Rock Mechanics & Mining Sciences* 45 278–288.

[33] **Copur H., Balcı C., Tumaç D., Avunduk E., Çomaklı R, Polat C. Tokat M.** (2014) ‘’Roadheader Selection and Performance Prediction for Excavation of Galleries of a Coal Mine in Amasya-Suluova Region’’ 19 th Coal Congress of Turkey May

CURRICULUM VITAE

Name Surname: Can Polat

Place and Date of Birth: Bursa, 21/06/1989

EDUCATION:

B.Sc.: Istanbul Technical University Mining Engineering

PROFESSIONAL EXPERIENCE:

2013-2014 Rock Mechanization Laboratory (Research Engineer)

2014- Geodata Engineering S.p.A.

PUBLICATIONS

- N. Ilci, M. Temel, S. Sezgin, T. Akpınar, S. Guarasio, **C. Polat**, N. Bilgin (2013)"Clogging and squeezing effect of marl- clayey limestone on the performance of a hard rock TBM in Suruc Tunnel, Turkey" World Tunneling Congress Geneva.
- N. Ilci, M. Temel, S. Sezgin, **C. Polat**, N. Bilgin (2013) '' Effect of Cutter Clogging on the Performance of a Tunnel Boring Machine (In Turkish) Proceedings of the 3rd international symposium on underground excavation for transportation November 59-64.
- C. Balci, R.Comakli, **C. Polat**, F.S. Sarbangholi (2013) '' Analysis of the TBM performance Parameters Using Boreability İndex'' Proceedings of the 3rd international symposium on underground excavation for transportation November 133-138.
- Copur H., Balcı C., Tumaç D., Avunduk E., Çomaklı R, **Polat C**. Tokat M. (2014) ''Roadheader Selection and Performance Prediction for Excavation of Galleries of a Coal Mine in Amasya-Suluova Region'' 19 th Coal Congress of Turkey May.